Mineral diagenesis and petrology of the Dala Sandstone, central Sweden

ALA ADIN ALDAHAN

AlDahan, Ala Adin, 1985 04 15: Mineral diagenesis and petrology of the Dala Sandstone, central Sweden. *Bulletin of the Geological Institutions of the University of Uppsala,* N.S., Vol. 12, pp. 1–48. Uppsala. ISSN 0302-2749.

The Dala Sandstone, of Proterozoic age, is the most extensive sedimentary unit in central Sweden. The rocks are quartz sandstones, lithic sandstones, feldspathic sandstones, arkoses and greywackes with intercalations of shales and siltstones less than 1 m thick. The Öje Basalt divides the sedimentary sequence into two parts. Dolerite dikes and sills of various compositions cut the sedimentary sequence, and in some parts the basalt. The clastic sediments were deposited in a dominantly continental environment. The detrital components of the sandstones are mainly quartz, feldspar and rock fragments. The most common diagenetic minerals are quartz, illite, chlorite, hematite, titanium minerals, calcite and feldspar. Diagenetic illite and chlorite were formed by alteration of detrital feldspars and biotite by authigenesis, and by aggradation crystallization of the fine-crystalline interstitial clay minerals. The sources of iron and titanium for hematite and titanium minerals, respectively, are mainly detrital biotite and ilmenite. The origin of authigenic quartz is mainly the silica produced from alteration of detrital grains, pressure solution of quartz, and replacement of detrital grains by calcite. Calcite and epidote are common as cement in sandstones close to dolerite. The diagenetic chlorite and most of the illite are Fe-rich and generally well crystallized. Their chemical composition and the crystallinity index of illite, as well as the general absence of diagenetic mixed-layer clay minerals (e.g. illite–smectite) and kaolinite, suggest their formation in the temperature range between 150 and 200°C and at a maximum pressure of 1.5 kb.

Ala Adin AlDahan, Department of Mineralogy and Petrology, Institute of Geology, University of Uppsala, Box 555, S–751 22 Uppsala, Sweden, 1st December, 1984.

Contents

Introduction

Diagenetic processes and products in sedimentary rocks have been paid increasing attention during the last thirty years. The availability of developed techniques with good resolution for the fine-crystalline mineral particles have been good aids in providing more feasible evidence of the crystallization behaviour of diagenetic minerals. The efforts, however, have concentrated on rocks younger than the Palaeozoic, because they are mainly connected in one way or another with oil production. The study of Precambrian clastic sequences is very scattered in Sweden. Among the important contributions are the works of Gorbatschev (1962a, 1962b, 1967) and Morad (1983, 1984). A survey of worldwide literature also shows a scarcity of studies on diagenesis in Precambrian clastic rocks. The reasons may partly be their commonly metamorphosed state and the shortage of information on mineral occurrence and equilibria of reactions in the field of high-grade diagenesis to very low-grade metamorphism.

Previous work

The name Dala Sandstone – earlier called "the red sandstone of Dalecarlia" – was given by Törnebohm (1873) to the large sandstone area in the north-western part of the Dalarna province of Sweden (Fig. 1). The rocks, which are sandstones, shales, conglomerates and associated igneous rocks, are ascribed to the "Jotnian" (Törnebohm 1896). This term was introduced by Sederholm (1895, in Sederholm 1897) for the youngest Precambrian sedimentary evolution and the upper division of the Algonkian, in which the Dala Sandstone and some other sedimentary sequences, e.g. the Visingsö Group, were included. Olivecrona (1920) verified the description of the stratigraphy of the Dala Sandstone as it was presented by Törnebohm already in 1873. He rejected the proposal of Frödin (1920), who considered the Dala Sandstone to have been conformably overlain by Cambrian rocks.

Presence of sedimentary structures, e.g. ripple marks and cross-beddings, together with the sedimentary association and tectonic setting of the area have led many workers to assign the deposition of the Dala Sandstone to a dominantly continental environment (Olivecrona 1920, v. Eckermann 1937, Magnusson et al. 1960, Lundqvist 1968, 1979). A combination of river and wind transport together with shallow basin deposition under mostly arid to semi-arid conditions has been suggested by v. Eckermann (1937).

Radiometric measurements, K-Ar and Rb-Sr determinations, were directly (Magnusson 1960) or indirectly (e.g. Welin & Blomqvist 1964, Lundqvist 1968) used to estimate the absolute age of the Dala Sandstone. A minimum value of 900 to 1000 m.y. was suggested by the above authors, while the data given by Patchett (1978) and Lundqvist (1979) indicate a minimum age of 1220 m.y. The spread of the age determination of the dolerites (Magnusson 1960, Gerling et al. 1966, Patchett 1978) that postdate the Dala Sandstone together with difficulties encountered in the radiometric measurements still leaves unanswered the question of the assignment of the exact age. However, the deposition of other Jotnian rocks in the Nordingrå region was suggested to occur during the interval 1385−1245 m.y. (Welin & Lundqvist 1975).

Aim and scope of the study

Although there has been some work on the regional geology of the Dala Sandstone, detailed petrologic and mineralogic information on the rocks belonging to it is lacking. The rocks outcrop in a large area in central Sweden, which makes stratigraphic controls a complicated task to perform. Therefore, minor

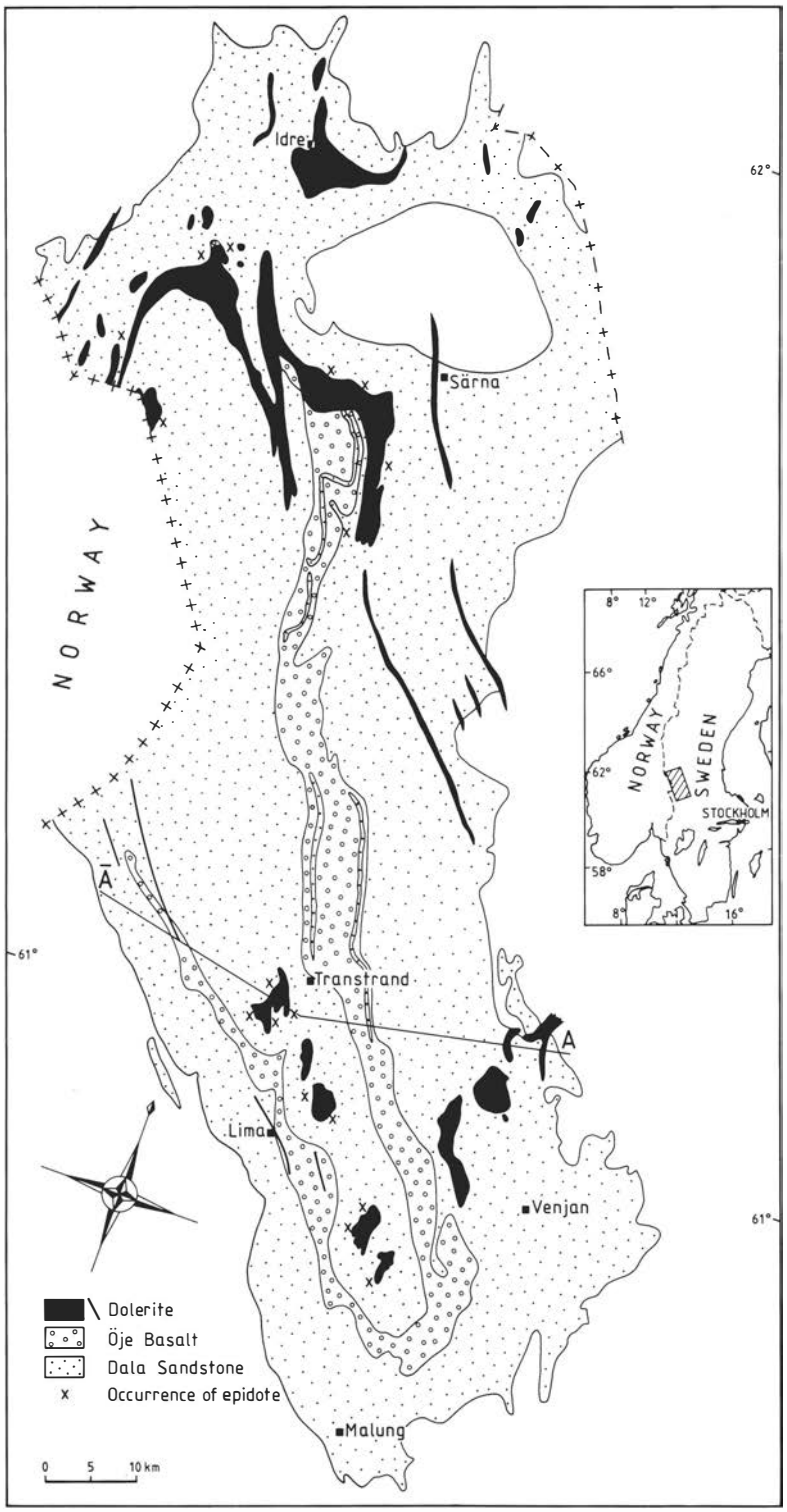

Fig. 1. A simplified geologic map of the studied area showing the distribution of the Dala Sandstone rocks and the associated igneous bodies (after Hjelmqvist 1966).

variations on local scale is beyond the scope of this study; instead an overall regional variation has been emphasized. Among the problems being studied are the mineral diagenesis in the sandstones, the factors acting in the diagenesis, the crystal-chemical variation in, mainly, clay minerals and in other minerals. An attempt is also made to relate the stages of minerals diagenesis to their conditions of formation.

Sampling and analytical techniques

Samples

About five hundred samples of the Dala Sandstone, from outcrops, tunnels and boreholes covering most of the area in Figure 1 were used for this study. Most of the samples were provided by Professor B. Collini, Uppsala. The samples were taken wherever possible with special attention to all lithologic variations. A few samples of the Öje Basalt were also collected for general identification. Most of the samples were thin sectioned and subjected to detailed examination using the transmitted light microscope. Information about the sampling localities is available from the Department of Mineralogy and Petrology, University of Uppsala.

Modal analysis

The modal composition of the sandstones was determined by the point-counter method. A test sequence was first carried out on thin sections of five samples in order to find the optimum number of points. In these a total of 300, 500 and 1000 points were counted and no significant differences were observed between the results when counting 500 or 1000 points. The 500 points per thin section were used for point-counter analysis of 100 samples, a large number of which are presented in tables for the different types of sandstones. The mineral components counted are mono- and polycrystalline quartz, potassium feldspar, plagioclase, detrital mica, quartz cement, interstitial clay, calcite cement, rock fragments and other constituents, e.g. iron and titanium oxides and other heavy minerals. The framework of sandstone classification presented by Füchtbauer (1959) was used in this work (Fig. 2).

Bulk chemical analysis

The total chemical composition of selected shales and siltstones and the different types of sandstone was determined. The analysis method used was wet-chemical analysis following Kolthoff & Sandell (1952). K_20 and Na_20 were determined by means of an atomic absorption spectrophotometer.

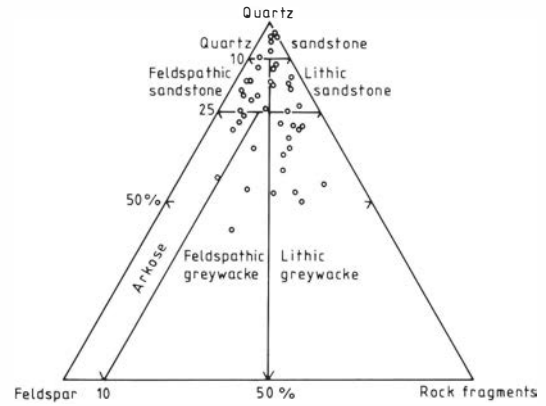

Fig. 2. Classification of the sandstones studied (after Füchtbauer 1959).

Electron-microscope and microprobe analysis

A JEOL scanning electron microscope with EDAX attachment was used in the examination of the rocks. For this purpose pieces of sonic-washed and dried samples were mounted on holders and coated with a thin layer of gold.

The chemical composition of individual minerals was determined in thin sections using a Cambridge microprobe analyser operating at a 75° take-off angle. The beam size was about 2 μm and usually only grains with sizes larger than this were analyzed. The results of the analyses were corrected for background, dead time, absorption fluorescence and atomic number effect by the use of a computer programme.

X-ray diffraction analysis

The clay-mineral fraction (less than 2μm) in sixty-five sandstones and twenty-five shales was separated by gentle crushing and subsequent sedimentation (see Galehouse 1971). Oriented samples were analysed at a rate of 2θ 1°/min, in the interval 2θ 2°−65°, using Ni-filtered CuKα radiation. The identification of the clay minerals was done by examination of samples as air-dried without further treatment, heated for one hour at 550°C and ethyleneglycol (EG) vapour saturated for twenty-four hours at 65°C. Treatment with dilute hydrochloric acid for twenty-four hours at 80°C was performed on some samples. Whole-rock samples of fifty selected shales and sandstones were also examined. X-ray analysis was performed on concentrates of titanium minerals, which were collected from some sandstone samples, using tetrabromethane of specific gravity 2.97 and subsequent separation by the Frantz magnetic separator.

General geological setting

Tectonics and structures

On a regional scale the rocks of the Dala Sandstone show almost horizontal stratification. The measurements of dips and strikes suggest that a NW–SE striking syncline with gently dipping limbs is the best fitted structural form (Collini pers. comm.). Steeply dipping stratification and schistosity up to 90° are observed along the south-western border of the area and are related to thrusting by Dalslandian movements in the late Proterozoic (Hjelmqvist 1966, Lundqvist 1979, Collini pers. comm.). Inside the border zone, right on to the Öje Basalt, the sandstone is slightly schistose and tilted or gently folded, with northeastwards decreasing intensity. Several faults striking chiefly in NW–SE and NNW–SSE are mentioned by Olivecrona (1920) and Hjelmqvist (1966).

The northernmost part of the area has been affected by the Caledonian orogenesis, which started in late Precambrian to early Palaeozoic times (Gee & Zachrisson 1979). The intensive east-west movement of the nappes resulted in local and regional deformation of the underlying bedrock, including the rocks of the Dala Sandstone.

The tectonic–igneous activities, which may be related to the formation of the Dala Sandstone rocks, can be summarized in three important events, pre-sedimentary, syn-sedimentary and post-sedimentary. The first one is sub-Jotnian igneous activity, which was responsible for the formation of the Dala Porphyries and Granites (Lundqvist 1979). The origin of these rocks is connected to magmatic differentiation associated with the closing phase of the Svecofennian orogeny (e.g. Hjelmqvist 1966, Lundqvist 1979).

The syn-sedimentary igneous activity is represented by the Öje Basalt. The basalt flows have been related to eruption of magma along fissures and fault zones, which were created by the collapse of the previous sub-Jotnian magma chamber (e.g. Lundqvist 1979). Increasing load of the sediments during the deposition of the lower part of the Dala Sandstone may have initiated the subsidence and hence the faulting.

The third event of the igneous acitivity, the post-sedimentary one, has resulted in the formation of dolerite dikes and sills. These dolerites represent the last stage in the magmatic history of the Jotnian in the area (Hjelmqvist 1966). The emplacement of the dolerites may be related to further fissuring and faulting caused by the increasing load of the sediment column and the associated basalts.

Basement, stratigraphy and lithology of the Dala Sandstone

Von Eckermann (1937) has discussed in detail the problem of the stratigraphic position of the Dala Sandstone. As to the lower boundary, the rocks rest on the sub-Jotnian complex (e.g. Sederholm 1927, v. Eckermann 1939, Hjelmqvist 1966, Lundqvist 1979). The lower part of this complex is composed of acidic and basic volcanics, porphyries and porphyrites and of quartzites, schists and conglomerates (the Lower Dala formation according to Hjelmqvist (1966)). The upper part, the Upper Dala formation (ibid.), consists of feldspar porphyries (the Älvdalen Porphyries) and porphyrites. Intercalations of the so-called Digerberg rocks (clastic rocks and volcanics), also occur (Hjelmqvist 1966). The Dala Granites, which are mostly reddish and coarse-grained, have also been included in the sub-Jotnian by Lundqvist (1979).

The lower Dala Sandstone. – The Dala Sandstone is divided into two parts, the lower and the upper, to differentiate between the sedimentary sequences below and above the Öje Basalt. The Öje Basalt is composed of lava flows that interrupted the sedimentation of the Dala Sandstone. The beginning of the lower part is marked, in many places, by conglomerates and sedimentary breccias. The thickness of this unit varies from place to place, but generally thicker beds are observed along the southwestern border of the area (Figs. 1 and 3). The breccias and the conglomerates are overlain by mostly pink quartz sandstones followed, with distinct contact, by feldspathic sandstones of grey, green and brown colours, and greywackes. Interlaminations of red and pale-grey arkose and grey-whitish quartz sandstone are observed in the upper layers of the lower part. In addition to these sandstones, thin intercalations (< 1 m) of red, brown, green, and dark-grey shales and siltstones are found.

The thickness of this part of the Dala Sandstone varies from south to north, as does also the thickness of the Dala Sandstone as a whole. It was estimated to 150–250 m (Törnebohm 1896) in the southern part of the area. Moving north, the thickness drops drastically to a total thickness of the whole Dala Sandstone of about 300 m (Törnebohm 1896).

An agate conglomerate, up to 60 cm thick, occurs at several localities between the quartz sandstones and the greywackes mentioned above, 20–35 m below the Öje Basalt (Collini pers. comm.). The pebbles of quartz and agate may originate from a body of a basalt older than the Öje Basalt which then has been eroded away, leaving only the pebbles.

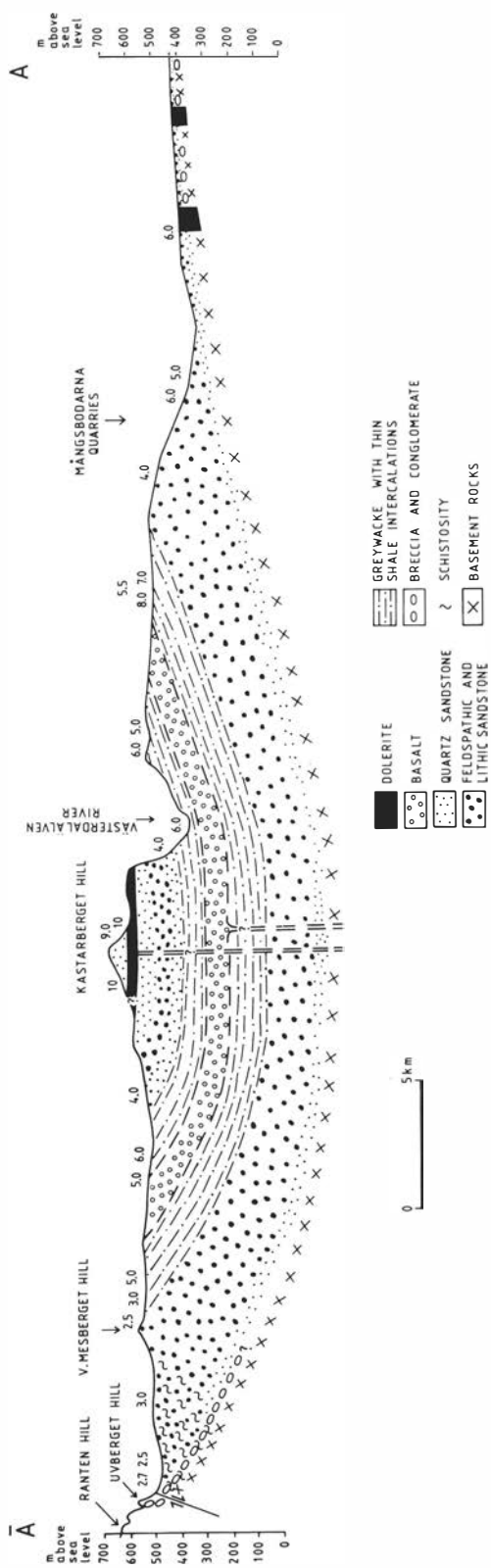

Fig. 3. Cross-section through the Dala Sandstone and the igneous rocks; for location see Figure 1. The numbers above the section are crystallinity indices of illite.

Among the common sedimentary structures in the lower part of the Dala Sandstone are regular and irregular laminations, simple and multiple cross-beddings, convolute bedding, symmetrical and asymmetrical ripple marks, desiccation cracks, shale-partings and raindrop imprints.

The Öje Basalt. – It is a large body of basalt which is composed of, at least locally, three flows with a NE–SW alignment (Fig. 1) and a total thickness of up to about 100 m (e.g. Törnebohm 1896, Hjelmqvist 1966). However, a thickness of up to 130 m is suggested by v. Eckermann (1939). The basalts may have flowed over non-friable sediments, slightly cemented sandstones. This is inferred from the presence of dredged sandstone beds in the bottom part of the basalt. If these beds were loose sediments, they would have been spread within the lava flow. Furthermore, fragments of sandstone, with a size of up to 30 cm, were observed within the basalt, in an outcrop 14.5 km NE of Malung. These fragments were probably parts of the sandstone beds, which suffered fragmentation during the fissuring and the eruption of the lava and were engulfed by the lava flow.

Pillow structures occur in the basalt at some places in the southern part of the studied area (Hjelmqvist 1966, Collini pers. comm.). They are small-scale pillows, mostly less than half a metre in diameter. As pillow structures are considered to result from subaqueous eruptions (e.g. Turner and Verhoogen 1960), at least part of the Öje Basalt must have erupted subaqueously.

The texture of the Öje Basalt is mostly porphyritic or amygdaloidal. The mineralogical composition mainly includes plagioclase, augite and chlorite, with substantial amounts of titanium minerals (leucoxene, sphene and rutile), calcite, epidote, hematite and occasionally magnetite. The amygdales are usually filled by calcite, chlorite, agate, quartz, chalcedony and locally by epidote and pumpellyite. v. Eckermann (1939) and Nyström (1982) reported the occurrence of prehnite also in some parts of the Öje Basalt.

Hitherto not much attention has been paid to the geology of the Öje Basalt. However, v. Eckermann (1939) considered the Öje Basalt to be a spilitic lava and more or less the effusive part of the later intrusive dolerites. Accurate age determinations are not available and the estimation of the age is based on the dolerites which cross-cut both the basalt and the clastic sequence. Adopting the value of 1220 m.y. as the age of the dolerites (p. 2), the sedimentation of the clastics and the eruption of the basalt predate this figure.

The upper Dala Sandstone. – This part of the sandstone, which overlies the Öje Basalt, does not differ much from the lower part as to composition (Fig. 3). In this part are also included those sandstone beds which occur in between the basalt with a thickness varying from 5 to 15 m. The sandstones are composed of, starting from the Öje Basalt upwards, grey-green greywackes, brown-red and pink feldspathic sandstones and pink-grey quartz sandstones. Thin beds of shales also occur, < 1 m thick. The estimation of the thickness of this part of the sequence imposes some problems due to erosion of the top layers. However, a range between 400 and 500 m is expected (Collini pers. comm.). A maximum thickness of the Dala Sandstone at about 800 m was suggested by Törnebohm (1896).

The grain size of the sandstones of the whole sequence of the Dala Sandstone varies between pebbly sandstones and fine-grained sandstones with, so far, no vertical or lateral trends observed. The fairly homogeneous lithology of the Dala Sandstone in both the upper and lower parts is probably a good justification to adopt a formation rank for the Dala Sandstone.

Phenomena of contact hydrothermal alteration of the sandstones and the shales are well pronounced in areas near the dolerite intrusions. The sandstones in such areas generally have brown or green colours, while the shales and siltstones became slightly metamorphosed and have developed banded textures with mostly violet to grey-black colours.

The dolerites. – Three major, mineralogically different, types of dolerites are encountered in the studied area. They occur as dikes and sills cross-cutting the clastics and basalt (Hjelmqvist 1966) and are thus virtually younger. The composition of the dolerites was described by Hjelmqvist (1966) as follows:

a – The Åsby Dolerite and related rocks are composed mainly of plagioclase, augite, olivine and ilmenite with accessory amounts of chlorite, amphibole, serpentine, magnetite and biotite.

b – The Särna Dolerite has about the same mineralogical composition as that of the Åsby Dolerite, but shows a micropoikilitic texture. Both dolerites grade locally into a monzonitic composition in which andesine, pyroxene, anorthoclase and quartz are the important constituents.

c – The quartz dolerites generally have a composition dominated by plagioclase, pyroxene and quartz in different ratios.

Petrology of the clastic rocks

The conglomerates and breccias

The basal conglomerates and breccias in the Dala Sandstone Formation have been observed in many areas along the contact with the basement rocks (Hjelmqvist 1966, Collini pers. comm.). Their boulders mostly originate from nearby basement rocks. Examinations of some localities combined with the description of Hjelmqvist (1966) indicate that the coarser fragments may reach a size of about 50 cm. Generally the boulders are subrounded to angular; the smaller the size the higher is the roundness. The dominating rocks among the boulders and pebbles are porphyries of different types, occurring in the basement surrounding the sandstone area. Other rock types occurring are quartz sandstones and, rarely, granites. The matrix of the conglomerates consists mainly of medium-grained sand particles of quartz and feldspar associated with quartz cement and occasionally interstitial illite and chlorite.

A number of specimens of agate conglomerate from different localities were examined. The dominating minerals in the pebbles are agate of mainly red colour and quartz. The pebbles may reach a size of 3 cm. Other pebbles observed are quartz sandstone and dark quartzite. All the pebbles are embedded in a matrix of light quartz sandstone or dark mica-rich sandstone.

The sandstones

According to the classification of Füchtbauer (1959) the sandstones investigated can be divided into six types (Fig. 2).

Quartz sandstones. – These are sandstones containing more than 90 % quartz (less than 10 % rock fragments and/or feldspar). They have pale-grey, pink or pale-red colour and are generally medium-grained. The composition is mainly monocrystalline quartz with minor amounts of feldspar, mostly microcline and felsitic rock fragments. The cementing material is predominantly quartz and illite (Table 1).

The red colour of these rocks is mainly attributed to hematite as interstitial pigment or, in some cases, grain coats. Heavy minerals are rare and, if any, mainly appear as grains of zircon, tourmaline, sphene and rutile.

Lithic and feldspathic sandstones and arkose. – The lithic sandstones contain more than 75 % quartz and have rock fragments in excess of feldspars (Fig. 2). The term was used by Gilbert (1955) for sand-

Table 1. Modal composition of some quartz sandstones.

Sample No.	Monocryst. quartz	Polycryst. quartz	Potassium feldspar	Plagioclase feldspar	Detrital micas	Quartz cement	Interstitial clay (illite)	Calcite cement	Rock fragments	Others
721b	55.7	–	–	–	–	22.3	20.3	–	1.7	–
1083a	63.3	–	1.0	0.7	–	20.7	12.3	–	2.0	–
523b	70.6	0.6	1.4	–	–	20.2	5.8	–	0.8	0.6
510d	54.4	0.4	3.4	–	1.8	15.2	16.0	–	1.0	7.8
596	61.3	0.3	3.0	1.6	–	31.3	1.5	–	1.0	–
565	61.1	–	2.8	1.5	–	25.2	8.2	–	1.2	–

stones with less than 90 to 95 % quartz plus chert and more rock fragments than feldspar. In the studied rocks, the lithic sandstones are usually pale-red in colour and medium-grained.

The feldspathic sandstones have principally the same composition as the lithic ones, but with more feldspar than rock fragments. The term was introduced by Pettijohn (1949) and is equivalent to the subarkose. The colour of the feldspathic sandstones is mainly pale-red but grey or greenish rocks are also encountered. They are generally medium-to coarse-grained.

The arkoses are very similar to the feldspathic sandstones in colour and texture. They contain, however, more than 25 % feldspar (Fig. 2; see also Pettijohn 1957).

The three types of sandstone mentioned are mainly composed of monocrystalline quartz, potassium feldspar, placioclase and rock fragments (Tables 2–4). Common types of rock fragments are

Table 2. Modal composition of some lithic sandstones.

Sample No.	Monocryst. quartz	Polycryst. quartz	Potassium feldspar	Plagioclase feldspar	Detrital micas	Quartz cement	Interstitial clay	Calcite cement	Rock fragments	Others
452	36.8	0.8	2.0	–	–	37.6	13.4	–	5.8	3.6
692a	49.7	0.3	2.0	2.7	–	40.0	–	–	4.6	0.7
716j	49.7	1.7	2.7	–	–	16.7	1.3	19.3	8.6	–
576c	61.6	1.0	3.0	–	–	7.2	11.2	0.8	9.6	5.6
569	50.0	0.8	2.2	3.4	–	15.2	8.6	5.6	6.6	7.6
463a	44.7	–	0.6	0.7	–	42.3	5.0	–	6.7	–

Table 3. Modal composition of some feldspathic sandstones.

Sample No.	Monocryst. quartz	Polycryst. quartz	Potassium feldspar	Plagioclase feldspar	Detrital micas	Quartz cement	Interstitial clay	Calcite cement	Rock fragments	Others
1161	57.6	1.8	4.4	1.6	–	19.2	9.2	–	5.6	0.6
1160	52.7	2.6	3.0	7.4	–	22.7	6.3	–	4.6	0.7
1159	53.0	–	2.0	11.0	–	21.0	9.7	–	3.3	–
1164	61.6	1.0	7.7	1.7	–	21.7	1.7	–	2.3	2.3
H18	42.8	9.4	10.2	–	0.2	6.2	28.2	–	2.8	0.2
H13	48.8	7.2	6.8	2.0	4.0	17.2	8.2	–	4.6	1.2
441	41.0	0.3	2.7	4.7	–	21.7	24.0	–	5.3	0.3
442b	48.3	6.0	3.3	2.0	–	26.4	11.0	–	2.0	1.0
501	39.0	0.6	4.7	1.3	–	28.7	24.3	–	1.4	–
464	47.0	–	1.3	8.0	–	38.0	4.0	–	1.7	–

Table 4. Modal composition of some arkoses.

Sample No.	Monocryst. quartz	Polycryst. quartz	Potassium feldspar	Plagioclase feldspar	Detrital micas	Quartz cement	Interstitial clay	Calcite cement	Rock fragments	Others
1128B	47.0	1.0	15.0	6.0	2.6	11.0	9.0	–	7.0	1.4
1155b	42.7	–	7.0	5.7	–	29.3	11.0	–	3.7	0.6
831	36.3	–	8.7	3.7	–	32.3	15.7	–	3.0	0.3
461	39.1	–	3.9	6.0	–	36.0	10.0	–	4.0	1.0

Table 5. Modal composition of some feldspathic greywackes.

Sample No.	Monocryst. quartz	Polycryst. quartz	Potassium feldspar	Plagioclase feldspar	Detrital micas	Quartz cement	Interstitial clay	Calcite cement	Rock fragments	Others
H5A	30.2	0.6	23.6	4.0	–	21.2	4.8	0.4	14.6	0.6
786a	35.3	2.3	9.0	8.4	–	23.0	7.0	–	15.0	–
1028	41.7	0.3	9.7	4.7	–	30.0	5.0	–	8.6	–

felsite, quartzite, sandstones and a few grains of mica schist. The source rocks of these fragments belong to the basement.

The cementing material in the sandstones is mainly quartz and clay minerals; illite dominates over chlorite. Calcite is the main type of cement in some lithic sandstones.

Greywackes. – This term has been a matter of controversy since the time of its introduction. It has mostly been used, however, as a genetic term to reflect an environment in which erosion, transportation, deposition and burial were so rapid that chemical weathering did not occur, as in active orogenic belts (e.g. Bates & Jackson 1980). Apart from its origin the term is used here for sandstones containing abundant rock fragments and feldspar (Fig. 2; see also Pettijohn 1975).

The greywackes are medium- to fine-grained and differ considerably in their mineralogical composition from the other types (Tables 5 and 6). In the Dala Sandstone they are next in abundance after the lithic, feldspathic and quartz sandstones. The feldspathic greywackes are less common than the lithic ones, with generally lower amounts of interstitial clay minerals and polycrystalline quartz. Potassium feldspar dominates over rock fragments and the cement is primarily quartz. In addition to felsite, quartzite and schist, basaltic and argillaceous rock fragments are common, which indicates more basic source rocks than the acidic ones mentioned earlier. As to the greywackes occurring below the Öje Basalt, the basaltic rock fragments are derived from the reworking of a basalt probably older than the Öje Basalt. With a few exceptions the polycrystalline quartz is more common in the greywackes than in the other rock types. The dominant colours of the greywackes are brown and red followed next by greyish-red or greyish-green. The colour is mostly controlled by the ratio of illite to chlorite. High ratio usually characterizes the red and brown rocks and a low ratio the grey and greenish ones.

Chemical composition of the sandstones

Unlike the shales the use of chemical analyses in characterizing sandstones has not, so far, been paid much attention. This is mainly because the grain size of sandstones permits detailed microscopic studies, which is not possible in shales. Furthermore, the complexity of diagenesis in sandstones causes changes in the original characteristics of the rock, e.g., alterations of minerals and cementation. If, however, the chemistry of sandstones is discussed in the light of observations of diagenetic changes, then chemical analyses will turn out to be much more elucidative (see e.g. Pettijohn 1975, Turner 1974, Morad 1983, 1984). The chemical analyses of the

Table 6. Modal composition of some lithic greywackes.

Sample No.	Monocryst. quartz	Polycryst. quartz	Potassium feldspar	Plagioclase feldspar	Detrital micas	Quartz cement	Interstitial clay	Calcite cement	Rock fragments	Others
1163	47.3	4.7	4.3	3.3	–	19.4	9.0	–	12.0	–
1170	46.3	1.4	1.0	3.7	–	19.0	14.0	–	14.3	0.3
H15	33.8	3.4	8.0	4.6	5.6	8.4	7.0	–	25.2	4.0
1166a	49.0	3.0	1.3	5.7	–	7.0	14.0	–	14.3	5.7
512b	40.4	1.6	8.0	–	1.0	9.8	20.8	–	14.4	4.0
522	45.8	5.8	3.2	2.6	0.2	4.2	13.8	5.8	16.4	2.2
617h	54.6	1.8	2.0	3.4	–	20.8	5.2	–	11.4	0.8
548b	40.8	1.4	1.4	5.2	–	12.8	4.0	–	26.4	8.0
578	34.4	2.4	1.4	4.6	–	1.4	8.8	1.0	11.4	22.0
502a	31.6	3.4	8.0	4.0	–	15.4	14.0	–	18.8	4.8
525	37.4	1.2	6.4	9.8	–	13.4	10.0	–	17.8	4.0
617i	41.0	1.4	3.0	7.2	–	15.6	10.6	–	13.4	7.8
1098j	40.8	1.8	5.8	6.2	–	7.2	16.6	3.6	17.0	4.8

Table 7. Bulk chemical composition of the quartz sandstones.

	596	523b	565
SiO_2	95.8	93.7	93.1
TiO_2	0.07	0.10	0.10
Al_2O_3	0.97	2.6	2.5
Fe_2O_3	0.95	0.73	0.80
FeO	0.46	0.36	0.18
MgO	0.07	0.07	0.22
CaO	0.16	0.12	0.13
Na_2O	0.14	0.30	0.43
K_2O	0.46	0.77	0.50
Total	99.08	98.75	97.96

Table 8. Bulk chemical composition of the lithic sandstones.

	576c	569	692a
SiO_2	84.9	82.3	87.9
TiO_2	0.46	0.37	0.28
Al_2O_3	6.5	5.3	4.5
Fe_2O_3	1.1	1.9	0.30
FeO	0.25	0.56	0.35
MgO	0.48	0.32	0.70
CaO	1.7	3.8	0.81
Na_2O	0.59	2.4	2.2
K_2O	2.4	2.2	2.1
Total	98.38	99.2	99.14

Table 10. Bulk chemical composition of the arkoses.

	1128B	1155b	831
SiO_2	84.5	88.5	87.3
TiO_2	0.19	0.15	0.10
Al_2O_3	7.3	4.9	4.6
Fe_2O_3	2.0	1.3	0.60
FeO	1.2	0.14	0.29
MgO	0.21	0.35	0.19
CaO	0.13	0.09	0.10
Na_2O	0.65	1.2	0.10
K_2O	2.0	3.0	3.2
Total	98.18	99.63	96.48

investigated sandstones (Tables 7–12) fall within the ranges of sandstones presented by Pettijohn (1975). Besides the quartz sandstones, the other sandstones also show high contents of SiO_2. The sources of this silica are mainly quartz, feldspars and clay minerals.

The presence of quartzite and other silica-rich rock fragments, especially in the greywackes, undoubtedly causes the generally high SiO_2 content in the greywackes. The K_2O content is related to presence of potassium feldspars (predominantly microcline and microperthite), illitic clay minerals and mica; to these and to interstitial chlorite the $A1_2O_3$ content is also related. The MgO is also contributed mainly from chlorite and biotite. The iron in the sandstones is shared mainly by iron oxides, clay minerals and biotite. Rutile, anatase and sphene are the main holders of TiO_2. CaO is contained primarily in calcite cement and to some extent in sphene. The source of Na_2O is primarily plagioclase.

To make use of the chemical parameters, the percentages of K_2O against that of the interstitial clay (Fig. 4A) and the ratio SiO_2/Al_2O_3 against that of quartz/(feldspar + rock fragments)(Q/(F+RF); Fig. 4B) were plotted. The contribution of K_2O, SiO_2 and Al_2O_3 does not entirely come from the plotted entities (as only interstitial clay or Q/(F+RF). This may have resulted in a wide field of distribution of the points in Figures 4A and B. Despite that, a trend towards positive correlation exists between the variables. As to Figure 4A, this may again mean that increasing content of interstitial clay is associated with increasing K_2O content of the rocks. In Figure 4B the same positive correlation trend is de-

Table 9. Bulk chemical composition of the feldspathic sandstones.

	H13	H18	1161	1164	1159	441	501
SiO_2	82.4	80.6	90.4	85.0	88.4	80.8	88.8
TiO_2	0.23	0.21	0.10	0.11	0.10	0.16	0.07
Al_2O_3	9.3	9.4	4.0	4.3	5.5	9.3	5.6
Fe_2O_3	2.2	1.6	1.4	0.68	0.73	1.5	0.98
FeO	0.53	1.8	0.22	0.14	0.13	0.32	0.30
MgO	0.58	0.55	0.14	0.07	0.25	0.36	0.06
CaO	0.45	0.26	0.13	2.3	0.36	0.44	0.17
Na_2O	0.48	0.48	0.09	0.79	0.22	1.3	0.50
K_2O	3.1	2.8	2.6	2.5	3.1	4.2	2.2
Total	99.27	99.70	99.08	95.89	98.79	98.38	98.68

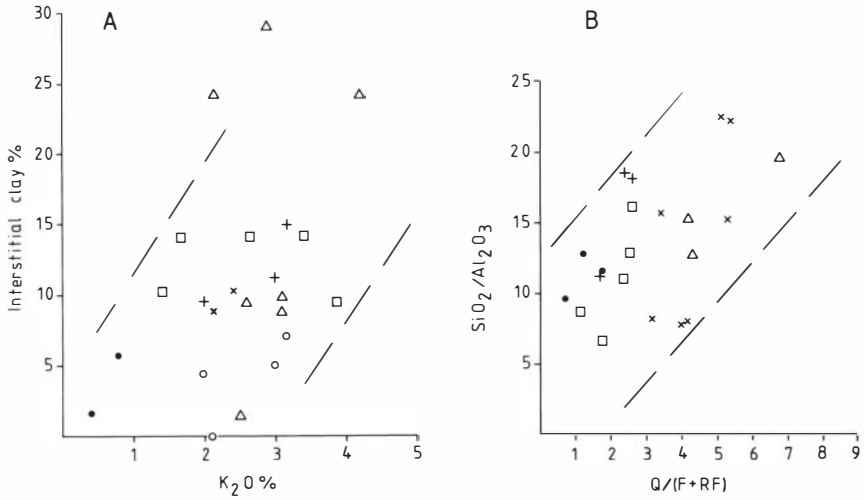

Fig. 4. The relation between K_2O and interstitial clay (A) and the ratios SiO_2/Al_2O_3 and Q/(F + RF) (quartz/(feldspar + rock fragments); B), in the different types of sandstones studied. • = quartz sandstone, x = lithic sandstone, o = feldspathic sandstone, + = arkose, △ = lithic greywacke, and □ = feldspathic greywacke.

Table 11. Bulk chemical composition of the feldsphathic greywackes.

	H5A	786a	1028
SiO_2	80.6	82.0	85.4
TiO_2	0.20	0.12	0.09
Al_2O_3	8.2	6.4	7.3
Fe_2O_3	2.2	0.81	0.37
FeO	2.1	0.26	0.38
MgO	1.3	0.32	0.11
CaO	1.5	0.11	0.53
Na_2O	1.2	1.0	0.10
K_2O	2.0	3.2	3.0
Total	99.3	94.22	97.28

Table 12. Bulk chemical composition of the lithic greywackes.

	502a	617i	1163	1166a	1170
SiO_2	76.0	61.8	85.4	78.7	85.9
TiO_2	0.44	1.5	0.22	1.6	0.25
Al_2O_3	9.1	9.5	5.2	6.8	6.7
Fe_2O_3	1.7	5.3	1.7	5.1	0.56
FeO	3.9	2.9	0.09	0.40	0.20
MnO	0.09	0.11	n.d.	n.d.	n.d.
MgO	0.20	3.1	0.46	1.6	0.58
CaO	0.71	8.0	0.33	1.3	0.33
Na_2O	2.4	2.8	0.08	0.30	0.65
K_2O	3.3	1.2	3.9	1.7	2.7
Total	98.84	96.21	97.38	97.5	97.87

monstrated between SiO_2/Al_2O_3 and Q/(F+RF), which is interpreted to reflect maturity in sandstones (Pettijohn 1975).

An interesting relationship is found between the FeO/Fe_2O_3 ratio and the ratio of illite (10 Å)/chlorite (7 Å) (Fig. 5). The negative correlation trend in the distribution of the points (representing both sandstones and shales) indicates that the higher the chlorite content, the higher is the amount of FeO in the rocks, also observed by Morad (1983).

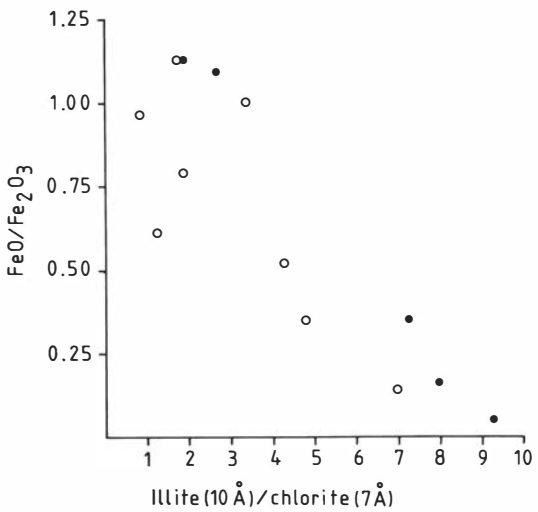

Fig. 5. The relation between the illite (10 Å)/chlorite (7Å) ratio and the FeO/Fe_2O_3 ratio in shales (•) and sandstones (o).

The siltstones and shales

These rocks grade into one another without any distinct boundary. Therefore the term shale, for simplicity, will be used throughout the text.

The colour varies from red to dark-grey and fissility characterizes the shales, which have fairly little silt-size material. The mineralogical composition of these rocks is size dependent. The higher the silt content, the higher is the amount of quartz and feldspar. The X-ray diffraction analysis shows that the main minerals in the shales are quartz, mica, chlorite and feldspar; substantial amounts of hematite, rutile and sphene are also found. The diffractograms of the clay fraction (<2 μm) disclose that chlorite, biotite and quartz dominate the green coloured rocks, whereas muscovite, illite and quartz are the dominant minerals in the red and brown coloured rocks. However, rock samples having different ratios of the above minerals display different tones of colour. The higher the chlorite content, the more the colour changes toward green, as in sandstones.

The chemical composition of the shales (Table 13) shows a great range of variation. This is a normal case in shale sequences and is interpreted as reflecting mainly the effect of grain size (Pettijohn 1975). The increase in the amount of coarse material is usually associated with increase in SiO_2 content. This correlates well with the observations from the studied shales where a higher SiO_2 means a higher amount of silt-size grains, mainly quartz. The most variable constituent is Na_2O, which is mainly related to albite and oligoclase. On the average, and compared to the sandstones, higher TiO_2, Al_2O_3, Fe_2O_3 and K_2O values are observed in the shales.

The detrital minerals of the sandstones

Quartz

Quartz is chemically ultrastable in most environments on the earth's surface. It is the most durable of the abundant minerals in sandstones, constituting an average of approximately 65 % (Blatt et al. 1980). Quartz is the predominant mineral in the rocks investigated and reaches, on an average, a content over 50 %. Monocrystalline quartz is the most common type, particularly in the quartz sandstones. The grains may be with or without inclusions. The type and distribution of inclusions in quartz may indicate the original source of the quartz grains. Folk (1968) and Blatt et al. (1980) distinguished three plausible types of inclusions that can reveal the source of detrital quartz. Those quartz grains, which are bubbly with vacuoles of liquid with or without gas inclusions, are derived almost exclusively from hydrothermal veins. Volcanic quartz is generally free from inclusions, while acicular inclusions of e.g. rutile, zircon and mica are common in granitic quartz. The most common inclusions in the quartz of the sandstones studied are vacuoles, microlites of mostly hematite, spherulitic zircon and tourmaline. Such inclusions may occur in both metamorphic and plutonic quartz. Needles of rutile, muscovite and biotite are also observed in some quartz grains, which may indicate a granitic origin. No special domain of inclusions in quartz was found vertically or laterally within the rocks investigated.

Extinction is another criterion of quartz, which Krynine (1946) used as a source-area indicator. Uniform to slightly undulatory extinction is the frequent type of extinction in the quartz studied. Quartz of plutonic origin is characterized by such an extinction. Strongly undulatory extinction is observed in the quartz grains of sandstones that have been affected by thrusting in the southwestern

Table 13. Bulk chemical composition of the shales.

	H4	H7	H24	H28	H30	H34	H59	571b	556	650a	1098i	1137a
SiO_2	69.3	52.7	47.2	43.2	45.1	52.6	61.2	56.9	68.5	67.0	64.9	61.2
TiO_2	1.0	1.9	2.1	0.98	3.2	1.5	0.49	0.85	0.65	1.0	1.2	1.3
Al_2O_3	11.2	20.9	21.3	25.6	26.4	22.4	17.7	18.7	15.3	11.6	13.6	13.0
Fe_2O_3	9.5	5.0	12.7	12.7	3.5	4.1	7.1	8.6	4.5	9.0	8.2	14.6
FeO	0.35	5.8	0.39	3.5	3.8	3.1	0.26	0.82	0.78	2.4	0.73	0.55
MnO	n.d.	0.11	n.d.	n.d.	0.05	n.d.	n.d.	n.d.	n.d.	0.13	n.d.	n.d.
MgO	0.70	2.0	1.4	1.2	1.5	1.3	1.2	2.2	1.8	2.6	2.7	1.8
CaO	0.91	1.7	1.2	0.87	1.6	0.98	0.87	1.4	0.38	0.83	0.98	1.0
Na_2O	0.00	0.10	0.00	0.10	1.3	0.00	0.1	0.96	1.9	0.00	1.4	0.00
K_2O	3.9	6.4	8.0	7.3	7.8	8.8	7.3	5.4	4.1	3.6	4.4	3.68
Total	96.86	96.61	94.29	94.45	94.25	94.78	96.22	95.83	97.91	98.16	98.11	97.13

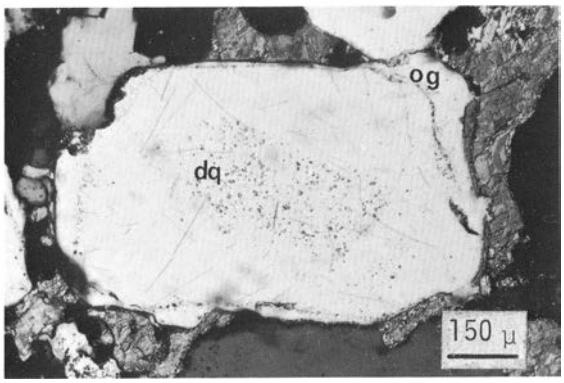

Fig. 6. A detrital quartz grain (dq) showing truncated overgrowth (og).

and northwestern parts of the area studied. The effects of tectonic and hydrothermal activity as well as diagenesis on the rocks put restriction on the use of the criterion of extinction. Polycrystalline quartz, showing sutured intercrystalline boundaries with uniform to slightly undulatory extinction and inclusions of mica, is characteristic of metamorphic origin (Krynine 1946, Blatt et al. 1980). Such grains are encountered in the studied sandstones and particularly in the feldspathic sandstones and the lithic greywackes. They are abundant in the upper part of the formation and their origin may be related to schists and quartzite of the sub-Jotnian complex. Quartz grains showing truncated overgrowth (Fig. 6) suggest derivation from reworked sandstones. They may indicate a contribution from sedimentary rocks in the basement. Another less common variety of detrital silica is the chalcedony. It is encountered in the greywackes below the basalt. The source rock of the chalcedony is certainly the same as that of the agate conglomerate mentioned earlier.

Feldspars

Feldspars such as microcline, microperthite, albite and oligoclase are present in all the sandstones studied. The potassium feldspars dominate over the plagioclases. This may be either due to primary domination of potassium feldspar in the source area or preferential elimination through weathering and during transportation and diagenesis. Plagioclases are expected to be more sensitive to alteration than potassium feldspar (Goldich 1938, Krauskopf 1979). The diagenetic alteration of the sandstones studied was so extensive that even most of the potassium feldspars were altered and fresh grains are uncommon. Acidic igneous and metamorphic rocks are considered the main source of sediments for the rocks of the Dala Sandstone Formation (e.g. Lundqvist 1979). It seems, therefore, that plagioclase feldspars were originally less in amount than the potassium feldspars.

The microcline occurs as subangular to rounded grains. They are commonly altered diagenetically into illite and chlorite and replaced by calcite.

Microperthite is common in the coarse-grained sandstones, particularly in the arkoses. The grains suggest derivation from a granite or pegmatite source (Folk 1968).

The albite and oligoclase show the same grain-shape and size characteristics as the microcline. As also occurred with microcline, they altered into illite and chlorite and were replaced by calcite.

Microprobe analyses of detrital microcline and albite (Tables 14 and 15) comprise almost pure end members. Such pure feldspars have been derived from plutonic (granitic) or metamorphic source rocks (Trevena & Nash 1981).

Micas and chlorite

Partially altered biotite and muscovite are minor

Table 14. Microprobe analyses of detrital microcline.

	1	2	3	4	5[a)]	6[a)]	7[a)]
SiO_2	63.90	63.15	63.80	63.59	63.50	63.31	63.35
Al_2O_3	18.67	18.44	18.25	18.54	18.29	18.40	18.17
FeO*	0.17	0.27	0.17	0.27	0.12	0.18	0.24
CaO	0.09	0.04	0.06	0.09	0.06	0.09	0.09
K_2O	16.50	16.06	17.08	17.05	17.02	16.22	16.92
Na_2O	0.25	0.64	0.97	0.75	0.22	0.98	0.63
Total	99.58	98.61	100.31	100.30	99.20	99.18	99.41
	Un-twinned	Perthitic	Poly-synthetic	Perthitic	Un-twinned	Un-twinned	Poly-synthetic

* FeO represents total iron.
All the grains are partially altered into illite; those with [a)] are replaced by calcite as well.

Table 15. Microprobe analyses of detrital albite.

	1	2	3	4	5	6[a)]	7[a)]
SiO_2	67.35	67.19	68.25	67.59	67.92	67.40	66.12
Al_2O_3	21.04	19.45	19.11	19.41	19.47	19.36	20.84
FeO*	0.51	0.01	0.01	0.01	0.12	0.05	0.01
CaO	0.06	0.17	0.18	0.13	0.08	0.07	0.62
K_2O	0.11	0.05	0.05	0.04	0.04	0.05	0.12
Na_2O	10.74	13.21	12.79	12.88	11.92	11.91	11.51
Total	99.80	100.09	100.39	100.05	99.55	98.84	99.22
	Untwinned		Albite–Carlsbad twin		Untwinned	Albite twin	

* FeO represents total iron.
All the grains are partially altered into illite; those with [a)] are replaced by calcite and quartz as well.

components among the detrital minerals in the studied sandstones. Some of the lithic greywackes and the feldspathic sandstones contain scattered, relatively large amounts of mica (up to 5.6 %). The size of the grains may reach 1 mm, with an average size of 0.03 mm. In the whole formation, biotite usually dominates over muscovite, which may be considered a reflection of the original mineralogy of the source rocks (see also Ljunggren 1954, Hjelmqvist 1966). Biotite has been used as source-area indicator and in some instances as indicator of the depositional environment (e.g. Krynine 1940, Lahee 1941, Füchtbauer 1974). This possibility could not be utilized for the rocks studied since all the grains of biotite are completely or partially altered by diagenesis. The chemical composition of the detrital muscovite (Table 16) shows that they vary from Fe-rich to Fe-poor types with almost similar potassium content.

Chlorite as primary detrital constituent is not common in the sandstones studied. However, if present, it is highly altered by the diagenesis.

Table 16. Microprobe analyses of detrital muscovite.

	1	2	3	4	5
SiO_2	50.38	52.78	45.77	46.61	50.80
Al_2O_3	24.62	24.54	34.28	36.69	30.22
FeO*	7.08	4.83	2.08	0.62	3.87
MgO	1.46	1.44	0.68	0.96	1.27
TiO_2	0.27	0.10	0.41	0.66	0.20
K_2O	9.51	9.50	9.50	9.42	9.36
Na_2O	0.01	0.01	0.00	0.00	0.03
MnO	0.07	0.07	0.04	0.01	0.12
Total	93.41	93.27	92.76	94.97	95.87

* FeO represents total iron

Heavy minerals

Heavy minerals are rarely found in the sandstones studied. However, a few particles of zircon, tourmaline, sphene, epidote, andalusite, rutile and magnetite have been observed. The low amount of heavy minerals, <0.5 %, may be attributed to intrastratal dissolution (Pettijohn 1975). However, a probable scarcity of heavy minerals in the source rocks is another explanation. The high degree of diagenetic alteration, which has affected the studied sandstones, may favour the possibility of later dissolution of the heavy minerals, in particular the sensitive ones such as amphiboles, pyroxenes and ilmenite. Unfortunately there is no direct evidence, but almost completely altered particles of ilmenite were proved to be the source of authigenic titanium minerals in the studied rocks (Morad & AlDahan 1982a).

Diagenesis in sandstones

At the depositional site and after sedimentation further alteration of the detrital minerals takes place. In addition, new minerals are formed, e.g. cement. Compaction starts also to influence the mineral particles as sedimentation proceeds. These two processes, cementation and compaction, contribute much to the reduction of the porosity of the sediment.

Cementation

Quartz cement. – Silica, in the form of quartz, is the most abundant cementing material in the studied sandstones. In the quartz sandstone, quartz cement as overgrowth and coarse-crystalline pore filling is the most common type. The pore-filling varie-

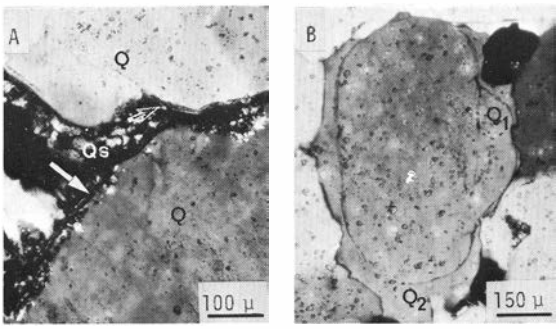

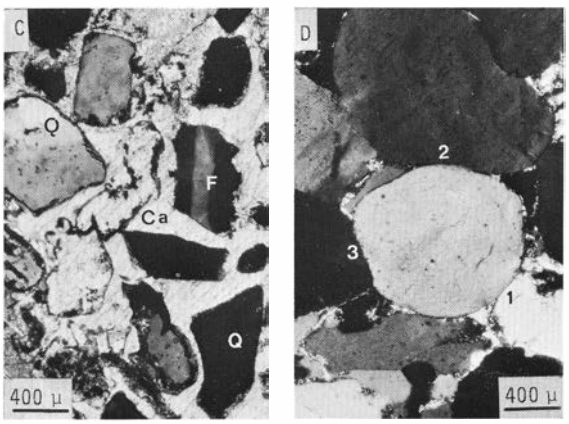

Fig. 7. A – Pore-filling quartz cement (Qs) enveloping illite coat (arrows); Q is detrital quartz. B – A detrital quartz grain showing two stages of quartz overgrowth (Q_1) and (Q_2). C – Quartz (Q) and feldspar (F) being replaced by calcite (Ca); observe the preserved boundaries, most probably from quartz which was completely replaced by calcite. D – Detrital quartz grains showing straight (1), concave–convex (2), and sutured (3) boundaries.

ty is the last cement to have been formed in these sandstones where it envelops the quartz overgrowth and the illite–hematite coat if present (Fig. 7A). The quartz overgrowth on the adjoining grains may weld together and close-up of pores occurs.

In samples from areas influenced by introduction of dolerites a second stage of quartz overgrowth is clearly observed (Fig. 7B). The silica needed for the second generation is probably derived from those nearby rocks in which quartz and feldspar were replaced by calcite (Fig.7C).

The shape of the boundaries between the quartz grains is observed to vary with respect to the type of cementing material. When quartz is the cement or the grains come in direct contact with each other, the intergranular boundaries are straight, concave–convex or sutured (Fig. 7D). The presence of clay coats on the detrital quartz grains usually enhances the formation of sutured boundaries. The clay coat, e.g. illite, found along the sutured boundary (Figs.

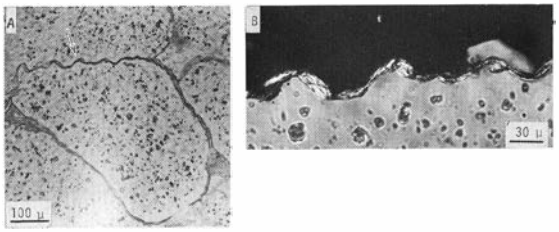

Fig. 8. A – Illite coat (arrow) along the sutured boundary between two quartz grains. B – The same as in A in larger magnification.

8A and B) usually tends to outline the individual or the resulting compound grain. Quartz as overgrowth locally shows triple- junction grain contacts (Fig. 9A).

Fine-grained quartz (chert) appears intergrown with interstitial clay particles (Fig. 9B) at the con-

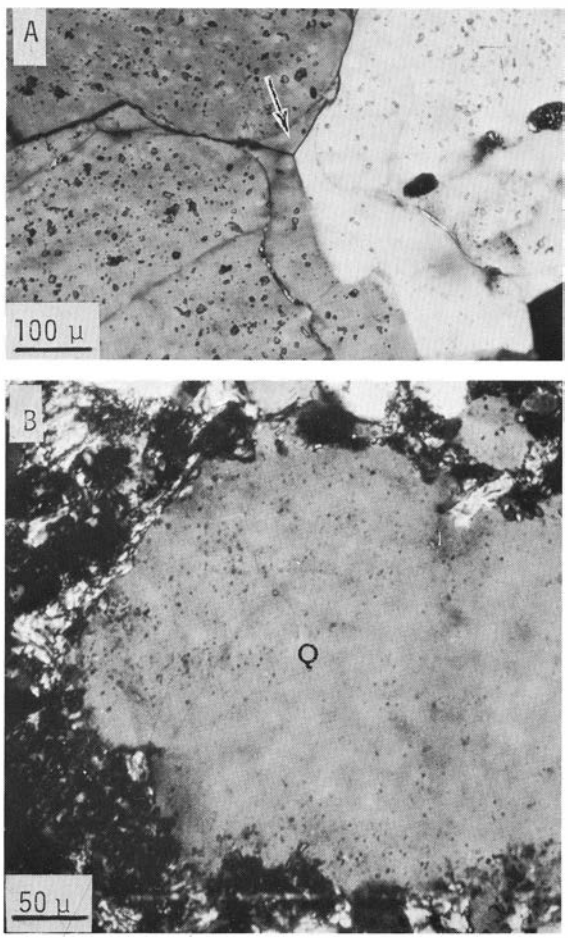

Fig. 9. A – Quartz overgrowth showing triple junction contact (arrow). B – Fine-grained quartz (chert) intergrown with illite and corroding detrital quartz grain (Q).

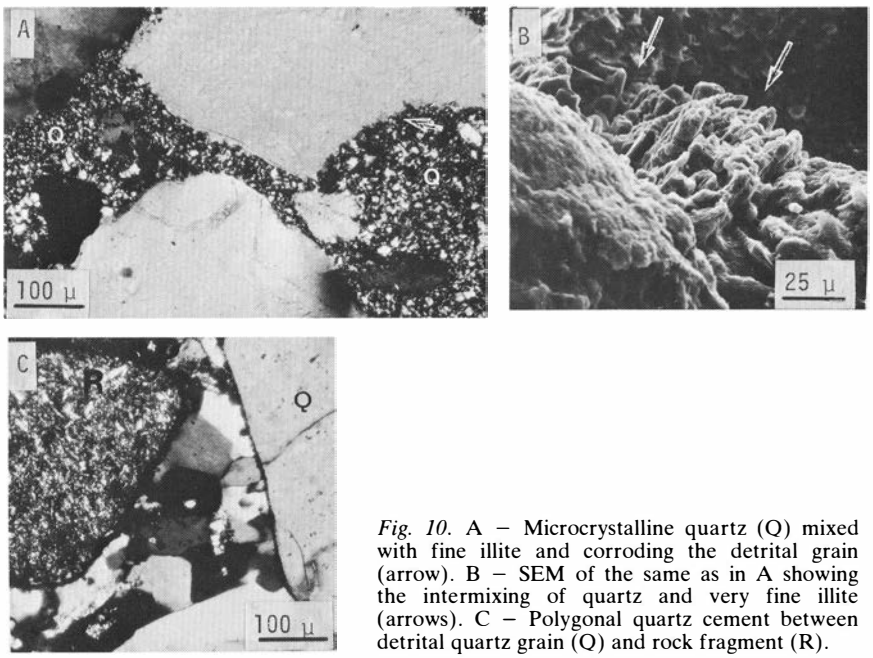

Fig. 10. A – Microcrystalline quartz (Q) mixed with fine illite and corroding the detrital grain (arrow). B – SEM of the same as in A showing the intermixing of quartz and very fine illite (arrows). C – Polygonal quartz cement between detrital quartz grain (Q) and rock fragment (R).

tact between quartz grains and interstitial clay. This phenomenon is rather common in clay-rich sandstones and is related to increasing stress with depth of burial (Dapples 1979).

Quartz cement also occurs in the form of microcrystals gathered as lumps or dispersed in between the interstitial clay minerals (Figs. 10A and B). This type of quartz cement is common in sandstones containing appreciable amounts of interstitial clay minerals. Corrosion of quartz and feldspar by clay minerals is a likely source of this quartz cement and has mostly been related to increasing depth of burial (e.g. Dapples 1979, Bjørlykke 1980).

Pressure solution has been considered as the source of silica for the formation of quartz overgrowth in many sandstones (e.g. Heald 1956, Füchtbauer 1974, Morad 1983, Houseknecht 1984). The presence of clay seams and coats on detrital quartz may hinder the formation of overgrowth as suggested by many authors (e.g. Pettijohn 1957, Bjørlykke 1980). This is most probably due to the exchange of Mg^{2+} and K^{+} by H^{+} on the surface of the chlorite and illite, which causes an increased pH in the surrounding solution. The increase of the pH will lead to inhibition of the quartz precipitation and instead pressure solution is intensified. Pressure solution creates overpressure in areas where clay is present and this may enhance the migration and precipitation of silica in the clay-free zones. The quartz sandstones in the Dala Sandstone Formation show higher contents of quartz overgrowth compared to the other types of the sandstones. This phenomenon can be explained by the argumentation given above.

Replacement of detrital and authigenic quartz by calcite cement in some lithic sandstones has resulted in selective dissolution of detrital quartz grains. Long straight boundaries, partly parallel to the c-axes, show lower degree of replacement than other parts of the grains. Hurst (1981) demonstrated that the surface-energy characteristics of quartz grains, which depend much on the crystallographic orientation and textural features (e.g. overgrowth and fractures), control their dissolution habit. By applying the results of Hurst, it seems that areas of the grains where selective dissolution has occurred could represent previous sites of high surface energy; most probably they were places of quartz overgrowth.

Euhedral crystals of quartz showing polygonal habit (Fig. 10C) are observed as cement in sandstones, adjacent to areas of dolerite, with only chlorite coat on the detrital grains. Straight and sutured boundaries as well as unequal-angle triple points are characteristics of these crystals, which suggests crystallization at high temperature (Spry 1969). Spry mentioned that at still higher temperature of crystallization straight boundaries and equal-angle triple points are developed in such grains. The silica needed for the formation of euhedral quartz cement has been furnished by nearby sandstones in which

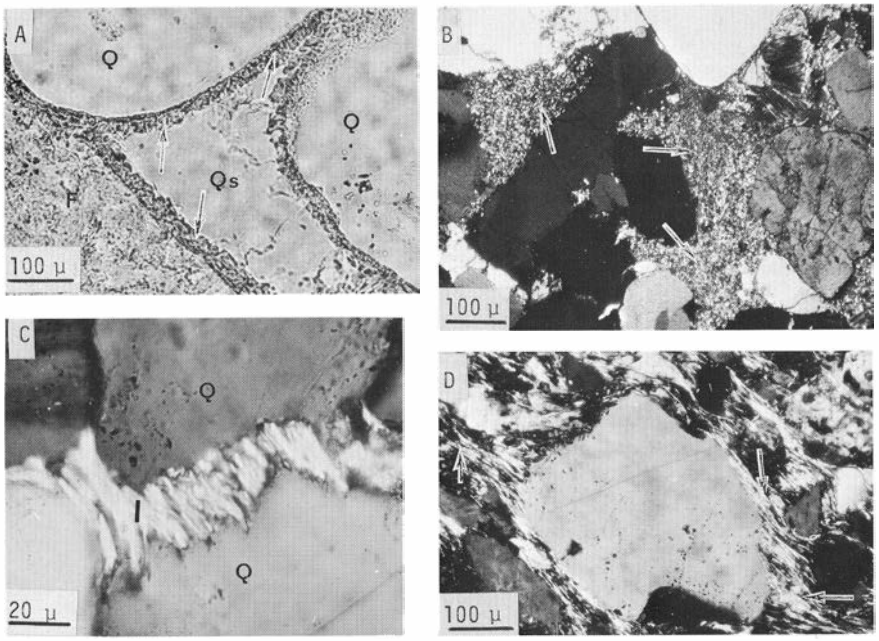

Fig. 11. A – Chlorite coat (arrows) on detrital quartz (Q) and feldspar (F); Qs is quartz cement. B – Pore-filling illite (arrows). C – Illite (I) protruding into quartz grains (Q). D – Lath-like illite (arrows).

hydrothermal fluids have dissolved quartz and feldspar. Calcite and epidote are common replacement minerals.

Clay-mineral cement. – Authigenic illite and chlorite as grain-coating and pore-filling cement (Fig. 11A and B) are abundant in the studied sandstones. They are next in abundance after the quartz cement. In some quartz sandstones, illite occupies most of the intergranular space and shows recrystallization in coarser crystals. It usually protrudes into the detrital quartz grains and forms an intergrowth with the margin of the grains (Fig. 11C). It seems that there have been at least two stages of generation of clay cement. The first stage includes the grain-coating cement. Together with the illite–hematite coat it is the earliest type of cement in the studied sandstones. The second stage is the formation of pore-filling clay cement, which may postdate and/or be contemporaneous with the precipitation of quartz cement.

In the southwestern part of the area, thrusting has resulted in recrystallization of the authigenic illite coat. The illite has grown as lath-like crystals perpendicular or obliquely to the grain wall, in a way interlocking with adjacent grains (Fig. 11D).

Hematite and titanium-mineral cement. – Hematite as coating around detrital particles and, mostly, as pore-filling, is a common cementing material in the red-coloured sandstones studied. The coat may appear in the form of dense masses of fine hematite crystals or as dispersed crystals within the illite coat (Fig. 12A). Fine-crystalline hematite is also found within the interstitial illite and chlorite. Most of the iron comes from the alteration of iron-bearing minerals, e.g. ilmenite, magnetite and biotite. Hydrothermal fluids, however, were another source in the rocks affected by the hydrothermal activity.

Titanium minerals such as rutile and sphene are another common cementing material in many sandstones (see also Gorbatschev 1962a, Prozorovich 1970, Morad 1983). In the sandstones investigated, titanium minerals occur as pore-filling lumps of leucoxene and sphene or as single crystals (Fig. 12C and D). They are usually embedded in the quartz overgrowth or in interstitial illite and chlorite. They may also protrude into detrital grains of quartz and feldspars. Although not common, overgrowth of sphene around detrital grains of sphene is observed (Fig. 12B).

Calcite and epidote cement. – Calcite is a late cementing material in the rocks studied. Although it may occur scattered in most of the sandstones studied, it is mainly found in some lithic sandstones

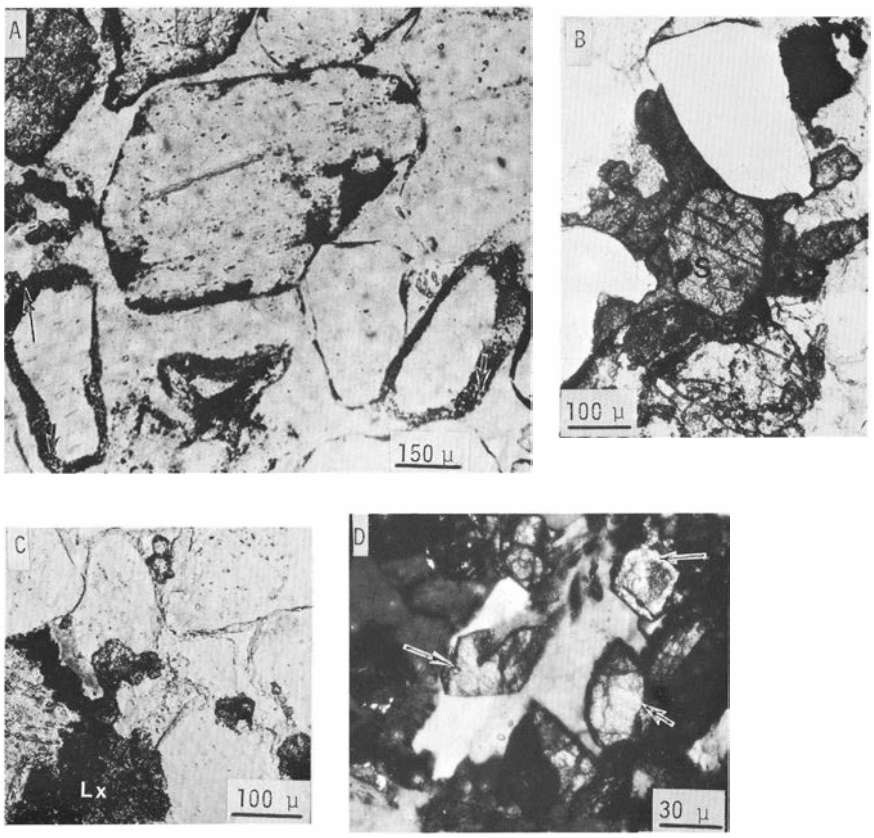

Fig. 12. A – Hematite coat (arrows) occurring as dense mass or mixed with fine illite. B – Overgrowth of sphene on detrital sphene (S). C – Lumps of leucoxene (Lx). D – Single crystals of rutile (arrows).

and in sandstones close to dolerites and basalts. In these sandstones calcite is usually associated with epidote. It appears as anhedral grains showing rhombohedral cleavage and sometimes twinning. Calcite is also found as fracture fillings where rhombohedral crystals of up to 1 cm in size are observed. The calcite cement may form a continuous framework where the detrital grains appear as floating particles (Fig. 7C). Partial or complete dissolution and replacement of the detrital grains have occurred. The replacement of quartz by calcite has been observed in many sandstones (e.g. Füchtbauer 1974, Pettijohn 1975, Blatt et al. 1980). Quartz starts to be effectively soluble at a pH above 9 (Krauskopf 1979) and at such a pH calcite precipitates. The rapid increase in the solubility of silica at a pH above 9 is attributed to the ionization of monosilicic acid as illustrated in the equations below (Wilding et al. 1977):

$$SiO_2 + 2H_2O \rightarrow H_4SiO_4$$

$$H_4SiO_4 + OH^- \rightarrow H_3SiO_4^- + H_2O.$$

Temperature is another factor that can facilitate the quartz-calcite replacement and, as with most minerals, the solubility of quartz increases linearly with increasing temperature (Lindström 1968). In contrast, at constant pressure, the solubility of calcite decreases with increasing temperature (temperatures up to that of diagenetic environment, $\leqslant$ 200°C). The replacement reaction of quartz by calcite may be expressed as follows:

$$SiO_2 + Ca^{2+} + HCO_3^- + 2OH^- \rightarrow CaCO_3 + +H_3SiO_4^-.$$

The soluble silica produced from the above reaction may have been transported and precipitated as quartz cement in other parts of the rocks, as mentioned earlier.

The calcite cement replaces not only quartz but also the feldspars partially or completely (Fig. 13A and B). The replacement affects both potassium feldspar and plagioclase without any preference. It is generally random and may start by the corrosion

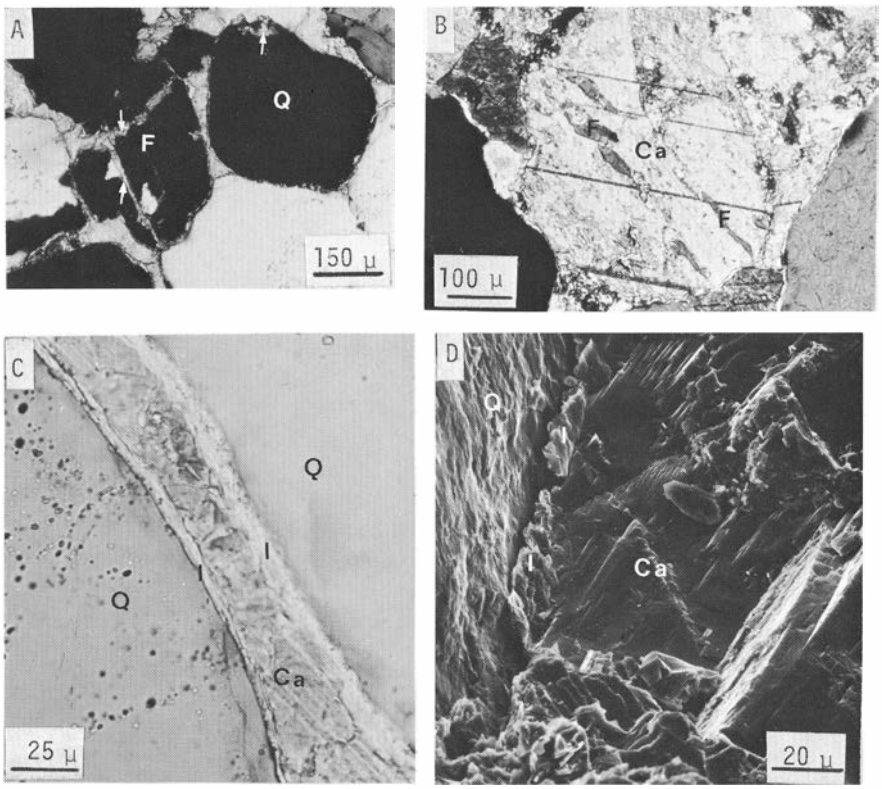

Fig. 13. A – Calcite (arrows) replacing detrital grains of feldspar (F) and quartz (Q). B – Calcite (Ca) replacing feldspar (F), which appears as remnant in the calcite. C – Illite coat (I) on detrital quartz grains (Q); the pore space is filled by calcite (Ca). D – SEM of part of C.

of the grain boundary and continue through the cleavages and fractures.

The presence of illite coats around detrital grains is found to hinder the replacement by calcite (Fig. 13D and C). It is observed that calcite enters detrital grains at points of fractures without a clay coat.

Epidote is another important cement in sandstones affected by hydrothermal activity, mostly near dolerites. It occurs as euhedral crystals or as granular aggregates, filling the pore space or as a coat around the detrital grains (Fig. 14). It is generally associated with authigenic minerals like calcite, titanium minerals, chlorite, illite and very rarely with quartz.

Compaction and porosity

Compaction is the process by which the original sediment loses some of its volume due to increasing overburden (see e.g. Wolf & Chilingarian 1976). Usually the fine-grained sediments (e.g. shales) are more sensitive to this process, because of the flakey nature of their minerals as well as the high amount of adsorbed water. The processes of compaction lead to textural changes in the sediments and they may even continue in the solid rocks. Among these textural changes are the change in porosity, grain shape and grain contact.

The changes are brought about by mechanical

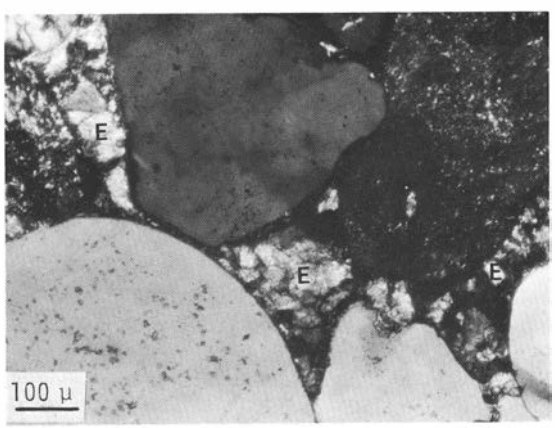

Fig. 14. Epidote (E) as grain-coating and pore-filling cement.

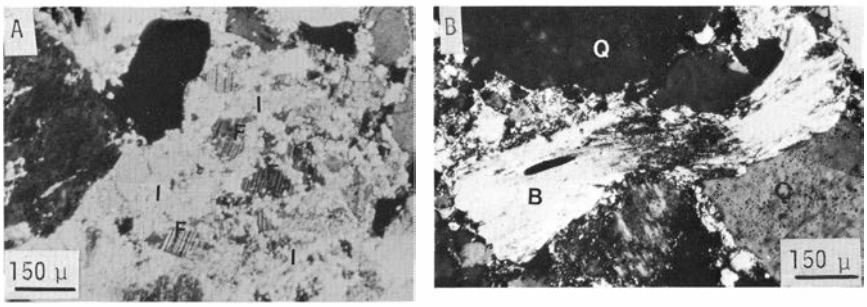

Fig. 15. A – Fragmented feldspar grain (F) within diagenetic illite (I). B – An altered biotite grain (B) bent between quartz grains (Q); the black dots on the biotite are leucoxene and hematite.

effect, which causes either physical changes, e.g. closer packing, crushing, deformation and/or physico-chemical alterations, e.g. dissolution, expulsion of adsorbed water, or biochemical ones, e.g. change in the partial pressure of H_2S.

One common feature which shows the effect of compaction in the studied sandstones is the deformation of the soft particles, the argillites and the altered feldspars. These particles were pushed through the interstitial space, most probably at the early stage of compaction without any appreciable cementation of the pore space. Fragmentation and redistribution of the altered feldspars are also observed (Fig. 15A). The process involves firstly the partial alteration of feldspar, e.g. into illite, and secondly the mechanical redistribution of the fragmented grain with increasing compaction at increasing depth of burial.

Mechanical compaction was an effective process in facilitating alteration of detrital biotites. A biotite grain between harder and non-flakey grains, e.g. quartz or feldspar, will be bent due to compaction (Fig. 15B). The process will then lead to compression and distortion along the cleavage planes in areas of high pressure grain contacts and to openings along the planes at areas of lower pressure. In these areas alteration of biotite into illitic clay and/or chlorite is common.

The shape of the contacts between the grains is considered to reflect the degree of compaction (Taylor 1950, Wolf & Chilingarian 1976). Generally, the concave-convex and the sutured contacts are late in the history of compaction compared to the straight and tangential ones. This phenomenon can easily be traced in those sandstones with low amounts of interstitial cement; best are the quartz sandstones. In these rocks, the concave–convex and sutured grain contacts are the most common types, which means high compaction effect. The effect of high compaction, under relatively deep burial conditions, may be better illustrated by the porosity values of sandstones. The results of 120 measurements of porosity of the sandstones studied show low values of both total and effective porosities. The highest may reach 7 %, but on an average they are below 3 %. Sandstones having such low values of porosity are known to have been buried at a minimum depth of 5,000 m (Maxwell 1964, Teodorovich & Chernow 1968). The decrease of porosity with depth is seldom linear and most of the results show non-linear relationship (e.g. Blatt et al. 1980). This fact may be related to complexity of the diagenetic processes during increasing burial and at different depth intervals. However, the data on porosity–depth relationships, at low porosity values as those of the present work, are scattered and not easily elucidated.

Two important textural factors, the grain parameters, e.g. size, shape and sorting, and the cementation, control the porosity of sandstones. The first factor is disregarded here, because the detrital grains in the studied sandstones are mostly altered by either compaction, replacement or overgrowth. This precluded establishing reliable measurements of grain parameters. To state the cement–porosity relationship was an easier task; it is shown in Figures 16A, B and C, and shows a noticeable negative correlation between the two parameters.

Mineralogy and textures of the diagenetic minerals

Apart from diagenetic quartz and calcite, which were thoroughly considered earlier in the text, the mineralogy and texture of the other diagenetic minerals are considered in this part. The minerals discussed are titanium and clay minerals as well as feldspars.

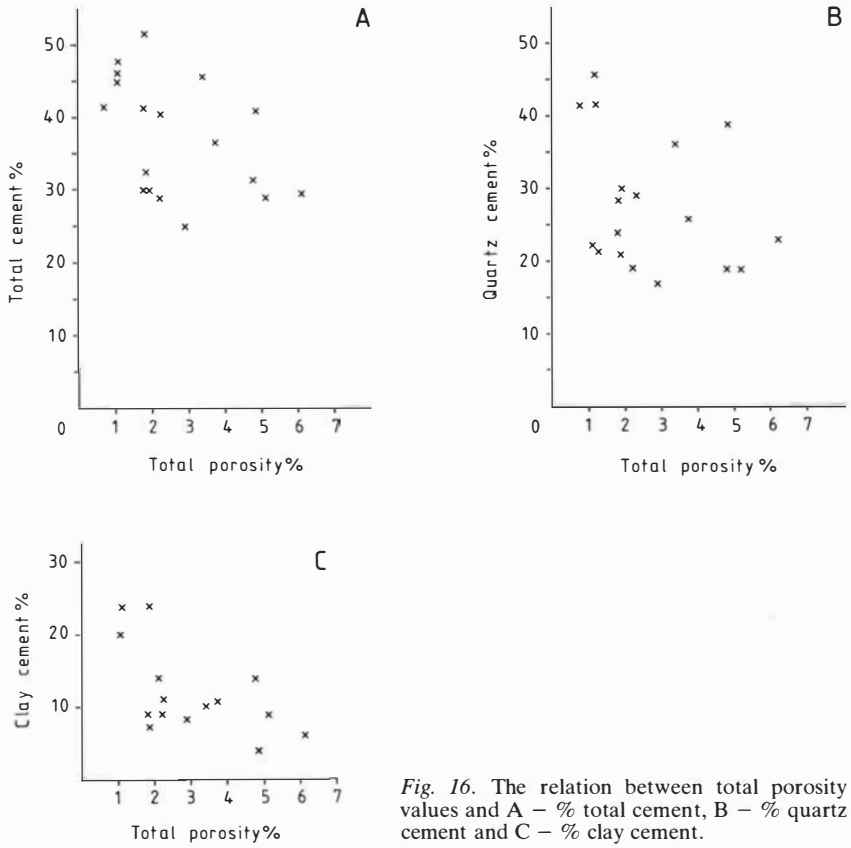

Fig. 16. The relation between total porosity values and A – % total cement, B – % quartz cement and C – % clay cement.

Titanium minerals

Authigenic titanium minerals, anatase, rutile and sphene, are found in all the rocks examined. They occur as single crystals or crystal aggregates in the form of interstitial cement or replacing detrital grains or, occasionally, as overgrowth on detrital sphene (Figs. 12B, C and D). The microscopic differentiation between titanium minerals is somewhat problematic when they occur as fine-crystalline aggregates. In such cases the term leucoxene is used, as adopted earlier by several authors (e.g. Shvestova 1975, Bates & Jackson 1980). In thin section, sphene appears as brown to almost colourless crystals with faint pleochroism, pale-brown to colourless. Large crystals show relatively small axial angle and high relief. Rutile and anatase display similar optical properties; prismatic habit and twinning are characteristics of rutile. Anatase has an acute bipyramidal or prismatic habit with uniaxial interference figure. The most dominant of the three titanium minerals is rutile followed by sphene. Anatase is not as common as the other two minerals. The transformation of anatase to rutile at increasing depth and temperature (Schulling & Vink 1967) may be the reason for its scarceness.

The microprobe analyses of authigenic rutile and anatase (Table 17) in their different textural forms showed that, in addition to Ti, they also contain Al, Fe, Si and Ca in variable percentages. Although not common, some analyses report the presence of Ca, Si and Al in rutile and anatase (e.g. Deer et al. 1962, Putnis & Wilson 1978). The presence of these elements in the rutile and anatase investigated is mostly related to microimpurities of sphene or other titanium minerals of intermediate composition.

The occurrence of more than one titanium mineral is much more pronounced in the leucoxene (Table 17). Iron is known to replace titanium in TiO_2, through either intergrowth of ilmenite or balance of a charge difference due to the substitution of Ti^{4+} by higher charged ions (e.g. Nb^{5+}, Ta^{5+}; Deer et al. 1962).

The average composition of authigenic sphene (Table 17) in three samples also indicates the presence of Al, Fe and Mg. Substitution of Ti by these

Table 17. Microprobe analyses of titanium minerals.

	Sphene			Anatase	Rutile	Leucoxene	
	1	2	3			1	2
SiO_2	30.65	30.25	30.91	0.22	0.27	0.31	0.47
Al_2O_3	2.26	3.21	2.81	1.05	0.95	1.83	1.92
FeO*	0.93	1.20	1.12	0.26	0.47	4.32	4.82
TiO_2	34.32	32.34	33.34	96.27	95.80	90.37	90.37
MgO	0.05	0.08	0.10	0.00	0.00	0.00	0.00
CaO	30.39	30.20	29.54	0.38	0.29	0.49	0.43
Total	98.60	97.28	97.82	98.18	97.78	97.32	98.01
	In altered biotite	In altered feldspar	With interstial illite	With interstitial chlorite	In altered feldspar	Crystal lumps within chlorite–illite cement	

* FeO represents total iron.

elements and Ca by, e.g., Sr, Ba and Na, was suggested (see e.g. Deer et al. 1962, Higgins & Ribbe 1976) to sustain charge balance. However, the substitutions $(Al,Fe)^{3+} + (F,OH)^{-} \leftrightarrows Ti^{4+} + O^{2-}$ were considered the most important (Higgins & Ribbe 1976); they may occur in the sphene studied.

Source of titanium. – Apart from hydrothermal activity, which will be discussed later, the diagenetic alteration of ilmenite and biotite is the most important source of titanium for the diagenetic titanium minerals. In the studied sandstones, the detrital grains of ilmenite were found to be partially or completely altered into titanium oxides. The alteration product is mainly leucoxene and rarely coarse crystals of rutile or anatase (Figs. 17A, C and D). The ilmenite grains sometimes keep their detrital form and locally their composition. In such grains the outer part has been altered into TiO_2 crystallites, projecting from the grain (Figs. 17E and F). The alteration of ilmenite into anatase and/or rutile has been concluded to take place through intermediate phases of iron–titanium mixtures (Brammall & Harwood 1923, Bailey et al. 1956, Temple 1966). The process involves subsequent increase in titanium and can simply be represented as

$$FeTiO_3 + 2H^+ \rightarrow TiO_2 + Fe^{2+} + H_2O.$$

The iron may be further oxidized to contribute in the formation of hematite or used as Fe^{2+} in the formation of interstitial chlorite or occasionally pyrite (Morad & AlDahan 1982a). The replacement of ilmenite by clay minerals, calcite and quartz is also observed (Fig. 18A–F).

Biotite is another evident source of titanium for the diagenetic titanium minerals. The mineral, in its altered form, is found to contain TiO_2 (Table 18). This amount of Ti is undoubtedly far below the original amount, i.e. before alteration. Unfortunately, fresh grains of biotite were not encountered in the studied sandstones and thus quantitative figures for the loss of titanium during alteration cannot be given. However, biotite grains, which hold

Table 18. Microprobe analyses of altered detrital biotites from sandstones.

	1	2	3	4	5
SiO	29.4	36.9	28.5	32.4	33.9
Al_2O_3	16.9	26.9	18.5	19.3	18.6
FeO*	31.4	19.5	30.5	22.5	22.7
MgO	3.5	2.3	3.9	4.9	7.5
K_2O	3.5	2.4	2.2	3.8	3.5
TiO_2	0.9	0.6	0.4	0.3	0.1
Total	85.6	88.6	84.0	83.2	86.3

* FeO represents total iron.

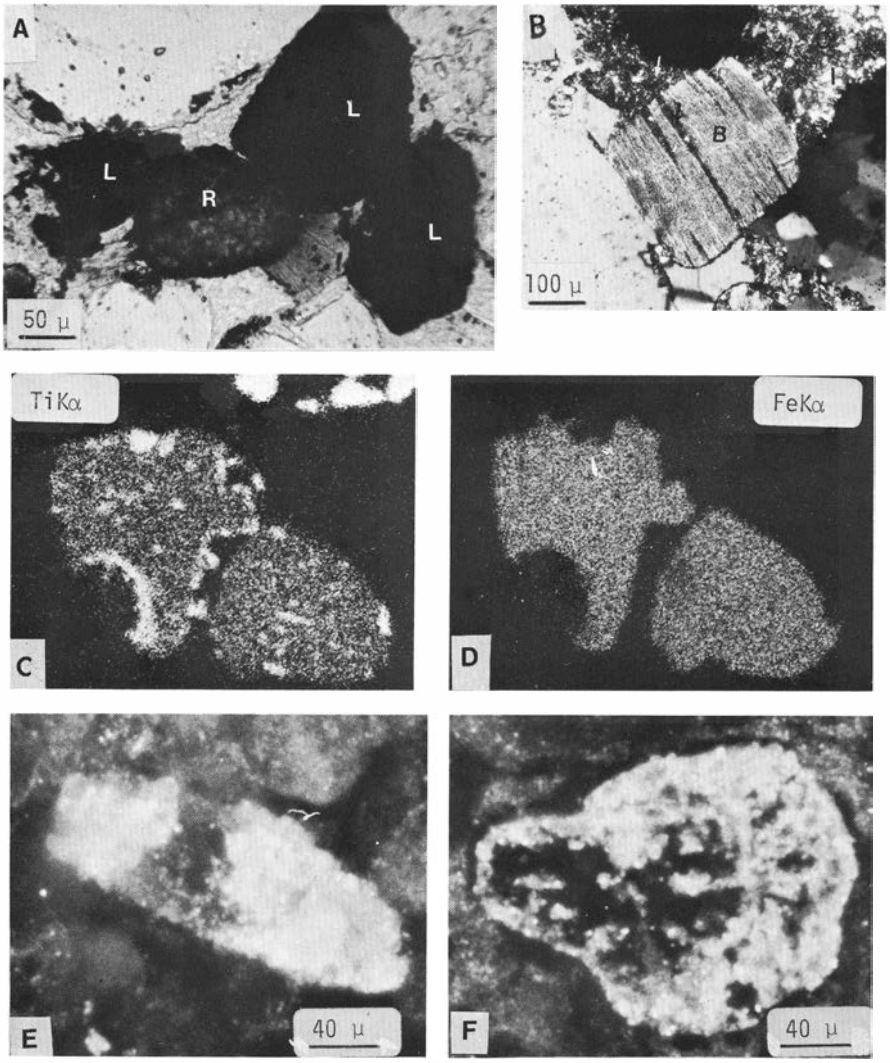

Fig. 17. A – Detrital ilmenites altered into leucoxene (L) and rutile (R). B – A biotite (B) altered into pseudomorphic illite, showing leucoxene (arrows) on the traces of cleavage planes and close to the grain; the surrounding is interstitial illite (I) and chlorite (C). C–D – A microprobe photo of Ti and Fe distribution of ilmenites randomly altered into TiO_2 polymorph (leucoxene). E–F – Ilmenites (grey and black tint) altered into crystals of rutile and leucoxene (white tint); reflected light.

different percentages of TiO_2 (Table 18), could be in different stages of alteration. Usually the most altered ones show the lowest titanium content.

Leucoxene and/or sphene are common alteration minerals along the cleavage planes of biotite and in its immediate surroundings (Fig. 17B). The process of formation of these minerals begins with dissolution and leaching. In general, and referring to no specific domain of condition, oxidizing environment may facilitate the release of titanium from the biotite (Gilkes et al. 1972, Gilkes & Suddhiprakarn 1979). The process is not well understood, but it may involve first the oxidation of the octahedral iron, $Fe^{2+} \rightarrow Fe^{3+}$, causing excess charge in that site. The charge balance may then be equated by the release of some titanium, mainly as $Ti(OH)_4$, crystallizing after dehydration as TiO_2 (Sherman 1952, Loughnan 1962, 1969). Further discussion about the alteration of biotite is presented later in the text.

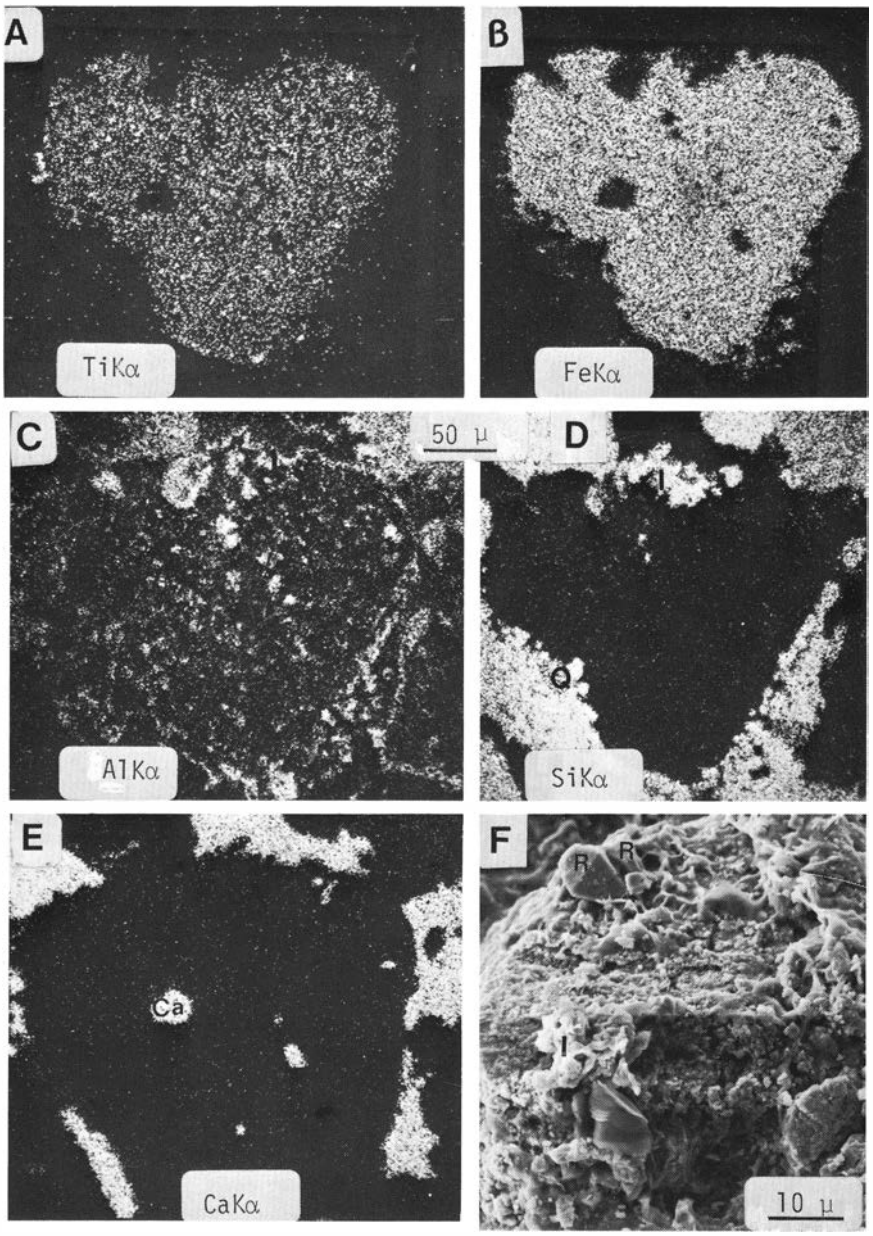

Fig. 18. A–E – Microprobe photo of partially altered ilmenite which is also replaced by calcite (Ca), quartz (Q) and illite (I). F – SEM of ilmenite altered into fine-crystalline leucoxene; the grain has also been replaced by illite (I) along its boundary. Rutile crystals (R) are shown projecting from the ilmenite surface.

Clay minerals

Illite and chlorite are the most common clay minerals in the studied sandstones. Kaolinite and mixed-layer clay minerals are, however, also found in the sandstones that are affected by hydrothermal activity. All these clay minerals have, in most cases, clear and distinctive X-ray diffraction patterns as well as microscopic properties.

The problem of differentiating diagenetic clay minerals from detrital ones was, and still is, of general interest. Many authors have discussed this problem, e.g., Sarkisyan (1971), Galloway (1974),

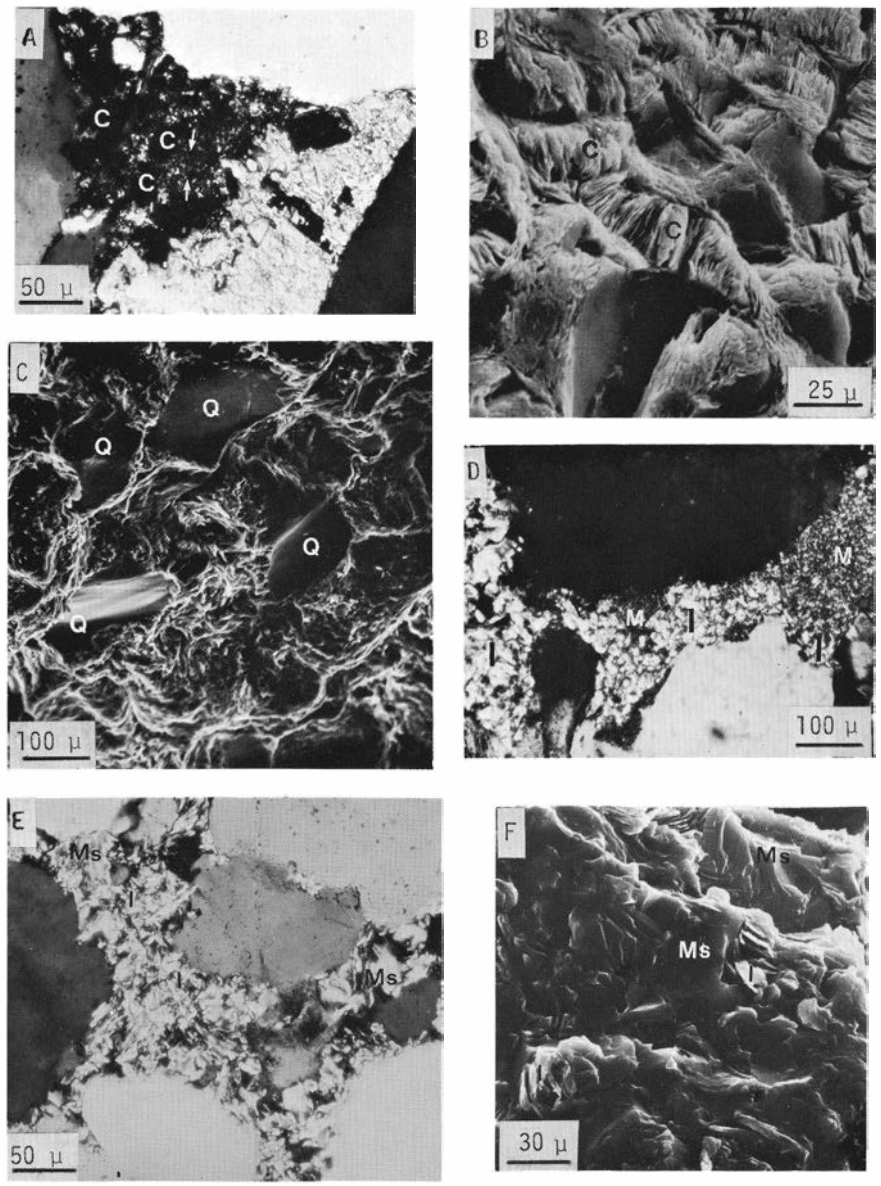

Fig. 19. A – Pore-filling chlorite (C) aggraded from fine chlorite and illite (arrows). B – Pore-filling and grain-coating chlorite (C) intergrown with each other due to high compaction. C – SEM of pore-filling illite, in most of the field, corroding detrital quartz (Q). D – Coarse illite flakes (I) aggraded from illite-chlorite matrix (M). E – Illite flakes (I) aggraded into muscovite (Ms). F – As in E (SEM).

Bjørlykke (1980) and Morad (1983). Wilson & Pittman (1977) presented many criteria which can help in differentiating between authigenic and clastic clay minerals. Among those, the following are considered the most reliable: a) delicacy of clay morphology, b) occurrence of clay as pore linings, absent only at grain contacts, c) composition radically different from that of associated allogenic clays. These and other criteria were used in establishing the diagenetic mode of the studied clay minerals.

The clay mineral suite in the sandstones studied can simply be divided into two groups. The first

includes those diagenetic minerals, which texturally are space fillings. They are inter- and intragranular fillings including pore fillings, grain coatings and fracture and vug fillings. Their mode of formation is crystallization from pore solution (authigenesis) and/or reaction of pore solution with interstitial authigenic and allogenic clay minerals (regeneration). The second group of clay minerals includes those formed by decomposition of unstable detrital minerals (e.g. feldspars and biotite). The processes involved in the production of clay minerals from detrital minerals are leaching, dissolution and replacement.

Pore-filling clay minerals. – Illite and chlorite are the important clay minerals in the pore space of the sandstones investigated. They usually fill the pore space without any particular orientation in relation to the detrital particles. Chlorite may occur as fine crystals, about 10 μm in size, and in some cases associated with illite (Fig. 19A). It is pale green or pale brown, when mixed with hematite, with fair relief, low birefringence and green-blue to greyish interference colour. Pore-filling chlorite is an abundant cementing material in the green-coloured and highly altered greywackes and feldspathic sandstones. It is more abundant in the coarser-grained than in the finer ones. The chlorite cement, in its different textural forms, is commonly found in those sandstones with relatively high content of altered biotite.

Pore-filling chlorite may also occur as coarse flakes, 10–30 μm in size, mostly aggraded from the fine-crystalline chlorite and illite (Fig. 19A). Due to high compaction of the sandstones, the flakey pore-lining clay minerals, chlorite and illite, are mechanically brought together to fill the pore space (Fig. 19B).

Pore-filling illite is an abundant mineral in all the types of sandstone studied, except for some of the green greywackes. The mineral is fine-crystalline (about 10 μm in size), colourless to pale-green or yellow, non-pleochroic and has low relief. The interference colours are yellow to orange of second order, as also are those of muscovite in the coarser flakes (about 50 μm). Illite is found to fill the pore space extensively and to corrode detrital quartz in some quartz sandstones (Fig. 19C).

The crystal form and the growth behaviour of individual crystals of illite and chlorite and other authigenic minerals (e.g. quartz) are good arguments for their authigenic origin. The crystallization of these clay minerals presumably took place from solutions rich in K^+, Si^{4+}, Al^{3+}, (Fe^{2+}, Fe^{3+}) and Mg^{2+}. The ratios of the ions (e.g. $[K^+]/[H^+]$, $[Fe^{2+}+Mg^{2+}]/[H^+]$) control the crystallization paths (Millot 1970, La Iglesia & van Oosterwyck-Gastuche 1978). Chlorite crystallizes at high $[Fe^{2+}+Mg^{2+}]/[H^+]$ ratio and illite at high $[K^+]/[H^+]$ ratio. The cations needed for the crystallization process are mostly derived from the decomposition of detrital feldspars and biotite and partly from the circulating meteoric water.

Pore-filling illite and chlorite were also observed as coarse flakes (up to 50 μm), which formed by crystallization from solution and/or regeneration from fine-crystalline illite and chlorite matrix (Fig. 19D). In some samples the illite flakes are aggraded into muscovite (Figs. 19E and F), as also evidenced by their chemical composition. Compared to the illite, the muscovite contains more potassium and aluminium and shows higher interference colours.

Kaolinite as pore-filling cement is rare and, if present, is usually associated with illite or mixed-layer illitic clay. It occurs as colourless flakes, about 10–20 μm in size with low relief and grey interference colour. It is often found, as mentioned above, at places affected by hydrothermal activity and is assumed to be formed from hydrothermal fluids.

Grain-coating clay minerals. – Authigenic clay minerals occurring as coats around detrital grains have been reported in many sandstones (Hayes 1970, Wilson & Pittman 1977, Morad 1983). Illite is the most common coat-forming clay mineral in the sandstones studied. It occurs in three different textures: as single layer of platelet crystals arranged parallel to the grain surface (Fig. 20A), as flakey crystals arranged perpendicular or obliquely to it (Fig. 20B) or as lath-like crystals occurring both parallel and obliquely to the grain surface (Fig. 11D). The latter type is found in the quartz and lithic sandstones which have been affected by thrusting in the southwestern part of the area (Fig. 1). It is presumably a product of recrystallization of earlier illitic coat.

The chlorite coat (Fig. 20C) is common in the greywackes and some feldspathic sandstones below and above the Öje Basalt. It is often encountered as a multilayer coat, best observed by the SEM examination (Fig. 20D). Both chlorite and illite coats are observed to corrode detrital grains (Fig. 20C). They may also project through the later pore-filling cement and form a sort of intergrowth (Figs. 11A and 20D). This manner of growth as well as the delicacy of the crystals preclude possibility of detrital origin.

The grain-coating cement is the earliest cement in the sandstones studied. It envelops all types of detrital grains and is usually missing at points of contact. As in the pore-filling clay minerals, the cations

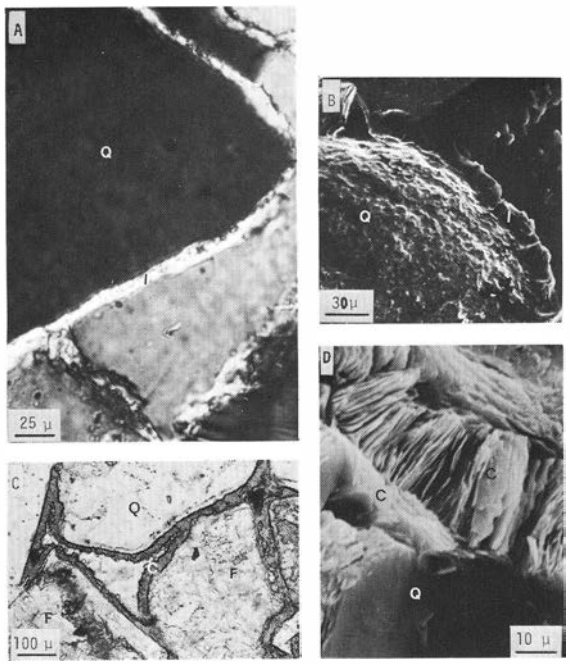

Fig. 20. A – Illite (I) as grain-coat platelets parallel to the grain wall of quartz (Q). B – Illite coat (I) occurring perpendicular to the grain wall of quartz (Q) (SEM). C – Chlorite coat (C) on detrital quartz (Q) and feldspar (F). D – Multilayer coat of chlorite flakes (C) on detrital quartz (Q) (SEM).

needed were derived mainly from the alteration of biotite and feldspars at the early stage of diagenesis.

Fracture- and vug-filling clay minerals. – Although not common, illite and chlorite are observed as fillings in the fractures of detrital grains of quartz and feldspar (Fig. 21A). These clay minerals are usually similar to the associated pore-filling variety both microscopically and chemically. This observation adds another positive argument for their authigenic origin. They are presumably late in the diagenetic history, at deep burial, where the increased compaction has initiated fracturing in some of the detrital grains. Illite and chlorite may occasionally fill fractures and vugs in the rocks (Fig. 21 B). Most commonly they are encountered in areas close to dolerite intrusions.

Clay minerals as alteration products of feldspars. – These minerals, especially potassium feldspar, have been shown to alter into clay minerals during diagenesis (e.g. Walker et al. 1978, Foscolos et al. 1982, Hurst & Irwin 1982). In the sandstones investigated, the alteration of feldspar has resulted in the formation of illite and chlorite. The illite, as fine flakes, 10–20 µm long, is the dominant alteration product of potassium feldspars (Figs. 22 A and C). The alteration may be partial or extend into the whole grain.

Chlorite, as flakes of 20–30 µm in size or occasionally finer, is observed either as the only alteration product of feldspars or in many feldspar grains associated with illite (Fig. 22 B). It is abundant in those greywackes and feldspathic sandstones in which the grain-coat is also chlorite. The Fe and Mg needed for the formation of chlorite were mainly derived from decomposition of the associated detrital biotite.

Among the many criteria supporting in situ alteration of feldspars, the following could be mentioned:

1) The clay minerals are not bound to the cleavage and composition planes (selective alteration) as they commonly are in weathered feldspars (e.g. Berner & Holdren 1979).

2) Feldspars which have their edges converted into clay minerals are presumably diagenetically altered because the softness and delicacy of these

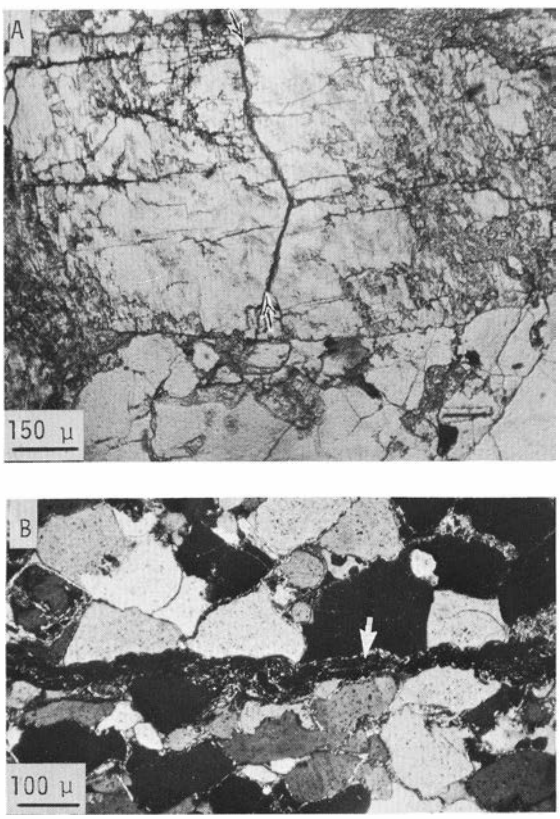

Fig. 21. A – Illite (arrow) as fracture filling in feldspar grain. B – Chlorite and illite as vug filling (arrow).

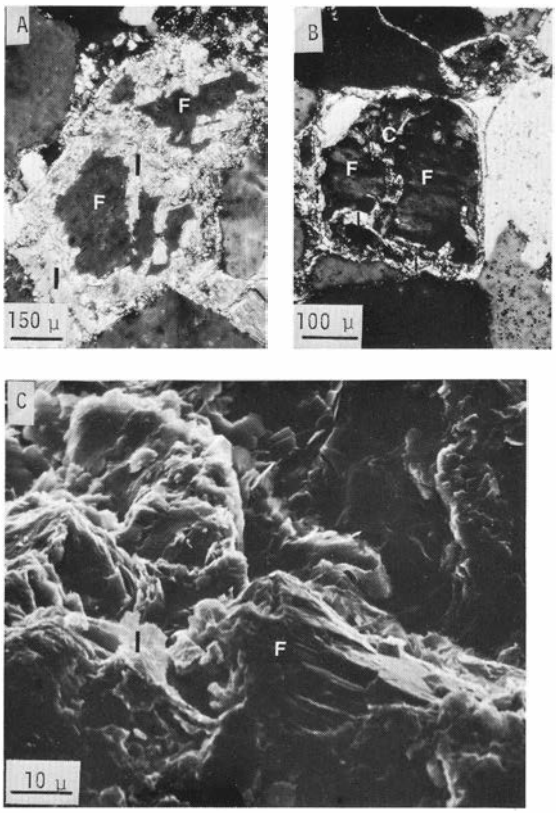

Fig. 22. A – Feldspar (F) altered into illite (I). B – Feldspar (F) altered into illite (I) and chlorite (C). C – SEM of part of A.

clay minerals preclude extended transport. Experimental work of Berner & Holdren (1979) also confirms such observations. They found that the clay-mineral coat formed as a result of feldspar weathering easily can be removed even by simple washing of the samples.

3) The clay minerals as alteration products of feldspar and as cement show the same mineralogy which indicates similar environment of formation, i.e. diagenetic environment. If, however, alteration has occurred by weathering, the feldspars are expected to show different alteration as they have been subjected to different environmental conditions in the source area and during transportation.

4) Diagenetically altered feldspars show clay minerals of uniform crystal size and rarely contaminated with iron oxides or "dirt" as is the case in weathered ones.

The literature on the degree and type of alteration of different types of feldspars gives no specific trend. In some cases potassium feldspar is observed preferentially altered compared to plagioclase; the reverse is also reported (e.g. Wilson & Pittman 1977, Walker et al. 1978, Almon 1981, Morad & AlDahan 1982b). In the investigated rocks, however, alteration is intensive in both plagioclase and potassium feldspar.

The processes and products of alteration of feldspars in the diagenetic zone depend on many factors including the chemistry of the pore solution, the degree of fluid circulation, pH–Eh conditions, temperature and pressure, and composition and grain size of the feldspars. Kaolinite is expected as a common alteration product of feldspars at high leaching conditions, i.e. high permeability, low cation concentration and low pH (<7):

$$\underset{\text{Na-}}{\text{K-}}\text{feldspar} + H_2O \rightarrow \text{kaolinite} + K^+ + Na^+ + H_4SiO_4.$$

At high $[K^+]/[H^+]$ ratio, illite is expected to form (e.g. Garrels & Christ 1965, Helgeson et al. 1969):

$$\underset{\text{Na-}}{\text{K-}}\text{feldspar} + H_2O \rightarrow \text{illite} + K^+ + Na^+ + H_4SiO_4.$$

The amount of K^+ ions produced in this reaction is obviously less than that in the previous one. However, in both reactions the produced K^+ may be consumed in the formation of authigenic illite in pore spaces.

Intermediate phase(s), illite–expandable clay, e.g. illite–montmorillonite, may form during the diagenetic alteration of feldspars (e.g. Walker et al. 1978), but such phases, however, were not encountered in the studied rocks. This may be due to the high grade of diagenesis which has resulted in the elimination of the unstable clay minerals (e.g. mixed-layer clay minerals and kaolinite).

The alteration of feldspars into chlorite has presumably occurred through direct reaction with pore solution rich in iron and magnesium, as

$$\underset{\text{Na-}}{\text{K-}}\text{feldspar} + Fe^{2+} + H_2O \rightarrow \text{chlorite} + Na^+ + \\ + K^+ + H_4SiO_4,$$

or by the chloritization of the illitized feldspars, as

$$\text{illite} + Fe^{2+} + Mg^{2+} + H_2O \rightarrow \text{chlorite} + K^+.$$

The produced K^+ may have contributed in formation of authigenic illite in pore spaces. The excess silica from the above reaction is usually found to crystallize as quartz.

Clay minerals as alteration products of biotite. – The detrital grains of biotite in the investigated sandstones are rarely encountered retaining their

texture or chemical composition. They are altered either partially, into hydrobiotite (Table 18), or completely, into illite and/or chlorite. The following criteria permit establishment of a diagenetic mode of alteration:

1) The presence of remnants of the altered biotite within the clay minerals formed (Fig. 23 A).
2) The crystal habit and composition of clay minerals along cleavage planes of biotite are the same as those of the surrounding clay cement.
3) The occurrence of relict cleavage traces marked, for example, by alignment of the clay or titanium minerals (Fig. 23 B).
4) Mechanically deformed biotite showing clay-mineral alteration in areas of deformation, with open or compressed cleavage planes (Fig. 23 C).

The alteration of biotite during diagenesis contributed a great part of the necessary cations to the formation of authigenic clay. In the rocks studied it was noticed, however, that in relatively oxidized rocks the alteration of biotite is mainly associated with illite and hematite. In reduced rocks, as evidenced by the presence of Fe^{2+}-rich chlorite and occasionally pyrite (see also Morad 1983, AlDahan & Morad 1983), the alteration product of biotite is predominantly chlorite. The reactions of these alterations can roughly be written as follows:

$$\text{Biotite} + H_2O \xrightarrow{\text{oxidation}} \text{illite} + K^+ + Fe^{3+} +$$

$$+Mg^{2+} + Ti^{4+},$$

$$\text{biotite} + H_2O \xrightarrow{\text{reduction}} \text{chlorite} + K^+ + Ti^{4+}.$$

Microprobe analyses of chlorites (Table 19) derived from alteration of biotite, show high contents of iron and presence of potassium. A relatively high content of iron is also observed in illites (Table 19). The mechanism of alteration of biotite into clay minerals involves opening of the interlayers associ-

Table 19. Microprobe analyses of illite (1–3) and chlorite (4–5) derived from the alteration of detrital biotites.

	1	2	3	4	5
SiO_2	44.3	43.9	44.5	25.4	26.9
Al_2O_3	22.0	25.5	33.5	17.7	18.7
FeO*	12.5	12.1	2.9	36.1	32.9
MgO	0.6	3.9	1.1	6.2	6.0
K_2O	6.7	3.6	4.2	0.5	1.2
TiO_2	0.2	0.6	0.3	0.1	0.1
Total	86.3	89.6	86.5	86.0	85.8

* FeO represents total iron.

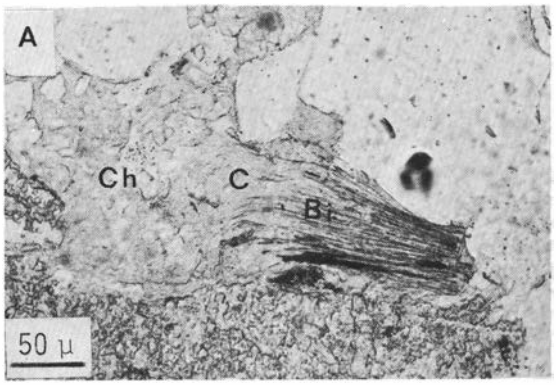

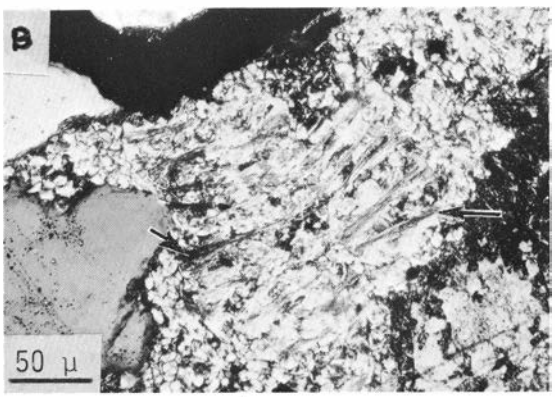

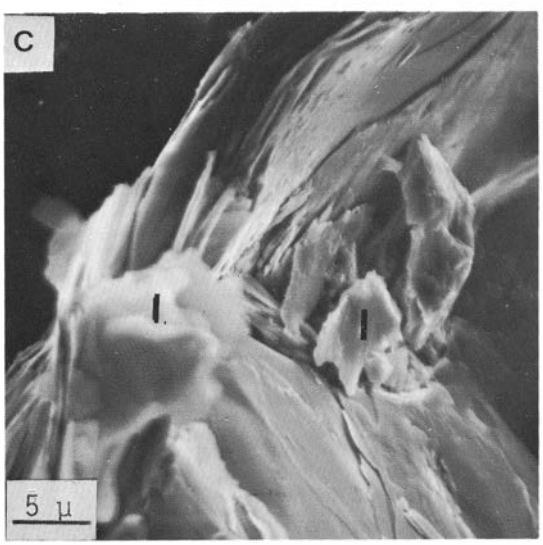

Fig. 23. A – A biotite (Bi) partially altered into chlorite (C) which merges into the surrounding pore-filling chlorite (Ch). B – A biotite completely altered into fine illite; the arrows show the relics of the biotite grain. C – SEM of mechanically deformed biotite showing illite flakes (I) at areas of deformation.

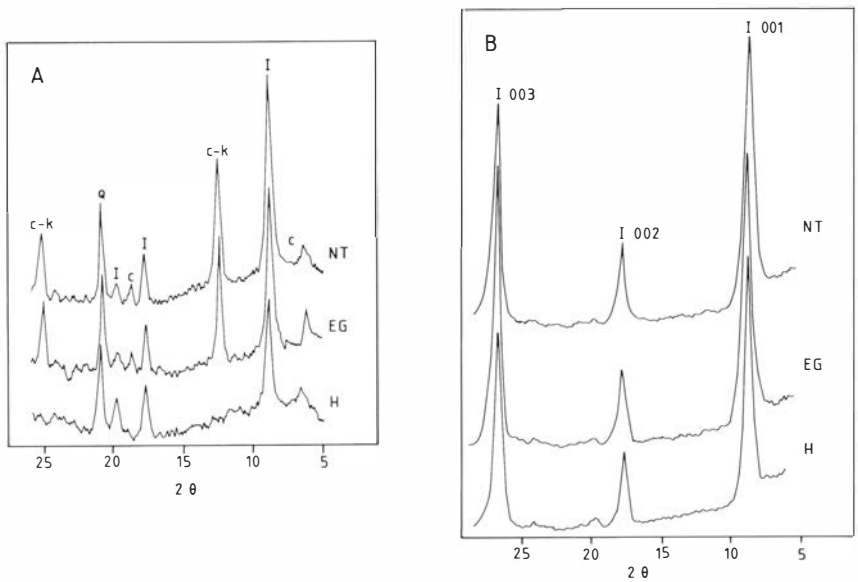

Fig. 24. X-ray diffraction patterns of diagenetic clay minerals. I = illite, c = chlorite, k = kaolinite, and Q = quartz. NT = non-treated, EG = ethylene-glycol treated, and H = heated to 550°C.

ated with release of K^+ and a probable subsequent expulsion of some octahedral cations (Fanning & Keramidas 1977). The processes may also involve a change in the valency of iron ($Fe^{2+} \rightarrow Fe^{3+}$), which is not yet well understood (see Gilkes et al. 1972, Norrish 1973). The concentration of K^+ in the solution plays a role in the alteration process when it is combined with the leaching potential of the environment (Fanning & Keramidas 1977). Lower K^+ concentration, for example, facilitates the decomposition of biotite while the degree of leaching significantly controls the alteration products, e.g. illite or kaolinite. However, as will be discussed later, the high grade of diagenesis of the investigated rocks may have caused the transformation of kaolinite into illite.

Crystal-chemical properties of diagenetic clay minerals

X-ray diffraction patterns. – As mentioned before, the diffraction peaks of the diagenetic clay minerals were in most cases separable and characteristic of the mineral in question. In some samples, however, the identification of the mixed-layer phases was somewhat problematic. They occur in small amounts and their peaks are masked by the more intensive ones. The occurrence of only one textural form of clay minerals (pore-filling, coating or alteration products) in one sample is uncommon. Hence the discussion hereafter deals with the different minerals apart from their textures.

The chlorite is characterized by a major peak at 7 Å and occasionally at 14 Å (Fig. 24 A). The whole spectrum, however, matches both the Fe–Mg chlorite (Shirozu 1969) and the chamosite (Brindley 1951, 1961). Upon heating, all the peaks disappeared except the basal 14 Å reflection, which was not affected and even, in some samples, intensified (Fig. 24 A). The ethylene-glycol (EG) treatment did not show any significant changes in the intensity of the peaks. The characteristic higher intensity of the even peaks relative to the odd ones of the investigated chlorite indicates that they have high iron contents (Brindley 1961). The sharpness of the 002 and 004 peaks may also suggest that the chlorite is well crystallized.

Illite was identified in most of the investigated rocks. The mineral is characterized by its basal reflections at about 10 Å, 5.0 Å and 3.32 Å. Another important reflection noticed is at about 4.48 Å (Fig. 24 B). All the analyzed samples are presumably well crystallized as indicated by the narrow peak width. The peaks were not affected by treatment with EG or by heating. Compared to the illites presented by Hower & Mowatt (1966), the ones investigated here may contain some expandable layers (less than 10 %), which were not detectable upon EG treatment or heating. It is, however, suggested that the occurrence of pure illite (without expandable layers) is not common (Weaver & Pollard 1973). The pronounced reflections at about 4.48 Å and 1.99 Å may suggest the presence of 3T, 1M and 1Md polytypes (see Levinson 1955).

Table 20. Microprobe analyses of authigenic illite. a = flaky in altered feldspar; b = flaky of different origin; c = particle coating; d = interstitial (vermicular); e = interstitial (microcrystalline).

	1[b]	2[b]	3[b]	4[b]	5[c]	6[b]	7[c]	8[b]	9[b]	10[b]	11[b]
SiO_2	51.55	50.22	45.35	45.57	44.73	44.14	43.70	46.73	46.30	47.16	50.17
Al_2O_3	24.29	26.10	31.40	29.63	29.96	23.62	30.11	29.87	22.59	25.01	23.82
FeO*	4.25	5.56	1.30	2.97	1.91	3.40	12.28	2.41	3.28	9.73	5.41
MgO	1.24	1.34	0.64	0.94	0.58	0.69	2.62	0.78	0.95	2.55	1.66
K_2O	8.88	8.57	10.98	10.88	6.93	9.95	8.67	11.17	11.22	8.83	9.40
TiO_2	0.03	0.17	0.17	0.09	0.17	0.55	0.13	0.05	0.20	0.02	0.02
MnO	0.04	0.07	0.03	0.04	0.07	0.04	0.38	0.00	0.00	0.00	0.00
Na_2O	0.00	0.00	0.00	0.00	0.00	0.00	0.00	0.00	0.00	0.00	0.00
Total	90.28	92.03	90.21	91.84	84.02	88.73	91.40	91.25	91.82	90.88	91.97
Number of ions based on 22^- charges											
Tet. Si	3.61	3.48	3.20	3.18	3.31	3.21	3.23	3.27	3.25	3.42	3.51
Al	0.39	0.52	0.80	0.82	0.69	0.79	0.77	0.73	0.75	0.58	0.49
Oct. Al	1.61	1.61	1.84	1.77	1.89	1.77	1.29	1.76	1.72	1.35	1.56
Fe	0.25	0.32	0.08	0.17	0.12	0.21	0.76	0.14	0.19	0.59	0.31
Mg	0.13	0.14	0.07	0.10	0.06	0.07	0.29	0.08	0.10	0.28	0.17
Oct. total	1.99	2.07	1.99	2.04	2.07	2.05	2.34	1.98	2.01	2.22	2.04
Int. K	0.79	0.76	0.99	0.97	0.65	0.92	0.82	1.00	1.00	0.82	0.83
Charge balance											
Inter.	0.79	0.76	0.99	0.97	0.65	0.92	0.82	1.00	1.00	0.82	0.83
Oct.	0.39	0.25	0.18	0.15	0.03	0.13	0.03	0.28	0.26	0.21	0.36
Tet.	0.39	0.52	0.80	0.82	0.69	0.79	0.77	0.73	0.75	0.58	0.49

	12[b]	13[e]	14[e]	15[d]	16[d]	17[d]	18[a]	19[a]	20[a]
SiO_2	46.74	45.75	50.86	51.16	52.64	51.37	53.08	44.41	47.05
Al_2O_3	23.82	22.95	25.93	26.33	23.71	24.13	22.89	29.44	23.16
FeO*	9.22	9.72	2.96	3.58	3.03	3.68	3.38	3.27	3.38
MgO	2.54	2.46	2.90	2.82	3.63	3.73	4.28	0.54	3.81
K_2O	9.45	0.13	9.84	9.22	9.88	9.43	9.03	9.93	9.03
TiO_2	0.02	0.02	0.02	0.02	0.00	0.00	0.00	0.00	0.00
MnO	0.00	0.00	0.00	0.00	0.10	0.10	0.00	0.40	0.10
Na_2O	0.00	0.00	0.00	0.00	0.10	0.10	0.00	0.00	0.00
Total	91.79	90.03	92.51	93.13	92.89	92.52	92.66	87.99	86.52
Number of ions based on 22^- charges									
Tet. Si	3.36	3.36	3.48	3.48	3.59	3.53	3.61	3.24	3.47
Al	0.64	0.64	0.52	0.52	0.41	0.47	0.39	0.76	0.53
Oct. Al	1.37	1.35	1.58	1.58	1.49	1.49	1.45	1.77	1.48
Fe	0.55	0.60	0.17	0.20	0.17	0.21	0.19	0.20	0.21
Mg	0.27	0.27	0.30	0.29	0.37	0.38	0.43	0.06	0.42
Oct. total	2.19	2.22	2.05	2.07	2.03	2.08	2.07	2.03	2.11
Int. K	0.87	0.86	0.86	0.80	0.86	0.83	0.78	0.92	0.85
Charge balance									
Inter.	0.87	0.86	0.86	0.80	0.86	0.83	0.78	0.92	0.85
Oct.	0.25	0.21	0.32	0.28	0.45	0.35	0.41	0.17	0.30
Tet.	0.64	0.64	0.52	0.52	0.41	0.47	0.39	0.76	0.53

* FeO represents total iron.

Small changes in the sharpness of the 10 Å peak upon heating as well as relatively broad peaks are observed in illites of sandstones near by dolerites. These observations suggest relatively higher content of expandable layers in these illitic minerals compared to those described above.

Chemical composition. – The microprobe analyses of illite and chlorite (Tables 20 and 22) are a representative selection from about 60 analyses of illite and 40 analyses of chlorite. The calculation of the structural formula is based on 28^- and 22^- charges for chlorite and illite, respectively, following Foster

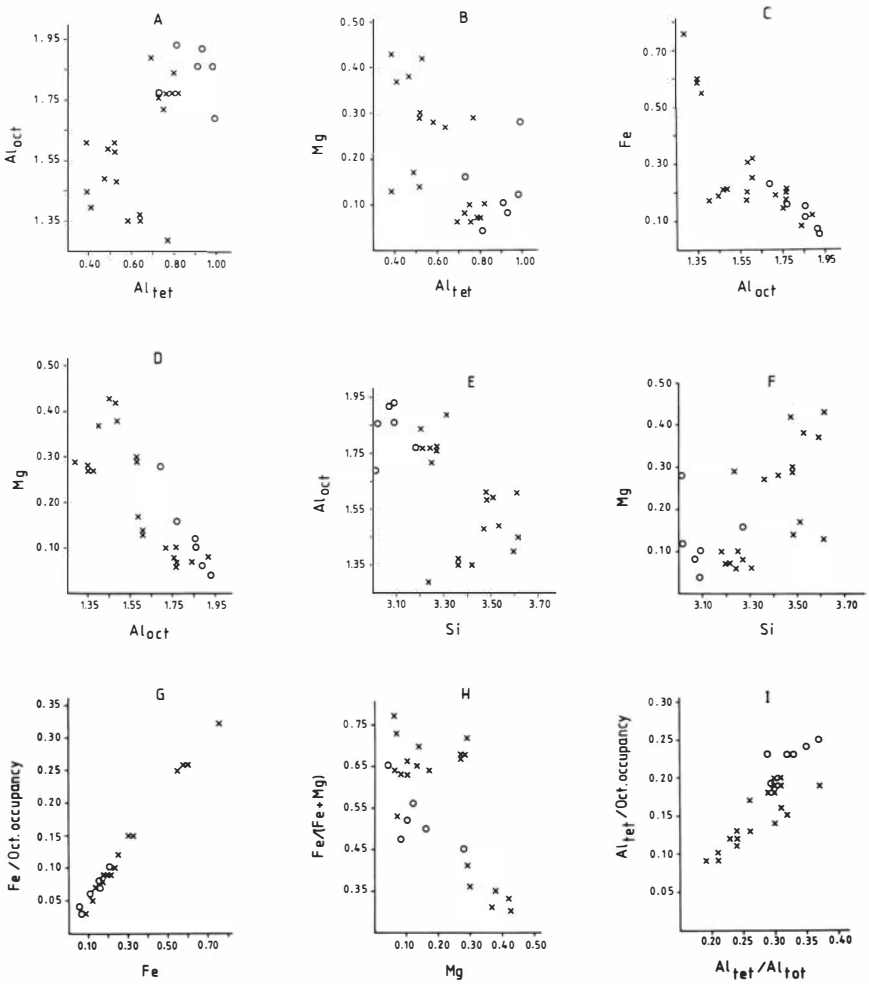

Fig. 25. A–I. The relation between the different cations and cation ratios in illite; x = diagenetic and o = hydrothermal.

(1956, 1962). All Si is referred to the tetrahedral sheet together with additional Al in order to bring the sum up to 4.00. The rest of the Al and all Fe and Mg were assigned to the octahedral sheet. Because of their negligible amounts Ti, Na and Mn were excluded from the structural formulae.

The microprobe analyses of diagenetic illite (Table 20) show no visible correlation between

Table 21. Correlation matrix for cations and cation ratios of illites.

	1	2	3	4	5	6	7	8	9	10
1 Si	0.00									
2 Al_{tet}	−0.99	0.00								
3 Al_{oct}	−0.65	0.63	0.00							
4 Fe	0.21	−0.19	−0.79	0.00						
5 Mg	0.60	−0.58	−0.82	0.38	0.00					
6 K	−0.39	0.40	0.18	−0.15	−0.25	0.00				
7 Fe/(Fe+Mg)	−0.32	0.31	0.14	0.40	−0.65	0.13	0.00			
8 Fe/Oct_{occ}	0.23	−0.22	−0.79	1.00	0.38	−0.15	0.41	0.00		
9 Al_{tet}/Al_{oct}	−0.87	0.89	0.22	0.25	−0.30	0.38	0.38	0.22	0.00	
10 Al_{tet}/Tet_{occ}	−1.00	0.99	0.65	−0.22	−0.60	0.37	0.31	−0.24	0.86	0.00

Table 22. Microprobe analyses of authigenic chlorite. a = pore lining and pore filling; b = interstitial (microcrystalline); c = flaky in altered feldspar.

	1[b]	2[a]	3[a]	4[a]	5[c]	6[c]	7[c]
SiO_2	29.25	21.38	22.32	21.82	24.59	29.89	24.47
Al_2O_3	18.51	22.32	20.84	18.48	17.95	18.18	17.94
FeO*	29.88	31.29	32.59	34.80	38.04	37.24	38.02
MgO	4.15	6.39	5.90	6.41	5.90	5.62	5.58
K_2O	2.19	0.10	0.10	0.10	0.00	0.00	0.00
TiO_2	0.34	0.00	0.00	0.00	0.00	0.00	0.00
MnO	0.46	0.57	0.66	0.76	0.65	0.66	0.66
Na_2O	0.00	0.11	0.10	0.00	0.00	0.00	0.00
Total	84.78	82.16	82.51	82.37	87.13	91.59	86.67
Number of ions based on 28^- charges							
Tet. Si	3.35	2.54	2.66	2.66	2.83	3.18	2.84
Al	0.65	1.46	1.34	1.34	1.17	0.82	1.16
Oct. Al	1.84	1.66	1.59	1.31	1.27	1.47	1.29
Fe	2.86	3.11	3.25	3.54	3.66	3.32	3.68
Mg	0.71	1.13	1.05	1.16	1.01	0.89	0.96
Oct. total	5.41	5.90	5.89	6.01	5.94	5.68	5.93
Charge balance							
Tet.	0.65	1.46	1.34	1.34	1.17	0.82	1.16
Oct.	0.66	1.46	1.37	1.33	1.15	0.83	1.15

* FeO represents total iron.

textural types and composition. They show, however, a range of variation in chemical composition similar to other data on illites (see Weaver & Pollard 1973, Merino & Ransom 1982). In general, the total layer charge is higher than that suggested, −0.75 per formula unit, by Bailey (1980).

The matrix of correlation (Table 21) shows three types of correlation:

1) First expectedly significant correlations, which may include, for example, the relation between $Al_{tet}-Si$, $Fe-Al_{oct}$, $Mg-Al_{oct}$ and $Fe-Al_{oct}$, indicating the common substitutions between these elements to maintain charge balance. As to the correlation between Al_{tet}/Al_{tot} and Al_{tet}, the higher amount of Al replacing Si, the lower is the amount that occupies the octahedral position, also indicated by the $Al_{tet}-Al_{oct}$ correlation.

2) The second type includes significant correlations which are not clearly understandable, for example the cases $Al_{tet}/Tet_{occupancy}-Mg$ and $Mg-Al_{tet}$.

3) In the third group (remaining correlations), the correlations are non-significant and do not permit reliable interpretations. It should be mentioned, however, that despite reporting iron as only Fe^{2+} and the uncertainty in the structural assignment of some elements, e.g. $Fe^{3+}\rightarrow Al_{tet}$, $Fe^{3+}\rightarrow K$, $Mg^{2+}\rightarrow K$, the correlation trends seem to be almost the same as those presented by Weaver & Pollard (1973).

Observable differences between diagenetic and hydrothermal illite are shown in Figures 25 A−I. The hydrothermal illites constantly contain large amounts of aluminium and sodium. It seems that, on the basis of the Al, Fe and Mg contents, the illites in general are separated into two groups (Figs. 25 A, D and H). This may mean that the amount of iron and probably magnesium rather than that of silicon may exert control on the substitution Al→Si in illites. In other words, the lower the Fe content, the higher the substitution of Al for Si. Further discussion on the conditions of formation of illites as reflected by their chemistry will be presented in the section on paragenesis.

The composition of the chlorites (Table 22) is relatively more homogeneous than that of the illites. Although high K_2O contents were observed in the microcrystalline interstitial chlorite, most probably due to presence of illitic impurities, the flakey chlorites show no remarkable variation in composition. However, all the different textural types fit more or less well into the formula of the tri-octahedral Fe-Mg chlorites (chamosite, Fig. 26). Chlorites having chamosite composition are known as authigenic minerals in sedimentary environments (e.g. Velde 1977).

The significant correlations between the octahedral cations, e.g. Fe−Mg, Fe/(Fe+Mg)−Mg (Table 23) reflect the common substitution between these elements. The particularly observable correla-

Table 23. Correlation matrix for cations and cation ratios of chlorites.

	1	2	3	4	5	6	7	8	9
1 Si	0.00								
2 Al_{tet}	−1.00	0.00							
3 Al_{oct}	0.09	−0.05	0.00						
4 Fe	−0.19	0.20	−0.18	0.00					
5 Mg	−0.04	0.01	−0.32	−0.86	0.00				
6 Fe/(Fe+Mg)	−0.01	0.03	0.15	−0.93	−0.98	0.00			
7 Fe/Oct_{occ}	0.10	0.11	−0.09	0.99	−0.91	0.97	0.00		
8 Al_{tet}/Al_{tot}	0.16	−0.13	0.62	−0.42	0.09	−0.17	−0.35	0.00	
9 Al_{tet}/Tet_{occ}	−1.00	1.00	−0.08	0.20	0.03	0.02	0.11	−0.15	0.00

tion between Fe and Mg may indicate the common substitution of $Fe^{2+} \rightarrow Mg^{2+}$ rather than Fe^{3+} in octahedral position. The occurrence of Fe, as mainly Fe^{2+}, in chlorite is also evident from the total chemical analyses of chlorite-rich sandstones. In these rocks the ratio FeO/Fe_2O_3 is found positively correlated with the chlorite content (Fig. 5) (see also Morad 1983).

In some analyses (Table 22) the tetrahedral Al is almost equivalent to the octahedral trivalent cations (in this case only Al; the octahedral sum is then close to 6 atoms per formula unit). The correlation between the amount of tetrahedral Al and the total octahedral occupancy was pointed out by Foster (1962). She interpreted the deviation of the octahedral sum from the theoretical value of six as due to lower occupancy of the octahedral position by an amount equal to one-half the excess of the octahedral trivalent cations, in this case only Al, over tetrahedral Al. This is well demonstrated by samples 1,2,3 and 6 in Table 22.

Figures 27 A–F show the distribution of the cations and cation ratios of the diagenetic and the hydrothermal chlorites. The trend of distribution is very similar for both types of chlorite, indicating almost the same cation relations.

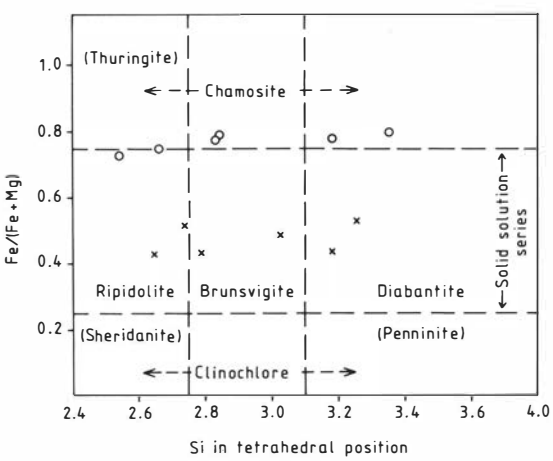

Fig. 26. Classification of chlorites (after Foster 1962 and Bayliss 1975); o = diagenetic and x = hydrothermal.

Authigenic feldspars

Authigenic feldspars are rare in the investigated sandstones. They occur mainly in the feldspathic sandstones of the lower layers of the upper part and in sandstones affected by hydrothermal solutions. Their composition is generally albitic (Table 24); a few crystals show potassic composition. Authigenic albite occurs as single crystals or as overgrowth on cores of detrital albite (Figs. 28 A, B and C). No marked chemical difference is observed between the core and the authigenic part. The authigenic part may grow either in optical and textural continuity with the detrital core with the same twinning habit (Fig. 28 A) or show differing growth habit.

The formation of the authigenic feldspars is presumably very late in the diagenetic history judging from the presence of associated pressure solution in the quartz and common occurrence of quartz overgrowth. In the same rocks the authigenic illite shows high degree of crystallinity.

The crystallization of feldspars is not temperature

Table 24. Microprobe analyses of authigenic albites and their detrital cores.

	Detrital core	Rim	Detrital core	Rim	Detrital core	Rim
SiO_2	66.25	66.00	66.10	66.14	65.84	66.75
Al_2O_3	20.53	19.98	19.52	19.39	19.93	19.88
FeO*	0.00	0.06	0.16	0.38	0.04	0.07
CaO	0.13	0.09	0.09	0.04	0.07	0.06
K_2O	0.03	0.09	0.09	0.10	0.05	0.02
Na_2O	11.50	11.45	11.18	11.45	11.23	11.15
Total	98.44	97.76	97.14	96.50	97.16	97.93

* FeO represents total iron.

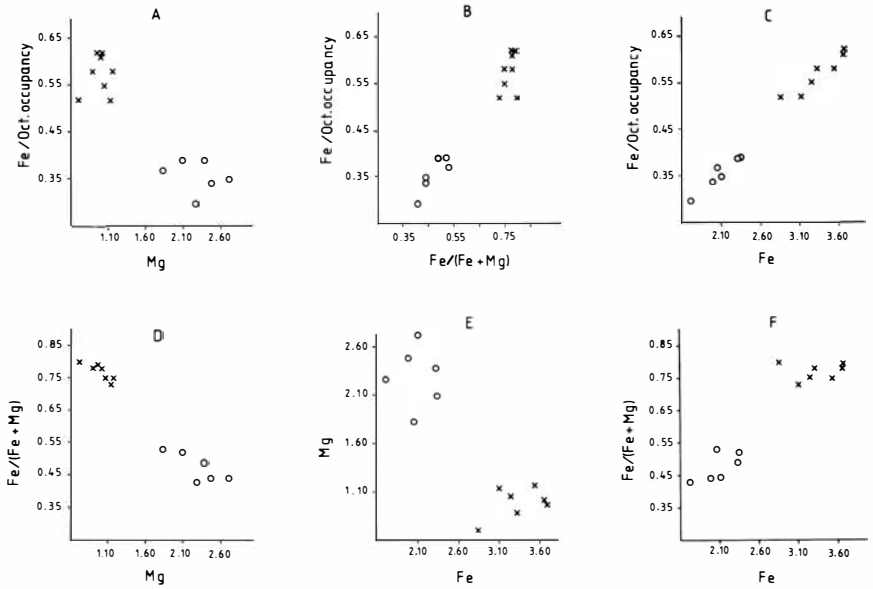

Fig. 27. A–F. The relation between the different cations and cation ratios of chlorite; x = diagenetic and o = hydrothermal.

dependent in the diagenetic environment (see Merino 1975, Huang 1977). Instead, the chemistry of pore solutions exerts the important control. Many authors, however, have stressed that in saturated solutions the ratio $[Na^+, K^+]/[H^+]$ is most critical in the formation of feldspars relative to other chemically compatible minerals (e.g. kaolinite, mica, Feth et al. 1964, Garrels & Christ 1965, Helgeson et al. 1969). The sodium needed for the formation of authigenic albite is presumably derived from the de-

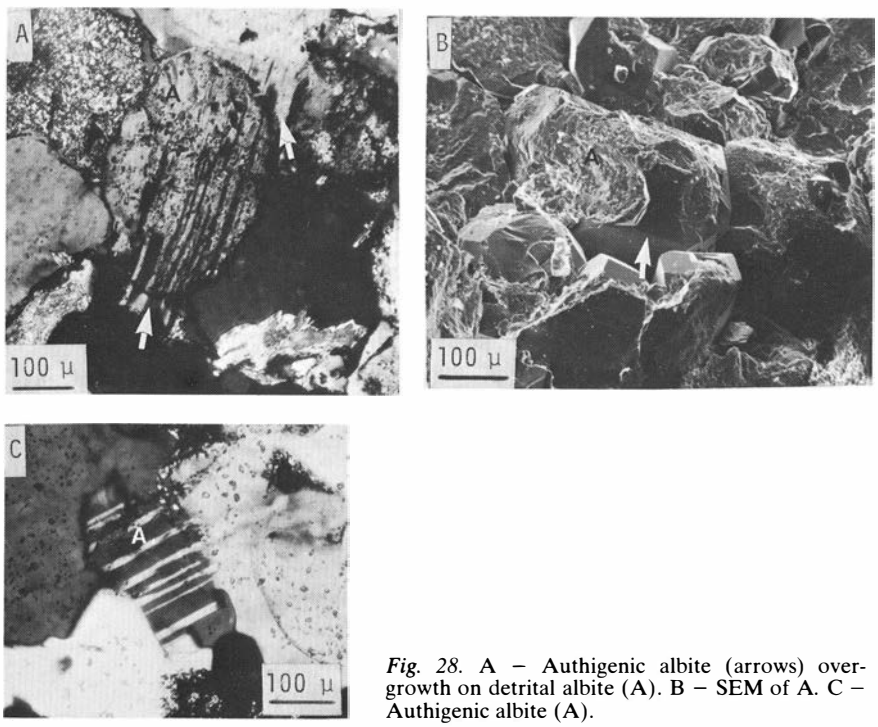

Fig. 28. A – Authigenic albite (arrows) overgrowth on detrital albite (A). B – SEM of A. C – Authigenic albite (A).

Table 25. Modal composition of some epidote-bearing sandstones.

Sample No.	Quartz	Potassium feldspar	Plagioclase feldspar	Quarts cement	Interstitial clay	Calcite cement	Rock fragments	Epidote	Others
455	27.7	2.7	15.3	22.0	7.0	10.6	4.7	6.0	4.0
617b	18.3	0.6	3.4	14.3	5.0	14.3	24.4	8.7	11.0
533	31.3	1.0	2.3	21.7	10.3	5.0	16.0	8.7	3.7
578	33.0	1.6	2.3	21.7	15.0	1.7	5.7	10.4	8.6
962D	40.0	1.0	2.0	19.7	5.7	–	12.6	11.7	7.3
588b	37.0	2.7	9.3	21.7	10.3	–	3.7	14.0	1.3
754a	37.3	1.7	2.7	15.3	14.0	2.3	2.7	15.3	8.7
620a	27.7	1.3	6.4	28.7	8.3	–	3.0	24.3	0.3
579c	34.3	2.0	0.7	29.3	2.0	–	1.0	30.0	0.7
886c	28.7	0.6	0.3	17.3	7.4	–	3.6	34.4	7.7
503h	25.0	–	0.3	25.0	2.7	–	1.0	44.3	1.7

Others = Ti-minerals and Fe-oxides.

composition of detrital plagioclases. These were, as previously mentioned, replaced by illite and/or chlorite.

Hydrothermal alteration

In areas close to or in the vicinity of the dolerites (Fig. 1) systematic sampling showed that the hydrothermal effect on the sedimentary rocks may continue to about 10 m away from the contact with the dolerite. However, the intensity of alteration and presence of epidote decrease drastically when comparing those samples at about 10–50 cm from the contact to those at about 10 m; in fact, only traces of epidote are observed in the latter. Nevertheless, it is found that in all areas marked in Figure 1, the shales were slightly metamorphosed and developed banded textures while the sandstones became harder and sometimes fractured. The fractures may extend to about 30 m away from the contact between dolerite and sedimentary rocks and are usually filled by epidote or calcite. Pyrite as crystals of about 0.2 mm is also observed in fractures filled by calcite and a green chlorite-like mineral, as shown by XRD. The minerals of hydrothermal origin in the basalts are calcite, chalcedony, chlorite, epidote, quartz, prehnite and pumpellyite. Prehnite was observed by v. Eckermann (1937) and prehnite and pumpellyite by Nyström (1982). These are found mainly as fillings in the amygdales of the basalt.

The mineralogical and chemical composition of hydrothermally altered sandstones, which contain different amounts of epidote, are shown in Tables 25 and 26. They differ characteristically from the sandstones already described, which have not been affected by hydrothermal solutions. They have lower amounts of detrital quartz, only traces of or no detrital mica and generally contain more plagioclase than potassium feldspar. Epidote in these sandstones occurs as single crystals or aggregates (Fig. 29A). Crystals showing prismatic or lath-like habits are also observed. The mineral has pale yellowish-green colour and is somewhat pleochroic with high relief and variable birefringence. It usually fills the pore space and replaces the earlier illite and quartz cement. Epidote also often replaces detrital quartz and feldspar (Fig. 29B). The replacement may be partial where epidote appears as crystals protruding into the detrital grains. More intense replacement also occurs; only remnants of the detrital grains are found (Fig. 29C).

The epidote has presumably formed through direct crystallization from the hydrothermal fluids and/or by reaction of these fluids with feldspar, quartz and illite. The common presence of epidote, calcite, titanium minerals, hematite and occasionally magnetite indicates that the hydrothermal fluids were rich in Fe, Ca, Ti and Mg. Magnesium, however, is found to be common in hydrothermal chlorite. Aluminium is another important element

Table 26. Bulk chemical composition of epidote-bearing sandstones.

	455	578	579C	886C
SiO_2	79.3	76.3	79.3	75.9
TiO_2	0.40	0.71	0.23	2.0
Al_2O_3	7.7	8.0	9.0	6.4
Fe_2O_3	3.3	4.8	1.7	4.6
FeO	0.54	0.69	0.28	1.5
MnO	0.01	0.00	0.00	0.05
MgO	0.07	1.6	0.32	0.89
CaO	3.0	1.8	4.2	6.2
Na_2O	1.3	1.2	0.66	0.85
K_2O	3.0	2.7	2.2	0.70
Total	98.62	97.80	97.89	99.09

which probably has been derived mainly from the interstitial clay minerals and the feldspars of the sandstones; it may, however, have been partially supplied by the hydrothermal fluids. The same sources as above, besides quartz, also supplied Si for the formation of epidote. The presence of calcite and hematite as well as the high content of Fe^{3+} in epidote (Table 27) suggest high to moderate f_{O_2} and f_{CO_2} during the crystallization of epidote (see Brown 1977, Bird & Helgeson 1980)

The hydrothermal chlorite differs in composition from the diagenetic ones (Table 28; cf. Table 22). High magnesium content characterizes the hydrothermal chlorites. They occur in the solid solution area of Figure 26 as ripidolite, brunsvigite and diabantite. These have, in thin section, pale-green colour, and are usually pleochroic with dark grey or violet interference colour (Fig. 30A).

The chemical composition of hydrothermal illite, on the other hand, does not differ much from that of diagenetic illite(Table 29; cf. Table 20). Higher content of aluminium in the tetrahedral position is, however, found in hydrothermal illites. They show, in thin section, interference colours similar to those of muscovite. The crystals are relatively large, about 0.05–0.10 mm in size, compared to those of diagenetic illite, mostly <0.02 mm (Fig. 30B).

Kaolinite and a mixed-layer clay mineral with basal spacing at 17 Å are observed in some sandstones, which do not contain much epidote. These minerals occur in minor amounts; their X-ray dif-

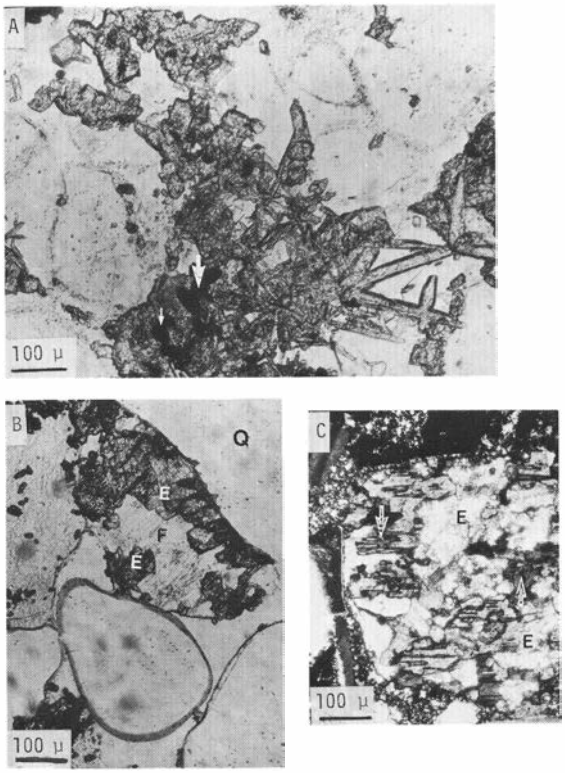

Fig. 29. A – Epidote, with high relief, occurring in different crystal forms within detrital quartz and quartz cement, with low relief; arrows are leucoxene. B – Epidote (E) replacing detrital quartz (Q) and feldspar (F). C – Epidote (E) replacing almost completely a feldspar (e.g. at arrows).

Table 27. Microprobe analyses of epidote.

	1	3	4	5
SiO_2	34.2	37.7	38.3	38.1
Al_2O_3	21.3	26.1	24.4	24.3
Fe_2O_3*	21.7	10.1	12.3	12.6
CaO	20.1	23.3	22.6	23.2
MgO	0.0	0.0	0.4	0.2
MnO	0.1	0.1	0.3	0.1
TiO_2	0.1	0.0	0.1	0.1
Total	97.5	97.3	98.4	98.6
Number of ions on the basis of 12.5 oxygens				
Si	2.81	2.98	3.03	3.01
Al	2.06	2.43	2.28	2.26
Fe	1.34	0.60	0.73	0.75
Ca	1.77	1.97	1.92	1.96
Pst % $\frac{Fe^{3+}+100^{1)}}{Fe^{3+}+Al}$	0.39	0.20	0.24	0.25
	Interstitial finely crystalline with hematite pigment	Radiating crystals	Fine prismatic crystals replacing quartz	Large crystal aggregate filling pore space

* Total Fe calculated as Fe_2O_3.
[1)] Pistacite content of epidote.

Table 28. Microprobe analyses of hydrothermal chlorite.

	1	2	3	4	5	6
SiO_2	29.23	27.74	30.07	28.76	24.99	25.53
Al_2O_3	18.37	20.80	16.99	17.44	18.28	26.22
FeO*	22.21	25.25	22.51	26.48	22.70	20.06
MgO	11.07	12.66	15.74	15.22	16.34	14.76
K_2O	1.54	0.02	0.57	0.04	0.03	0.04
TiO_2	0.17	0.10	0.02	0.02	0.30	1.06
MnO	1.24	1.37	0.00	0.00	0.44	0.19
Na_2O	0.00	0.00	0.00	0.00	0.06	0.01
Total	83.88	84.94	85.90	87.96	83.14	87.87
Number of ions based on 28⁻ charges						
Tet. Si	3.25	2.74	3.18	3.02	2.79	2.63
Al	0.75	1.26	0.82	0.98	1.21	1.37
Oct. Al	1.65	1.46	1.30	1.18	1.19	1.80
Fe	2.06	2.34	1.99	2.33	2.11	1.72
Mg	1.83	2.09	2.48	2.38	2.71	2.26
Oct. total	5.54	5.89	5.77	5.89	6.01	5.78
Charge balance						
Tet.	0.75	1.26	0.82	0.98	1.21	1.37
Oct.	0.73	1.24	0.84	0.96	1.21	1.37

* FeO represents total iron.

Table 29. Microprobe analyses of hydrothermal illite.

	1	2	3	4	5	6
SiO_2	44.77	45.74	46.58	46.71	45.43	47.89
Al_2O_3	33.87	36.61	36.39	36.81	34.77	31.12
FeO*	4.11	2.76	1.59	1.30	2.04	2.85
MgO	2.77	1.21	0.47	0.83	1.06	1.61
K_2O	10.47	10.14	9.95	10.11	10.13	9.18
TiO_2	0.03	0.13	0.13	0.58	0.84	0.01
MnO	0.00	0.03	0.02	0.06	0.00	0.00
Na_2O	0.16	0.44	0.48	0.35	0.43	0.20
Total	96.18	97.06	95.61	96.12	94.70	92.86
Number of ions based on 22⁻ charges						
Tet. Si	3.01	3.02	3.09	3.07	3.09	3.27
Al	0.99	0.98	0.91	0.93	0.91	0.73
Oct. Al	1.69	1.86	1.93	1.92	1.86	1.77
Fe	0.23	0.15	0.09	0.07	0.12	0.16
Mg	0.28	0.12	0.05	0.08	0.11	0.15
Oct. total	2.20	2.13	2.07	2.07	2.09	2.08
Int. K	0.90	0.85	0.84	0.85	0.87	0.80
Charge balance						
Inter.	0.90	0.85	0.84	0.85	0.87	0.80
Oct.	0.09	0.13	0.07	0.06	0.04	0.07
Tet.	0.99	0.98	0.91	0.93	0.91	0.73

* FeO represents total iron.

fraction peaks appear only when separating them within the clay fraction. The X-ray peaks of kaolinite were differentiated from those of chlorite by treatment with diluted hydrochloric acid. In thin section kaolinite is very similar to illite but has lower relief and grey interference colour. The mixed-layer clay mineral resembles kaolinite but is more greenish in colour (Figs. 31A, B and C). It may be an interstratified illite–kaolinite or illite–chlorite mineral.

Paragenesis

The term paragenesis has been widely used in metamorphic petrology to denote the co-existence of specific mineral phases under specified conditions (e.g. Winkler 1979). The state in sedimentary rocks is, however, different. The conditions of their formation are greatly limited in terms of temperature and pressure and only in few cases are they reflected in the mineralogy (e.g. evaporites, carbonates). Regarding clastic sequences, e.g. sandstones, there is much information about the relation of their diagenetic assemblages to temperature and pressure (e.g. Dunoyer De Segonzac 1970, Velde 1977, Hower 1981). In this respect, it seems that the term paragenesis can also be applied to sedimentary rocks when there is a possibility to characterize their diagenetic parageneses in terms of temperature and pressure (see also Hoffman & Hower 1979). Depending on the properties of single diagenetic minerals and/or association of many minerals, the zone of diagenesis may be divided into the following parageneses (information gathered from Frey 1970, Dunoyer De Segonzac 1970, Hower 1981, Boles 1981):

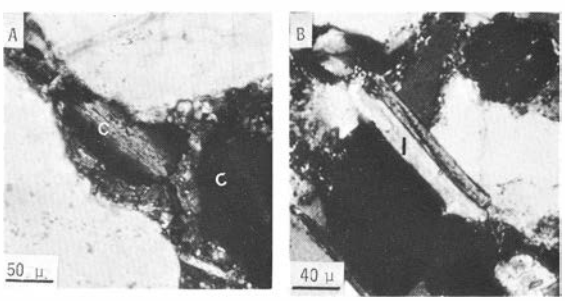

Fig. 30. A – Hydrothermal chlorite (C). B – Hydrothermal illite (I).

1 – Montmorillonite – kaolinite

2 – Kaolinite – mixed-layer clays

3 – 1M-1Md illite – chlorite

4 – 2M illite – muscovite – chlorite

increasing temperature and pressure ↓

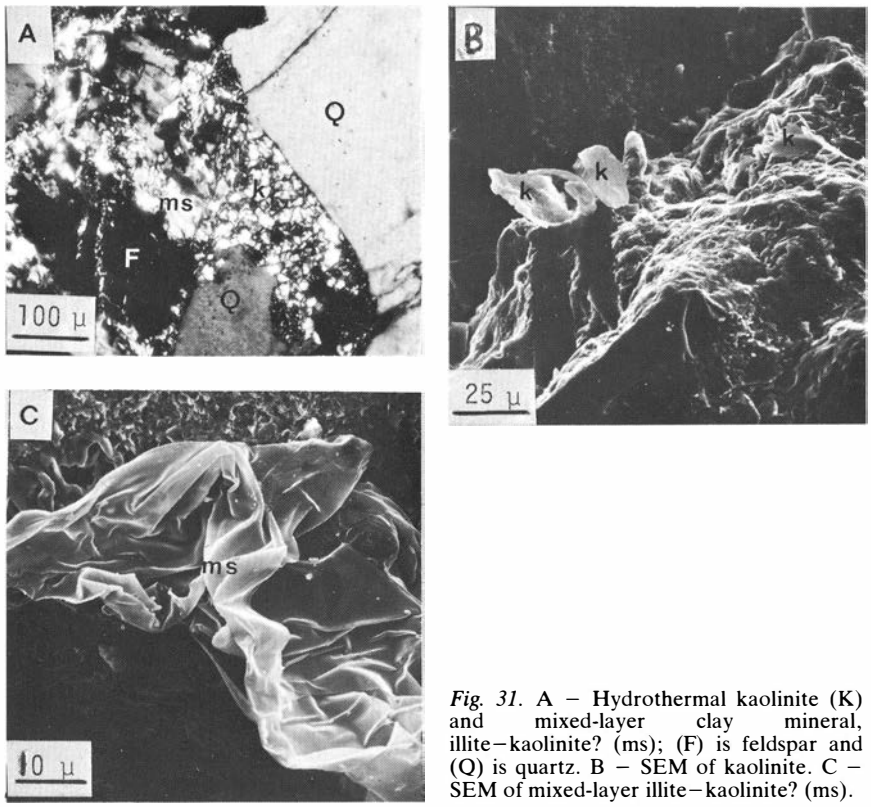

Fig. 31. A – Hydrothermal kaolinite (K) and mixed-layer clay mineral, illite–kaolinite? (ms); (F) is feldspar and (Q) is quartz. B – SEM of kaolinite. C – SEM of mixed-layer illite–kaolinite? (ms).

The sensitivity of clay minerals to minor changes in temperature and pressure within the intervals 25–200°C and 0 to about 1.5 kb (see the references mentioned above) has led several authors to use them as indicators of diagenetic grade. The discussion hereafter, on the diagenetic paragenesis, aims to show the chemical and structural changes in diagenetic clay minerals in relation to their parageneses. The associated mineral phases will also be discussed.

Principal transformations at normal T–P gradients

There is a wealth of data and evidence showing the effect of temperature and, to a lesser extent, that of pressure on the transformations of clay minerals (e.g. Burst 1959, Dunoyer De Segonzac 1970, Hoffman & Hower 1979). The increase of temperature with depth, the geothermal gradient, is considered normal and gradual when it falls in the range of 20–30°C/km (Dunoyer De Segonzac 1970, Winkler 1979, Hoffman & Hower 1979, Monnier 1982). In the studied area, direct measurements of temperature gradients are not available and therefore temperature gradients from the nearby areas have been adopted. Eriksson & Malmqvist (1979) gave values of geothermal gradients between 13 and 20°C/km in the area just southeast of the one studied. Malmqvist (pers. comm. 1984) believes that 20°C/km could be accepted as an average gradient, on a regional scale, in the area studied. He also assumes that values up to 30°C/km are not out of the question. For the purpose of this work and to account for the magmatic activity during the formation of the Öje Basalt and the intrusions of the dolerites, a regional temperature gradient of 25°C/km was considered.

Smectite. – Smectite is thermodynamically stable at the earth's surface conditions, being transformed with advancing diagenesis (increasing burial depth) as follows: smectite→mixed-layer clay→illite and/or chlorite→muscovite and /or chlorite (Perry & Hower 1970, Velde 1977, Boles & Franks 1979, Lahann 1980, Hower 1981, Garrels 1984). The type of phase formed depends on the chemistry of the pore solution. The ratios $[K^+]/[H^+]$, $[Fe^{2+}+Mg^{2+}]/[H^+]$ or simply $[K^+]/[Fe^{2+}+Mg^+]$ determine whether illite or chlorite will be formed. As mentioned, the source of these cations is mainly the diagenetic alteration of the detrital feldspars and biotites.

Experimental work and natural observations indicated that the transformation smectite→illite starts at about 50°C, which means at about 2 km burial depth (e.g. Eberl & Hower 1976, Inoue 1983). The illitic layers begin to dominate and the expandable smectite layers diminish and become less than 10 % at temperatures above 120°C (e.g. Hower 1981, Boles 1981). The appearance of muscovite together with illite indicates a more advanced stage of diagenesis, approaching the boundary to metamorphism (e.g. Velde 1977).

In the diagenetic environment of the investigated rocks, smectite and mixed-layer clays were not identified. This may complicate the judgement on the extent to which illite and chlorite are transformations from smectite or discrete diagenetic entities. A survey of literature discussing mostly rocks of diagenetic grades lower than the studied ones, shows that mixed-layer clay minerals are very common in most clastic sedimentary rocks (e.g. Dunoyer De Segonzac 1970, Weaver & Pollard 1973, Wilson & Pittman 1977, Walker et al. 1978, Foscolos et al. 1982, Morad 1983). This may favour the assumption that at least mixed-layer clay minerals as authigenic and alteration products of biotite and feldspar were present at an early stage and were transformed to their discrete entities during diagenesis. This is also in good agreement with the fact that mixed-layer clays were observed in sandstones and shales having almost similar source rocks, environment and age as those of the Dala Sandstone (see Morad & AlDahan 1982b, Morad 1983). The diagenetic illite and chlorite in the studied rocks are therefore presumably the results of both direct crystallization and/or transformation of unstable expandable clay minerals, e.g. smectite and/or mixed-layer clay minerals. In their present form, however, their crystallinity and chemistry reflect their diagenetic grade (paragenesis).

It is observed that the diagenetic clay-mineral assemblage in shales shows higher degree of diagenetic development than the associated sandstones (e.g. Hower et al. 1976, Hoffman & Hower 1979, Howard 1981), one important reason being differences in permeability. Sandstone has high permeability and the $P_{H_2O} = P_{hydraulic}$, whereas low permeability and $P_{H_2O} = P_{lithostatic}$ characterizes shales, especially at a burial depth more than one kilometre (e.g. Velde 1977). This difference in the partial pressure of water will change the thermal stability of more hydrous clay-mineral phases. The result is development of clay minerals with low water content, e.g. illite, in a shale, and clay minerals with high water content (illite–smectite) in a sandstone, even when the rocks are buried at the same depth. In the rocks studied no marked differentiation is observed between the clay mineral assemblage in the sandstone and that of the shales. Due to low permeability of the shales they may show low contents of expandable layers in illite. This was not possible to verify in the rocks studied, because, as mentioned above, the illite does not contain appreciable amounts of expandable layers either in the shales or in the sandstones.

Illite. – The diagenetic illites studied are dominated by phengitic and sericitic types (Fig. 32). Although data on the chemical composition of authigenic illites are scarce, illite of phengitic composition is considered common in deep burial diagenetic environment (Kossovskaya & Drits 1970, Dunoyer De Segonzac 1970, Velde 1977). Al-rich illite (sericite)

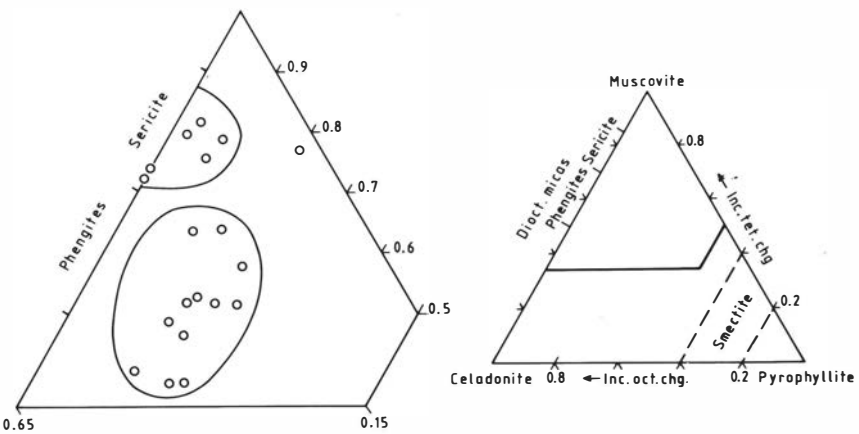

Fig. 32. The distribution of the studied diagenetic illites in the compositional triangle, muscovite–pyrophyllite–celadonite (the triangle is from Hower & Mowatt 1966). Inc. oct. chg. = increasing octahedral charge. Inc. tet. chg. = increasing tetrahedral charge.

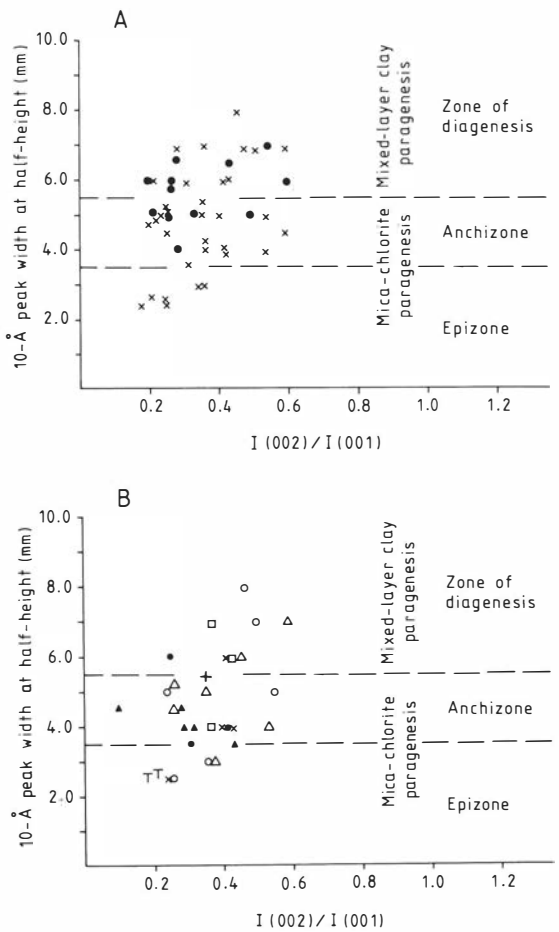

Fig. 33. The relation between peak-width and intensity ratio (002)/(001) in illites, A – in shales (●) and sandstones (x), B – in the sandstone types. ● = quartz sandstone, x = lithic sandstone, o = feldspathic sandstone, + = arkose, △ = lithic graywacke, and □ = feldspathic greywacke. ▲ = illite in epidote-bearing sandstones from the hydrothermal areas, T = illite from the thrusted zone in the southwestern part of the area studied.

and muscovite were observed in samples at dolerite areas (see Fig. 1), in the deeper part of the rock sequence and in the thrust zone, respectively, which indicates high grade of diagenesis (2M illite–muscovite–chlorite paragenesis; see also Velde 1977). In the rest of the studied sequence, the low temperature polytypes of illite (3T, 1M and 1Md) are observed as previously described on p. 30.

The crystallinity index of illite (CI) is a commonly used indicator for diagenetic conditions (Kübler 1964, Dunoyer De Segonzac 1970, Islam et al. 1982). The plot of the I(002)/I(001) against the 10Å peak width at half height of glycolated <2μm fraction (Fig. 33A and B) shows that the rocks of the Dala Sandstone grade from the zone of diagenesis into the epizone. The samples in the epizone came from localities in hydrothermally affected areas and from the thrust zone in the southwest. Disregarding these localities, the rest of the samples have a range of illite crystallinity between 0.35 and 0.80 2θ. It seems that there has been no sharp crystallinity change between the different parts of the formation, although a general trend of increasing crystallinity with depth is observed (Fig. 3). Despite the small number of the plotted points, the trend of increasing crystallinity with decreasing porosity (Fig. 34) also points towards a high grade of diagenesis. Deterioration in the CI is found in some samples as they come close to the dolerites (Fig. 3) because of the earlier mentioned existence of expandable mixed-layers in the illitic minerals (p. 30). In Figure 33B the CI in the different types of sandstones shows no marked differences. The epidote-bearing sandstones, however, show relatively limited values of CI and fall within the anchizone.

The relation between the composition of illite and its crystallinity has been investigated (e.g. Esquevin 1969, Velde 1977); a general trend of higher potassium and lower silica, iron and magnesium contents is observed with increasing temperature. This may be true in the studied illites if they are compared to illites from higher- or lower-grade rocks (see Morad & AlDahan 1982b), but within the studied rocks there is no special correlation.

Chlorite. – Iron-rich chlorites, such as those investigated, were frequently observed in diagenetic environments (Grim 1970, Weaver & Pollard 1973, Velde 1977). Such chlorites, having chamosite composition and both 7 Å and 14 Å reflections, are

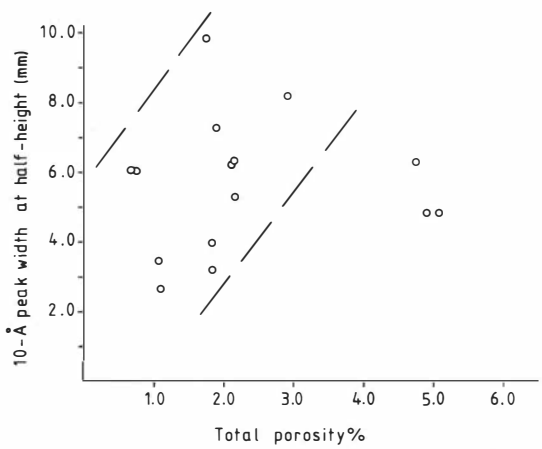

Fig. 34. The relationship between total porosity and crystallinity of illite in some of the samples studied.

expected to transform towards the more stable 14 Å chlorite structure at increasing T–P conditions (Hayes 1970, Velde 1977). This transformation takes place at a thermal energy level where mixed-layer clays are no longer stable, i.e. about 120°C.

The well crystallized habit of the studied chlorites is another indicator of high T–P conditions encountered by their host rocks (cf. Hayes 1970).

The partitioning of homologous ions (Fe^{2+}–Mg^{2+}) between the co-existing illite and chlorite depends upon variation in temperature and pressure conditions (Ramberg 1952). At low temperature the partitioning is not very clear and instead segregation occurs (Velde 1977). The Fe^{2+} will concentrate in one phase, chlorite, and Mg^{2+} in the other, illite. This segregation may have occurred in the studied co-existing phases, but as the valency of the iron in the microprobe analysis is not known, the problem cannot be solved. However, it is generally found that the chlorite contains much more iron, predominantly as Fe^{2+}, than the illite (Fig. 35). The ratio Fe/Mg seems generally to be low in illites compared to chlorites. It is particularly observed in those illites co-existing with chlorites (Table 20, analyses 14, 16 and 20). This suggests that the illite concentrates Mg in preference of Fe^{2+} whereas the chlorite does the reverse.

In brief, the crystal-chemical properties of the studied diagenetic clay minerals suggest diagenetic temperature above 150°C and at the most around 200°C. This is indicated from the presence of phengitic and sericitic illites with practically no expandable layers, as well as with an absence of mixed-layer clay minerals and kaolinite, together with the presence of well crystallized and iron-rich chlorite. These associations are characteristics of parageneses 3 and 4 (1M-1Md illite–chlorite and 2M illite–muscovite–chlorite; p. 38). This implies a minimum depth of burial of about 4000 m; if an average geothermal gradient is assumed at about 25°C/km.

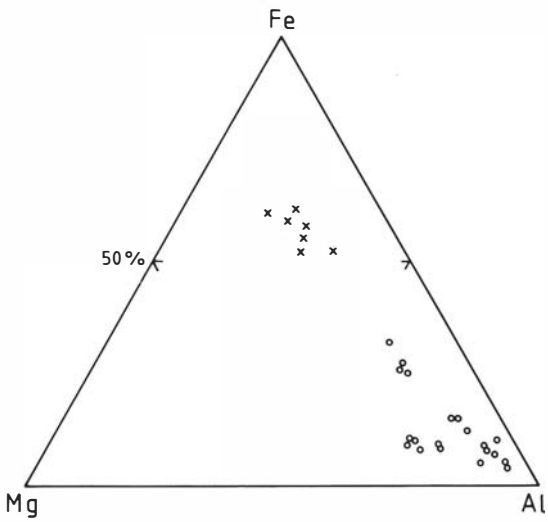

Fig. 35. Ternary plot of Fe–Mg–Al of diagenetic illite (o) and chlorite (x).

Principal transformations at high T–P gradients

In the areas of dolerite intrusions there has obviously been higher increase in temperature and possibly pressure as well. The case was no longer a normal burial diagenesis; higher temperature and supply of hydrothermal fluids involved a change.

The evidence at hand, presence of epidote and illite, preserved sedimentary texture and dissolution-replacement of the detrital grains by epidote and calcite (see also p. 36), suggests a maximum temperature of 300°C. The important transformation in the clastic rocks in the hydrothermally affected area are:

1) Transformation of illite into mixed-layer clays (an illite–kaolinite or illite–chlorite phase) and/or increasing amount of expandable layers and deteriorating degree of crystallinity.

2) Formation of Mg-rich chlorite from the interstitial illite and chlorite.

3) Recrystallization of some illite into coarser crystals of muscovite habit.

These transformations are arranged with increasing distance from the dolerites and may also vary depending on the original interstitial clay (chlorite or illite dominating). In the first two transformations it seems that the hydrothermal fluids were an important factor, whereas in the latter the temperature played a greater role. The formation of mixed-layer clays in hydrothermal environment is not as clearly understood as in the diagenetic environment. However, mixed-layer clays were reported as either associated directly with volcanic activity or occurring in geothermally active areas (e.g. Sudo & Shimoda 1978).

Summary of diagenetic events and conditions

Due to progressive burial, the sediments will encounter new conditions after deposition. The relatively more sensitive minerals will obviously start to adjust themselves to these new conditions. The first, dominating type of alterations to take place are redox reactions (e.g. Berner 1971, Dapples 1979). Highly oxidizing conditions and high per-

meability are expected at the early stage of burial; therefore the alteration of biotite and feldspar is, to a great extent, a function of them.

Hydrolysis of feldspar results in production of K^+ (Wollast 1967, Siegel & Pfannkuch 1984); the rate of the hydrolysis was found to be pH dependent. The produced potassium may be mobilized. The rate of leaching will then control the alteration product of feldspar. High rate usually favoured the formation of kaolinite relative to the illitic clay minerals. Part of the octahedral Fe^{2+} in biotite may be oxidized at this stage of diagenesis and is expelled from the octahedra. It contributes to the formation of the red colour of the rocks, occurring as hematite. The hydrolysis of biotite may also cause the extraction of K^+ and formation of hydrobiotite. It is suggested, however, that the further oxidation of biotite may increase the bond strength, which holds K^+, due to conversion of the OH^- to O^{2-} (e.g. Ross & Rich 1974). This may reduce the further alteration of biotite at this diagenetic stage. The alteration also depends highly upon the leaching rate, as in feldspar.

At the early stage of burial the formation of clay coats of illite or chlorite and hematite coats as well as pigment on the detrital grains is assumed to take place. The high concentration of the released cations around the detrital particles, due to adsorption, has probably favoured the formation of the authigenic illite, chlorite and hematite.

With increasing thickness of the overburden the sediments become more compacted with continuous decrease of porosity and permeability. The circulation of the pore fluids is reduced and the concentration of the cations derived from the alteration of unstable particles is increased. The dewatering of argillaceous sediments results in an addition of fluids to the more permeable sandstone beds (see e.g. Rieke & Chilingarian 1974). The detrital particles begin to be subjected to pressure solution. The result is precipitation of quartz overgrowth which is shown to envelop the earlier clay coats. The formation of pore-filling clay cement belongs also to this stage of diagenesis. The alteration of detrital feldspar and biotite presumably continues but probably at a lower rate. The cations released at this stage are presumably kept in the close vicinity of the detrital grains. This conclusion is based on the assumption that illitization of kaolinite took place at this stage, hence its absence due to increase of the $[K^+]/[H^+]$ ratio. However, due to supply of more potassium than required for illite authigenesis and excess of silica, authigenic potassium feldspar is expected to crystallize (Helgeson et al. 1969). As mentioned earlier, a few crystals of authigenic potassium feldspar were in fact observed. According to Nicholls (1976) this may indicate that ratios as high as log $[K^+]/[H^+] \sim 5.5$ at log $[H_4SiO_4] \simeq 4$ rarely were reached in the studied rocks. Instead, the ratio of $[Na^+]/[H^+]$ seems to have reached the concentration level of crystallization of albite. The two parageneses, kaolinite – mixed-layer clays and 1M-1Md illite – chlorite, may belong to this stage of diagenesis. In the rocks studied only the latter was observed.

The third important event in the diagenetic history of the studied rocks is the increasing influence of temperature and pressure, in addition to solution chemistry, as in paragenesis 4 (2M illite–muscovite–chlorite). This stage is characterized by almost complete diminishing of porosity and permeability where diagenetic reactions were accomplished on a micro-environmental scale. The kaolinite and mixed-layer clays are completely absent (see Morad & AlDahan 1982b). The prevailing diagenetic changes are transformation and recrystallization reactions. Illite is found to recrystallize into coarser crystals and in some cases into muscovite. The process presumably involves the extended fixation of K^+ in the illite as proposed by Kazintsev (1968). At this stage of diagenesis a possible increase of the effective porosity may set in, due to release of an appreciable amount of bound water associated with relative decrease of the particle size of the clay minerals (Rieke & Chilingarian 1974). This will enhance and speed up the reactions by supplying additional fluids. The local transport of silica from the high pressure zone (with sutured quartz-grain contacts) to that of lower pressure (overgrowth area) may have been facilitated by the new additional pore fluids (cf. Houseknecht 1984). Table 30 summarizes the sequence of major diagenetic events described above.

The expected maximum diagenetic temperature and pressure conditions which have affected the rocks of the Dala Sandstone Formation are about 200°C and 1.5 kb. This estimation is based on observations such as absence of mixed-layer clays and kaolinite, recrystallization of illite into muscovite and development of triple junction and quartzite-like textures in some of the quartz sandstones. Such developments in clastic sequences are related to approximately the same T–P conditions by other authors in other areas (e.g. Hoffman & Hower 1979, Boles 1981, Islam et al. 1982).

The conditions of diagenesis were influenced by the dolerites at their areas of intrusion. This has caused both increase in the temperature of the pore fluids and addition of new mineralizing solutions. The present evidence, as mentioned earlier, supports the estimation of temperature around 300°C and relatively shallow depth for the alteration of the

Table 30. Sequence of major diagenetic events in the rocks studied.

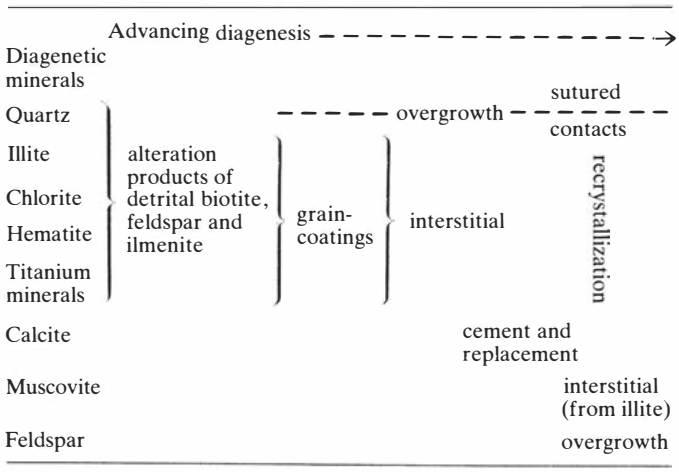

clastics (sandstones and shales). In other words, the injection of the dolerites has occurred during the continuing burial of the sediments, i.e. before they reached their final burial as estimated at a minimum depth of about 4000 m. The circulating hydrothermal fluids gave rise to formation of epidote, calcite, titanium minerals, chlorite, kaolinite, albite, quartz, hematite and minor amounts of magnetite and mixed-layer clay minerals.

If, however, temperatures higher than 300°C and/or deep burial conditions were attained, other minerals, e.g. pumpellyite, prehnite, actinolite and andradite, are expected to occur. Besides, the rocks would show textures of metamorphic grades rather than their present sedimentary ones.

Conclusions

The mineralogy of the Dala Sandstone rocks, being mainly quartz-dominated, suggests derivation mostly from acidic igneous rocks, gneisses and sandstones. These are common constituents of the basement rocks in the area studied and its surroundings. The domination of biotite over muscovite in the sandstones studied is well related to composition of the basement rocks. The scarcity of heavy minerals in the sandstones is presumably related to intrastratal dissolution.

The diagenetic clay minerals were formed by authigenesis, alteration of detrital biotite and feldspars and aggradation crystallization of interstitial clay minerals. The sources of cations for their formation were mainly decomposition of the detrital biotite and feldspar and partly circulating meteoric water. Detrital biotites and ilmenite were important sources of Ti for authigenic anatase, rutile and sphene. The alteration of Si-bearing detrital grains, the transformation of diagenetic clays and pressure solution were the main source of silica in the rocks studied.

A high grade of diagenesis characterizes the rocks studied which is best suggested by common absence of illite–smectite and kaolinite. These minerals are known to transform to the more stable phases, i.e., illite and/or chlorite, by increasing temperature and pressure, i.e., increasing depth of burial. Other features that suggest high grade of diagenesis are sutured contacts between quartz grains, presence of authigenic sphene and the almost complete loss of porosity.

The high grade of diagenesis in the rocks studied has resulted in the generally low content of expandable layers in the illitic minerals as well as in their high iron content. This effect, high grade of diagenesis, is also reflected by the good crystallinity of the illites. The chlorites also show good crystallinity and high content of iron, occurring as Fe–Mg trioctahedral chlorites and chamosite.

The sequence of diagenetic minerals as it is shown in Table 30 represents a series of processes which were finally controlled by a temperature of about 150 to 200°C and a pressure of about 1.5 kb. These estimations are based on the chemistry and the paragenesis of diagenetic minerals. The clastic rocks in areas close to the dolerites have been exposed to temperature and possibly pressure higher than those which affected the other parts of the rock sequence. This has resulted in the formation of

metamorphic minerals (e.g. epidote, chlorite) and texture. The hydrothermal fluids have been affecting both the detrital and diagenetic minerals causing their replacement or alteration. Epidote and calcite are among the important replacement minerals, whereas chlorite, kaolinite and mixed-layer illite–kaolinite (?) are the important alteration products. Maximum temperature reached at the areas of hydrothermal alteration might be about 300°C.

Acknowledgements. – I am grateful to Bengt Collini for supervising this work and for providing samples, thin sections and porosity data. He also critically read the manuscript and for this and for his kindness and encouragement I am much obliged.

I express my thanks to Hans Harryson for the help with the electron-microprobe analyses and to Anne-Marie Karlson and Brita Almquist for making the wet-chemical analyses. Thanks are also due to Christina Wernström, who kindly drafted the figures and to Olle Wallner for making the thin sections. Assar Lindberg and Martin Feuer are acknowledged for preparation of photographs.

I am greatly indebted to Kersti Gløersen for typing the manuscript and for her generous help during the whole research period. Thanks are also due to Hans Annersten for his continuous encouragement and to Jari Sillanpää for his help in programming.

I thank my friend Sadoon Morad for help, support and fruitful discussions.

Finally, a fellowship from the Ministry of Higher Education and Research, Baghdad, Iraq, is gratefully acknowledged.

REFERENCES

AlDahan, A. A & Morad, S. 1983: The alteration of biotite in sedimentary rocks: a petrographic and mineralogic investigation. *Terra Cognita 3,* 177. Paris.

Almon, W. 1981: Depositional environment and diagenesis of Permian Rotliegendes sandstones in the Dutch sector of the southern North Sea. *In* Longstaffe, F.J. (ed.): *Short Course in Clays and the resource geologist.* Mineral. Assoc. Can., 119–147.

Bailey, S. 1980: Structure of layer silicates. *In* Brindley, G. & Brown, G. (eds.): *Mineral. Soc. Monogr. 5,* 1–124. London.

Bailey, S., Cameron, E., Speeden, H. & Weege, R. 1956: The alteration of ilmenite in beach sands. *Econ. Geol. 51,* 263–279.

Bates, R. & Jackson, J. 1980: *Glossary of geology.* 2nd ed. Am. Geol. Inst., Fallschurch, Virginia.

Bayliss, P., 1975: Nomenclature of the trioctahedral chlorites. *Can. Mineral. 13,* 178–180.

Berner, R. 1971: *Principles of chemical sedimentology.* 240 pp. McGraw-Hill, New York.

Berner, R. & Holdren, G. 1979: Mechanism of feldspar weathering. II. Observation of feldspars from soils. *Geochim. Cosmochim. Acta 43,* 1137–1186.

Bird, D. & Helgeson, H. 1980: Chemical interaction of aqueous solutions with epidote-feldspar mineral assemblage in geologic systems: I. Thermodynamic analysis of phase relations in the system $CaO–FeO–Fe_2O_3–Al_2O_3–SiO_2–H_2O–CO_2$. *Am. J. Sci. 280,* 907–941.

Bjørlykke, K. 1980: Clastic diagenesis and basin evolution. *Rev. Inst. Invest. Geol., Univ. Barcelona 34,* 21–44.

Blatt, H., Middleton, G. & Murray, R. 1980: *Origin of sedimentary rocks.* 2nd ed. 782 pp. Prentice-Hall, Inc., Englewood Cliffs, New Jersey.

Boles, J. R. 1981: Clay diagenesis and effect on sandstone cementation (case histories from the Gulf Coast Tertiary). *In* Longstaffe, F. J. (ed.): *Short Course in Clays and the resource geologist,* 148–168. Mineral. Assoc. Can.

Boles, J. R. & Franks, S. G. 1979: Clay diagenesis in Wilcox sandstones of southwest Texas: Implication of smectite diagenesis on sandstone cementation. *J. Sediment. Petrol. 49,* 55–70.

Brammall, A. & Harwood, H. 1923: The occurrence of rutile, brookite and anatase on Dartmoor. *Mineral. Mag. 20,* 20–26.

Brindley, G. W. 1951: The crystal structure of some chamosite minerals. *Mineral. Mag. 29,* 502–525.

Brindley, G. W. 1961: Chlorite minerals. *In* Brown, G. (ed.): *The X-ray identification and crystal structures of clay minerals,* 242–296. Mineral. Soc., London.

Brown, E. 1977: Phase equilibria among pumpellyite, lawsonite, epidote and associated minerals in low-grade metamorphic rocks. *Contrib. Mineral. Petrol. 64,* 123–136.

Burst, J. F. 1959: Postdiagenetic clay-mineral environmental relationships in the Gulf Coast Eocene. *Proc. Natl. Conf. Clays and Clay Miner 6,* 327–341. Pergamon Press, London.

Dapples, E. 1979: Diagenesis of sandstones: *In* Larsen, G. & Chilingar, G. (eds.): Diagenesis in sediments and sedimentary rocks. *Dev. in sedimentol. 25A,* 31–97. Elsevier, Amsterdam.

Deer, W., Howie, R. & Zussman, M. 1962: *Rock-forming minerals 3.* 270 pp. Longmans, London.

Dunoyer De Segonzac, G. 1970: The transformation of clay minerals during diagenesis and low-grade metamorphism: A review. *Sedimentology 15,* 281–346.

Eberl, D. & Hower, J. 1976: Kinetics of illite formation. *Geol. Soc. Am. Bull. 87,* 1326–1330.

v. Eckermann, H. 1937: The Jotnian formation and the sub-Jotnian unconformity. *Geol. Fören. Stockholm Förh. 59,* 19–58. Stockholm.

v. Eckermann, H. 1939: A contribution to the knowledge of the Öje Diabase. *Geol. Fören. Stockholm Förh. 61,* 177–192. Stockholm.

Eriksson, K. & Malmqvist, D. 1979: A review of the past and the present investigations of heat flow in Sweden. *In* Čermak, V. & Ryback, L. (eds.): *Terrestrial heat flow in Europe.* 267 pp. Springer-Verlag, Berlin.

Esquevin, J. 1969: Influence de la composition chimique des illites sur leur cristallinité. *Bull. Cent. Rech. Pau–S.N.P.A. 3,* 147–154.

Fanning, D. & Keramidas, V. 1977: Mica. *In* Dixon, J. B. & Weed, S. B. (eds.): *Minerals in soil environments,* 195–258. Soil Science Society of America, Madison, Wisconsin.

Feth, J., Robertson, C. & Polzer, W. 1964: Source of mineral constituents in water from granitic rocks, Sierra Nevada, California and Nevada. *U.S. Geol. Surv. Water Supply Paper 1535-I.*

Fieremans, M. & Bosmans, H. 1982: Colour zones and the transition from diagenesis to low-grade metamorphism of the Gedinnian shales around the Stavelot Massif (Ardennes, Belgium). *Schweiz. Mineral. Petrogr. Mitt. 62,* 99–112.

Folk, R. C. 1968: *Petrology of sedimentary rocks.* 170 pp. University of Texas, Texas.

Foscolos, A., Reinson, G. & Powell, T. 1982: Controls on clay-mineral authigenesis in the Viking sandstone, central Alberta. 1. Shallow depths. *Can. Mineral. 20,* 141–150.

Foster, M. D. 1956: Correlation of dioctahedral potassium micas on the basis of their charge relations. *U.S. Geol. Surv. Bull. 1036–D.*

Foster, M. D. 1962: Interpretation of the composition and a classification of the chlorites. *U.S. Geol. Surv. Bull. 414–A.*

Frey, M. 1970: The step from diagenesis to metamorphism in pelitic rocks during Alpine orogenesis. *Sedimentology 15,* 261–279.

Frödin, G. 1920: Om de s.k. prekambriska kvartsit-sparagmitformationerna i Sveriges sydliga fjälltrakter. *Sver. Geol. Unders. C299.* Stockholm.

Füchtbauer, H. 1959: Zur Nomenklatur der Sedimentgesteine. *Erdöl und Kohle 12,* 605–613. Industrieverlag von Hernhaussen K.G., Hamburg.

Füchtbauer, H. 1974: *Sediments and sedimentary rocks 1.* 464 pp. Wiley & Sons, Inc., New York.

Galehouse, J. 1971: Sedimentation analysis. *In* Carver, R. (ed.):*Procedures in sedimentary petrology,* 69–94. Wiley-Interscience, New York.

Galloway, W. 1974: Deposition and diagenetic alteration of sandstone in northeast Pacific arc-related basins: Implication for greywacke genesis. *Geol. Soc. Am. Bull. 85,* 379–390.

Garrels, R. 1984: Montmorillonite/illite stability diagrams. *Clays and Clay Minerals 32,* 161–166.

Garrels, R. & Christ, C. 1965: *Solutions, minerals and equilibria.* 450 pp. Harper & Row, New York.

Gee, D. & Zachrisson, E. 1979: The Caledonides in Sweden. *Sver. Geol. Unders. C789.* Uppsala.

Gerling, E. K., Lobal-Zucenko, S. B. & Borisenko, N. F. 1966: New data on the absolute age of the Jotnian of the Baltic Shield. *Dokl. Akad. Nauk SSSR 166:3,* 674–677. (In Russian.)

Gilbert, C. 1955: Sedimentary rocks. *In* Williams, H. Turner, F. & Gilbert, C (eds.): *Petrography,* 251–384. Freeman and Co., San Francisco.

Gilkes, R. & Suddhiprakarn, A. 1979: Biotite alteration in deeply weathered granite. I. Morphological, mineralogical and chemical properties. *Clays and Clay Minerals 27,* 349–360.

Gilkes, R., Young, R. & Quirk, S. 1972: The oxidation of octahedral iron in biotite. *Clays and Clay Minerals 20,* 303–315.

Goldich, S. 1938: A study of rock weathering. *J. Geol.* 46, 17–58.

Gorbatschev, R. 1962a: The Pre-Cambrian sandstone of the Gotska Sandön boring core. *Bull. Geol. Inst. Univ. Uppsala 39,* 1–30.

Gorbatschev, R. 1962b: Dolerite intrusions and cementation of the Jotnian sandstone in the Mälaren area, central Sweden. *Geol. Fören. Stockholm Förh. 84:2,* 65–87. Stockholm.

Gorbatschev, R. 1967: Petrology of Jotnian rocks in the Gävle area, east central Sweden. *Sver. Geol. Unders. C621.* Stockholm.

Grim. R. E. 1970: *Clay mineralogy.* 596 pp. McGraw-Hill, New York.

Harland, W. B., Cox, A. V., Llewellyn, P. G., Pickton, C. A. G., Smith, A. G. & Walters, R. 1982: *A geologic time scale.* XI + 131 pp. Cambridge University Press, Cambridge.

Hayes, J. 1970: Polytypism of chlorite in sedimentary rocks. *Clays and Clay Minerals 18,* 285–306.

Heald, M. 1956: Cementation of Simpson and St. Peter sandstones in part of Oklahoma, Arkansas and Missouri. *J. Geol. 64,* 16–30.

Helgeson, H., Brown, T. & Leeper, R. 1969: *Handbook of theoretical activity diagrams depicting chemical equilibria in geologic systems involving an aqueous phase at one atm and 0° to 300°C.* 253 pp. Freeman, Cooper & Co., San Francisco, California.

Higgins, J. & Ribbe, P. 1976: The crystal chemistry and space groups of natural and synthetic titanites. *Am. Mineral. 61,* 878–888.

Hjelmqvist, S. 1966: Beskrivning till berggrundskarta över Kopparbergs län. *Sver. Geol. Unders. Ca40.* Stockholm.

Hoffman, J. & Hower, J. 1979: Clay mineral assemblages as low grade metamorphic geothermometers: Application to the thrust faulted distributed belt of Montana, USA. *In* Scholle, P. & Schluger, P. (eds.): *Aspects of diagenesis,* 55–79. SEPM, Spec. publ. no. 26. Tulsa, Oklahoma.

Houseknecht, D. 1984: Influence of grain size and temperature on intergranular pressure solution, quartz cementation, and porosity in a quartzose sandstone. *J. Sediment. Petrol. 54,* 348–361.

Howard, J. 1981: Lithium and potassium saturation of illite/smectite clays from interlaminated shales and sandstones. *Clays and Clay Minerals 29,* 136–142.

Hower, J. 1981: Shale diagenesis. *In* Longstaffe, F. J. (ed.): *Short Course in Clays and the resource geologist,* 60–80. Mineral. Assoc. Can.

Hower, J., Eslinger, E., Hower, M. & Perry, E. 1976: Mechanism of burial metamorphism of argillaceous sediments: I. Mineralogical and chemical evidences. *Geol. Soc. Am. Bull. 87,* 725–737.

Hower, J. & Mowatt, T. 1966: The mineralogy of illites and mixed-layer illite/montmorillonites. *Am. Mineral. 51,* 825–854.

Huang, P. M. 1977: Feldspars, olivines, pyroxenes and amphiboles. *In* Minerals in soil environments, 553–595. Soil Science Society of America, Madison, Wisconsin.

Hurst, A. 1981: A scale of dissolution for quartz and its implication for diagenetic processes in sandstones. *Sedimentology 28,* 451–459.

Hurst, A. & Irwin, H. 1982: Geological modelling of clay diagenesis in sandstones. *Clay Minerals 17,* 5–22.

Inoue, A. 1983: Potassium fixation by clay minerals during hydrothermal treatment. *Clays and Clay Minerals 31,* 81–91.

Islam, S., Hesse, R. & Chagnon, A. 1982: Zonation of diagenesis and low-grade metamorphism in Cambro-Ordovician flysch of Gaspé Peninsula, Québec Appalachians. *Can. Mineral. 20,* 155–167.

Kazintsev, E. 1968: Pore solutions of Maykop Formation of Eastern Pre-Caucasus and methods of squeezing of pore waters at high temperature. *In* Bogomolov, G. a.o.(eds.): *Pore solutions and methods of their study (A symposium),* 178–190. Izd. Nauka i Tekhnika, Minsk.

Keller, W.D. 1955: *The principles of chemical weathering.* 88 pp, Lucas, Columbia.

Kolthoff, I. & Sandell, E. 1952: *Textbook of quantitative inorganic analysis.* 759 pp. MacMillan, New York.

Kossovskaya, A. & Drits, V. 1970: The variability of micaceous minerals in sedimentary rocks. *Sedimentology 15,* 83–102.

Krasintseva, V. & Korunova, V. 1968: Influence of pressure and temperature on composition of extruded solutions during mud compaction. *In* Bogomolov, G.a.ao.

(eds.): *Pore solutions and methods of their study (A symposium),* 191–204. Izd. Nauka i Tekhnika, Minsk.

Krauskopf, K.B. 1979: *Introduction to geochemistry.* 2nd ed, 617 pp. McGraw-Hill, New York.

Krynine, P. 1940: Petrology and genesis of the Third Badford Sand. *Bull. Pennsylv. State Coll. Min. Ind. Exp. Sta. 29,* 13–20.

Krynine, P. 1946: Microscopic morphology of quartz types. *Proc. 2nd Panam. Congr. Min. Eng. Geol. 3,* 35–49

Kübler, B. 1964: Les argiles, indicateurs de métamorphisme. *Rev. Inst. Franç Pétrol. 19,* 1093–1112.

Lahann, R. W. 1980: Smectite diagenesis and sandstone cement: The effect of reaction temperature. *J. Sediment. Petrol. 50,* 755–760.

Lahee, F. 1941: *Field geology,* 5th ed., 833 pp. McGraw-Hill, New York.

La Iglesia, A. & van Oosterwyck-Gastuche, M. 1978: Kaolinite synthesis. I. Crystallization conditions at low temperature and calculation of thermodynamic equilibria. Application to laboratory and field observations. *Clays and Clay Minerals 26,* 397–408.

Levinson, A. 1955: Studies in the mica group: Polymorphism among illites and hydrous micas. *Am. Mineral. 40,* 41–49.

Lidström, L. 1968: Surface and bond-forming properties of quartz and silicate minerals and their application in mineral processing techniques. *Acta Polytech. Scand. 75A,* 149.

Ljunggren, P. 1954: *The region of Hålia in Dalecarlia, Sweden.* 141 pp. Ph. D. thesis, University of Lund, Sweden.

Loughnan, F. 1962: Some considerations in the weathering of silicate minerals. *J. Sediment. Petrol. 32,* 284–290.

Loughnan, F. 1969: *Chemical weathering of the silicate minerals.* 154 pp. American Elsevier, New York.

Lundqvist, Th. 1968: Precambrian geology of the Los-Hamra region, central Sweden. *Sver. Geol. Unders. Ba23.* Stockholm.

Lundqvist, Th. 1979: The Precambrian of Sweden. *Sver. Geol. Unders. C768.* Uppsala.

Magnusson, N. 1960: Age determination of Swedish Precambrian rocks. *Geol. Fören. Stockholm Förh. 82,* 407–432. Stockholm.

Magnusson, N., Thorslund, P., Brotzen, F., Asklund, B. & Kulling, O. 1960: Description to accompany the map of the pre-Quaternary rocks of Sweden. *Sver. Geol. Unders. Ba16.* Stockholm.

Maxwell, J. C. 1964: Influence of depth, temperature, and geologic age on porosity of quartzose sandstone. *Bull. Am. Assoc. Pet. Geol. 48,* 697–709.

McHardy, W., Wilson, M. & Tait, J. 1982: Electron microscopy and X-ray diffraction studies of filamentous illitic clay from sandstones of the Magnus field. *Clay Minerals 17,* 23–39.

Merino, E. 1975: Diagenesis in Tertiary sandstones from Kettleman North Dome, California. I. Diagenetic mineralogy. *J. Sediment Petrol. 45,* 320–336.

Merino, E. & Ransam, B. 1982: Free energies of formation of illite solid solutions and their compositional dependence. *Clays and Clay Minerals 30,* 29–39.

Millot, G. 1970: *Geology of clays,* 429 pp. Springer-Verlag, New York.

Monnier, F. 1982: Thermal diagenesis in Swiss molasse basin: implication for oil generation. *Can. J. Earth Sci. 19,* 328–342.

Morad, S. 1983: Diagenesis and geochemistry of the Visingsö Group (Upper Proterozoic), southern Sweden: a clue to the origin of colour differentiation. *J. Sediment. Petrol. 53,* 51–65.

Morad, S. 1984: Diagenetic matrix in Proterozoic greywacke sandstones from Sweden. *J. Sediment. Petrol. 54,* 1155–1166.

Morad, S. & AlDahan, A. A. 1982a: Authigenesis of titanium minerals in two Proterozoic sedimentary rocks from southern and central Sweden. *J. Sediment. Petrol. 52,* 1295–1305.

Morad, S. & AlDahan, A. A. 1982b: Mineralogy and crystal-chemistry of clay minerals related to diagenesis and very low-grade metamorphism of two Proterozoic sedimentary sequences from Sweden. *UUDMP research report 33.* 118 pp. Uppsala.

Nicholls, G. 1976: Weathering of the earth's crust. *In* Riley, J. & Chester, R. (eds.): *Chemical oceanography,* 91–101. Academic Press, London.

Norrish, K. 1973: Factors in the weathering of mica to vermiculite. *In* Serratosa, J. (ed.): *Proc. Int. Clay. Conf., Div. de Ciencias, 417–432.* Madrid.

Nyström, S. 1982: *Extent of host rock alteration – a control of pumpellyite composition in burial metamorphosed rocks from central Sweden,* 49 pp. Ph. D. thesis, University of Stockholm, Sweden.

Olivecrona, H. 1920: Om Västerdalarnas sandstensformation och dess tektonik. *Geol. Fören. Stockholm Förh. 42,* 323–362. Stockholm.

Patchett, J. 1978: Rb/Sr ages of Precambrian dolerites and syenites in southern and central Sweden. *Sver. Geol. Unders. C747.* Stockholm.

Perry, E. & Hower, J. 1970: Burial diagenesis in Gulf Coast pelitic sediments. *Clays and Clay Minerals 18,* 165–177.

Pettijohn, F.J. 1949: *Sedimentary rocks.* 1st ed., 526 pp. Harper & Brothers, New York.

Pettijohn, F.J. 1957: *Sedimentary rocks.* 2nd ed., 718 pp. Harper and Brothers, New York.

Pettijohn, F.J. 1975: *Sedimentary rocks.* 3rd ed., 628 pp. Harper & Row, New York.

Prozorovich, G. 1970: Determination of the time of oil and gas accumulation by epigenesis studies. *Sedimentology 15,* 41–52.

Putnis, A. & Wilson, M. 1978: A study of iron-bearing rutiles in the paragenesis TiO_2–Al_2O_3–P_2O_5–SiO_2. *Mineral. Mag. 42,* 255–263.

Ramberg, H. 1952: *The origin of metamorphic and metasomatic rocks.* 317 pp. The University of Chicago Press, Chicago.

Rieke, H. & Chilingarian, G. 1974: Compaction of argillaceous sediments. *Dev. in sedimentol. 16.* 424 pp, Elsevier, Amsterdam.

Ross, G. & Rich, C. 1974: Effect of oxidation and reduction on potassium exchange of biotite. *Clays and Clay Minerals 22,* 355–360.

Sarkisyan, S. 1971: Application of the scanning electron microscope in the investigation of oil and gas reservoir rocks. *J. Sediment. Petrol. 41,* 289–292.

Schulling, R. & Vink, B. 1967: Stability relations of some titanium minerals (sphene, perovskite, rutile, anatase). *Geochim. Cosmochim. Acta 31,* 2399–2411.

Sederholm, J. 1897: Om indelningen af de prekambriska formationerna i Sverige och Finland och om nomenklaturen för dessa äldsta bildningar. *Geol. Fören. Stockholm Förh. 19,* 20–53. Stockholm.

Sederholm, J. 1927: Om de jotniska och s.k. subjotniska bergarterna. *Geol. Fören. Stockholm Förh. 49,* 397–426. Stockholm.

Sherman, G. 1952: The titanium content of Hawaiian soils and its significance. *Proc. Soil Sci. Soc. Am. 16,* 15–18.

Shirozu, H. 1969: "Discussion". *In* Kodama, H. (eds.): Hydrous mica complexes. *Proc. Int. Clay Conf. 2. 64 pp. Tokyo.*

Shvestova, I. 1975: Mixed rutile-anatase leucoxene. *Dokl. Acad. Sci. 194,* 130–133.

Sibley, D. & Blatt, H. 1976: Intergranular pressure solution and cementation of the Tuscarora orthoquartzite. *J. Sediment. Petrol. 46,* 881–896.

Siegel, D. I. and Pfannkuch, H. D. 1984: Silicate mineral dissolution at pH 4 and near standard temperature and pressure. *Geochim. Cosmochim. Acta 48,* 197–201.

Spry, A. 1969: *Metamorphic textures,* 350 pp. Pergamon Press, London.

Sudo, T. & Shimoda, S. 1978: Clays and clay minerals of Japan. *Dev. in sedimentol. 26.* 326 pp, Elsevier, Amsterdam.

Taylor, M. 1950: Pore-space reduction in sandstones. *Bull. Am. Assoc. Pet. Geol. 34,* 701–716.

Temple, K. 1966: Alteration of ilmenite. *Econ. Geol. 61,* 695–714.

Teodorovich, G. & Chernov. A. 1968: Character of changes with depth in productive deposits of Apsheron oil-gas-bearing region. *Sov. Geol. 4,* 83–93.

Trevena, A. & Nash, W. 1981: An electron microprobe study of detrital feldspar. *J. Sediment. Petrol. 51,* 137–150.

Turner, F. & Verhoogen, J. 1960: *Igneous and metamorphic petrology.* 694 pp. McGraw-Hill, New York.

Turner, P. 1974: Origin of red beds in the Ringerike Group (Silurian) of Norway. *Sediment. Geol. 12,* 215–235.

Törnebohm, A. E. 1873: Über die Geognosie der schwedischen Hochgebirge. *K. Sven. Vetenskapsakad. Handl. Bih. 1.* Stockholm.

Törnebohm, A. E. 1896: Grunddragen af det centrala Skandinaviens bergbyggnad. *K. Sven. Vetenskapsakad. Handl. 28:5.* Stockholm.

Velde, B. 1977: Clays and clay minerals in natural and synthetic systems. *Dev. in sedimentol. 21.* 218 pp, Elsevier, Amsterdam.

Walker, T., Waugh, B. & Grone, A. 1978: Diagenesis in first-cycle desert alluvium of Cenozoic age, southwestern United States and northwestern Mexico. *Geol. Soc. Am. Bull. 89,* 19–32.

Weaver, C. & Pollard, L. 1973: The chemistry of clay minerals. *Dev. in sedimentol. 15.* 213 pp, Elsevier, Amsterdam.

Welin, E. & Blomqvist, G. 1964: Age measurements on radioactive minerals from Sweden. *Geol. Fören. Stockholm Förh. 86,* 33–50. Stockholm.

Welin, E. & Lundqvist, Th. 1975: K-Ar ages of Jotnian dolerites in Västernorrland Country, central Sweden. *Geol. Fören. Stockholm Förh. 97,* 83–88. Stockholm.

Wilding, L., Smeck, N. & Drees, L. 1977: Silica in soils: quartz, cristobalite, tridymite and opal. *In* Dixon, J. B. & Weed, S. B. (eds.): *Minerals in soil environments,* 471–552. Soil Science Society of America, Madison, Wisconsin.

Wilson, M. & Pittman, E. 1977: Authigenic clays in sandstones: recognition and influence on reservoir properties and paleoenvironmental analysis. *J. Sediment. Petrol. 47,* 3–31.

Winkler, H. 1979: *Petrogenesis of metamorphic rocks.* 334 pp. Springer-Verlag, New York.

Wolf, K. & Chilingarian, G. 1976: Compaction of coarse-grained sediments, II. *Dev. in sedimentol. 18B.* 645 pp. Elsevier, New York.

Wollast, R. 1967: Kinetics of the alteration of K-feldspar in buffered solutions at low temperature. *Geochim. Cosmochim. Acta 31.* 635–648.

Printed by Ekenäs Tryckeri AB, Ekenäs, Finland April, 1985.